



EX LIBRIS
UNIVERSITATIS
ALBERTENSIS

The Bruce Peel
Special Collections
Library

University of Alberta

Library Release Form

Name of Author: Xiaofei Dong

Title of Thesis: Fading Statistics of Diversity Techniques

Degree: Master of Science

Year this Degree Granted: 2001

Permission is hereby granted to the University of Alberta Library to reproduce single copies of this thesis and to lend or sell such copies for private, scholarly or scientific research purposes only.

The author reserves all other publication and other rights in association with the copyright in the thesis, and except as herein before provided, neither the thesis nor any substantial portion thereof may be printed or otherwise reproduced in any material form whatever without the author's prior written permission.

University of Alberta

Fading Statistics of Diversity Techniques

by

Xiaofei Dong




A thesis submitted to the Faculty of Graduate Studies
and Research in partial fulfillment of the
requirement for the degree of Master of Science

Department of Electrical and Computer Engineering

Edmonton, Alberta

Fall, 2001



Digitized by the Internet Archive
in 2025 with funding from
University of Alberta Library

<https://archive.org/details/0162014920530>

University of Alberta

Faculty of Graduate Studies and Research

The undersigned certify that they have read, and recommend to the Faculty of Graduate Studies and Research for acceptance, a thesis entitled Fading Statistics of Diversity Techniques submitted by Xiaofei Dong in partial fulfillment of the requirements for the degree of Master of Science.

To the memory of my father

Abstract

Multipath propagation causes signal fading in wireless systems. The rate of occurrence of signal fades and the durations of the fades are important parameters for wireless communication system design. They provide valuable aid in selecting bit rate, frame length and codes for digital systems and in assessing outage probabilities for both digital and analog system design. Diversity is often used to mitigate fading and thus, alter the level crossing rate and fade duration. In this thesis, analytical results are derived for average level crossing rate (LCR) and average fade duration (AFD) of different diversity combining methods operating on Rayleigh, Ricean and Nakagami fading input branches. The diversity methods considered are maximal ratio combining (MRC), equal gain combining (EGC) and selection combining (SC). New results for average level crossing and average fade duration of MRC diversity operating on independent and identically distributed (iid) Ricean fading channels are given in exact closed-forms. Precise approximation of the two quantities for EGC are presented as a infinite series. It is shown from these results that diversity reduces the level crossing rate and reduces the fade duration as the fading signal spends more time around its root-mean-square value (rms).

In practical systems, the assumption that diversity branches are identically distributed is seldom true. We present new solutions for the average LCR and AFD of maximal ratio combining with unbalanced channels with diversity order two, three and four. It is shown

that reasonable imbalance of branch powers is acceptable and the greatest improvement is from no diversity to dual-branch diversity. Exact closed-form solutions are also derived for selection combining in generalized fading models, including Rayleigh, Ricean and Nakagami. The results apply to arbitrary diversity orders and branch powers.

In diversity systems, the input branches are sometimes correlated due to insufficient separation. We show that MRC is optimal even without decorrelating the inputs. It is also shown that the performance measures of a MRC diversity system in correlated fading can be obtained from an equivalent, independent branch model. New analytical results for the average LCR and AFD of a MRC system in correlated fading are presented.

Acknowledgments

I would like to express my sincere thanks and gratitude to Dr. Norman C. Beaulieu for his continuous guidance, encouragement, friendship, technical expertise and financial support which have made this thesis possible. Special thanks to David Young for the continuous help on simulation, documentation and other technical issues.

I would like to thank my sister Xiaodai for her technical insights and advice, as well as the long time support and encouragement. I thank my brother-in-law Tao Lu for the technical advice and discussion.

I thank my father for the love and encouragement he left, and the moral supports throughout the years.

I am grateful to my boyfriend Huanzhou for the encouragement, technical discussion and help with references.

This thesis was financially supported through research assistantships provided by the Natural Sciences and Engineering Research Council (NSERC) and the Alberta Informatics Circle of Research Excellence (iCore), Queen's University Graduate Awards, and Queen's University Graduate Fellowship.

Contents

1	INTRODUCTION	1
1.1	Overview	1
1.2	Multipath Fading Environment	2
1.2.1	Short-term Fading Model	3
1.2.2	Rayleigh Fading	7
1.2.3	Ricean Fading	7
1.2.4	Nakagami- m Fading	8
1.3	Diversity Methods	9
1.3.1	Maximal Ratio Combining	12
1.3.2	Equal Gain Combining	13
1.3.3	Selection Combining	15
1.4	Thesis Outline and Contributions	15
2	Level Crossing Rate and Fade Duration	18
2.1	Definitions	18
2.2	The Average Level Crossing Rate and Average Fade Duration of a Gaussian Process	19

2.3	The Average Level Crossing Rate and Average Fade Duration of a Nakagami Fading Signal	23
3	Average Level Crossing Rate and Average Fade Duration of MRC Diversity	25
3.1	System Model	26
3.2	Independent and Identically Distributed Ricean Fading Model	27
3.2.1	The Average Level Crossing Rate	27
3.2.2	The Average Fade Duration	31
3.2.3	Simulation	31
3.3	Independent and Identically Distributed Rayleigh Fading Model	37
3.4	Independent Rayleigh Fading Models with Unbalanced Branch Powers . . .	38
3.4.1	The Average Level Crossing Rate	38
3.4.2	The Average Fade Duration	42
4	Average Level Crossing Rate and Average Fade Duration of EGC Diversity	46
4.1	General Expressions for Level Crossing Rate and Fade Duration	47
4.2	Obtaining the PDF of the Equal Gain Output Signal Envelope	48
4.2.1	Ricean Fading	48
4.2.1.1	Independent Ricean Fading Branches with Non-identical Powers	49
4.2.1.2	Independent Ricean Branches With Identical Signal Powers	52
4.2.1.3	Simulation and Numerical Computation	53
4.2.2	Rayleigh Fading	56
4.2.3	Nakagami Fading	56

5	Average Level Crossing Rate and Average Fade Duration of SC Diversity	58
5.1	Average Level Crossing Rate	59
5.2	Average Fade Duration	64
5.3	Discussion of Correlated Inputs	65
6	Average Level Crossing Rate and Average Fade Duration of Diversity in Correlated Fading	67
6.1	Optimal Maximal Ratio Combining with Correlated Diversity Branches . .	69
6.2	Average Level Crossing Rate and Average Fade Duration in Correlated Fading	73
6.3	Discussion of EGC and SC in Correlated Fading	82
7	Summary and Conclusions	85
	References	88
	Vita	94

List of Figures

1.1	Normalized Rayleigh fading signal envelope at $f_m = 90$ Hz.	10
1.2	Receiver structure of a coherent maximal ratio combiner.	13
1.3	Normalized signal envelope of a four-branch maximal ratio combining diversity system operating with iid Rayleigh branches at $f_m = 90$ Hz.	14
2.1	Normalized average level crossing rate of a Rayleigh fading envelope.	21
2.2	Normalized average fade duration of a Rayleigh fading envelope.	22
3.1	Average normalized level crossing rate of MRC for different diversity orders with $K = 7$ dB.	32
3.2	A branch input normalization where the average LCR is normalized to one branch power [Yacoub, <i>Elect. Letters</i> , Jan. 2000].	34
3.3	Average normalized fade duration of MRC for different diversity orders with $K = 7$ dB.	35
3.4	A branch input normalization where the AFD is normalized to one branch power [Yacoub, <i>Elect. Letters</i> , Jan. 2000.]	36
3.5	The average normalized LCR of MRC for branch signals with an exponentially decaying input signal power profile with decay factor 1.	43

3.6	The normalized AFD of MRC for branch signals with an exponentially decaying input signal power profile with decay factor 1.	45
4.1	Average normalized level crossing rate of EGC operating on iid Ricean fading branches for different diversity orders with $K = 7$ dB.	54
4.2	Average normalized fade duration of EGC operating on iid Ricean fading branches for different diversity orders with $K = 7$ dB.	55
5.1	Average normalized level crossing rate of SC for different diversity orders with exponentially decaying mean branch signal power profile with decay factor 0.25.	63
5.2	Average normalized fade duration of SC for different diversity orders with exponentially decaying mean branch signal power profile with decay factor 0.25.	66
6.1	Coherent maximal ratio combining operating on correlated inputs, (a) without decorrelation (b) with decorrelation	70
6.2	The average normalized LCR of MRC with adjacent branch spacings equal to one wavelength.	76
6.3	The normalized AFD of MRC with adjacent branch spacings equal to one wavelength.	77
6.4	The average normalized LCR of MRC in Rayleigh fading with equal correlations between all branches.	80
6.4	The average normalized LCR of MRC in Rayleigh fading with equal correlations between all branches, cont'd.	81

6.5 The normalized AFD of MRC in Rayleigh fading with equal
correlations between all branches of $R_{r_{ij}} = 0.604 \dots \dots \dots 83$

Acronyms

Acronym	Definition
AFD	Average Fade Duration
AWGN	Additive White Gaussian Noise
CDF	Cumulative Distribution Function
EGC	Equal Gain Combining
iid	Independent and Identically Distributed
JCDF	Joint Cumulative Distribution Function
JPDF	Joint Probability Density Function
LCR	Level Crossing Rate
LOS	Line-of-sight
MRC	Maximal Ratio Combining
PDF	Probability Density Function
PSD	Power Spectrum Density
RV	Random Variable
SC	Selection Combining
SNR	Signal-to-Noise Ratio

Symbol Notation

Symbol	Definition
${}_1F_1(\alpha, \beta; z)$	Confluent hypergeometric function
\mathcal{A}_i	Random event i
A_n	Envelope of the n th arriving waves
B	Isometry matrix of a vector norm
b	Average power received by an isotropic antenna
b_n	The n th moment of the in-phase and quadrature components
$E(x)$	Expectation of X
$E_z(t)$	Electric field component
E_0A_n	Real amplitude of the n th wave in electric field
$F(x)$	Cumulative distribution function of X
f_m	Maximal Doppler spread
$f(x)$	Probability density function of X
$g(\tau)$	Autocorrelation function of the in-phase and quadrature components of the electric field
$h(\tau)$	Cross-correlation function of the in-phase and quadrature components of the electric field
I	Identity matrix

$I_0(x)$	Modified Bessel function of the first kind of order zero
$I_k(x)$	Modified Bessel function of the first kind of order k
J	Jacobian of a linear transformation
$J_0(x)$	Zero-order Bessel function of the first kind
K	Rice factor
K_i	Rice K factor of the i th diversity branch
M	Number of diversity branches
m	Nakagami- m fading parameter
	Non-zero mean of a Gaussian process
m_i	Nakagami- m fading parameter of the i th branch
N	Noise power
	Correlation matrix of the Gaussian noise vector
N_0	One-sided power spectral density of white Gaussian noise
N_R	Average level crossing rate
\hat{N}	Correlation matrix of the transformed noise vector
\mathbf{n}	Additive white Gaussian noise vector
$\hat{\mathbf{n}}$	Additive white Gaussian noise vector after the unitary transformation
$P(\mathcal{A}_i)$	Probability of event \mathcal{A}_i
Q	Unitary matrix
$Q_1(a, b)$	Marcum- Q function of order 1
$Q_M(a, b)$	Generalized Marcum- Q function of order M
\mathbf{q}_i	The i th eigenvector of a correlation matrix
R	Signal level R
	Correlation matrix of the complex Gaussian signals

R_{ij}	The (i, j) th element of the correlation matrix R
R_r	Envelope correlation matrix
R_{rms}	Root-mean-square value of a fading signal envelope
\hat{R}	Correlation matrix of transformed Gaussian signals
$r(t)$	Fading signal envelope
$\dot{r}(t)$	Time derivative of a fading signal envelope
$\dot{r}_i(t)$	Time derivative of the i th branch signal envelope in a M -branch diversity system
\hat{r}	Diversity combined signal envelope after a linear transformation
$\dot{\hat{r}}$	Time derivative of the diversity combiner output signal envelope after a linear transformation
$S(f)$	Power spectrum density function
s	Non-centrality parameter of a Ricean RV
\mathbf{s}	Signal vector
$s(t)$	Transmitted signal with normalized unit average energy
$s_i(t)$	The i th bandpass signal in an M -branch diversity system
$\hat{\mathbf{s}}$	Signal vector after the unitary transformation
T_c	In-phase component of the electric field
T_R	Average fade duration
T_s	Quadrature component of the electric field
$U(\cdot)$	Unit step function
$\text{Var}[x]$	Variance of X
x	A time instance of $x(t)$
$x(t)$	In-phase component of a complex Gaussian process

y	A time instance of $y(t)$
$y(t)$	Quadrature component of a complex Gaussian process
\mathbf{z}	Complex signal vector
$z_i(t)$	Received i th complex signal of an M -branch diversity system
z_i	A time instance of the received signal from the i th diversity branch
$\hat{\mathbf{z}}$	Complex signal vector after the unitary transformation
α_n	Azimuthal angle of arrival
δ	Decaying factor
$\Gamma(x)$	Gamma function
γ	Received signal-to-noise ratio
	Diversity combiner output signal-to-noise ratio
γ_i	Received signal-to-noise ratio of the i th branch
$\Gamma(\alpha, x)$	Incomplete Gamma function
$\hat{\gamma}$	Diversity combiner output signal-to-noise ratio after a linear transformation
Λ	Diagonal matrix with eigenvalues on the diagonal
λ	Wavelength of the carrier frequency
λ_i	The i th eigenvalue
v	Mobile speed
Ω	Average energy in the amplitude of fading
Ω_i	Average fading energy of the i th diversity branch
ω_c	Carrier frequency
ω_n	Doppler shift
ϕ_n	Random phase in the n th wave
$\phi_i(t)$	Phase of the complex fading random process $z_i(t)$

ρ	Normalized signal level
σ^2	Energy of the scattering components
$\dot{\sigma}^2$	Variance of the time derivative of a signal envelope
$\dot{\sigma}_i^2$	Variance of the time derivative of the i th branch signal envelope in an M -branch diversity system

Chapter 1

INTRODUCTION

1.1 Overview

The interest in wireless communications and wireless devices has exploded in the past two decades. It is predicted that by 2002, there will be one billion mobile users around the world, and 30-50 percent of business-to-customer e-commerce will be conducted through mobile devices in 2002.

In just 20 years, we have seen the evolution from a few phone calls to a tangle of competing technologies; TDMA, GSM, CDMA, and the list goes on. The first generation wireless communication technology (1G) was analog and was strictly for voice. The second generation (2G), features digital wireless networks and is still in use. It is promised that the third generation (3G) wireless communication systems will provide speeds up to 2 Mbps, and access to all kinds of digital information, such as music, photos, video and television. Researchers are already looking ahead to 4G, sometimes called “software-defined radio.” Needless to say, the basic principle of the fast-growing technology is to provide higher bit rates and data services in addition to pure voice. Japan has successfully used the packet-

switched connection technology to provide fast wireless internet services and has shown a huge potential market. The packet switching technology is also proposed for 3G systems. However, the wireless fading environment is as hostile as ever. Correct understanding of the fading behavior of the wireless channel is critical for deploying the new high-speed technology.

In this thesis, we investigate the statistical properties of the wireless fading channel. We want to give a quantitative description of the occurrence of deep fades and duration of fades, through the analysis of the average level crossing rate and average fade duration. These two parameters provide important performance measures in communication system design. In this thesis, we present the analytical results for the average level crossing rate and average fade duration of diversity systems.

This chapter is organized as follows. In Section 1.2, we review in some detail the characteristics of the multipath fading environment. The principles of diversity combining schemes are presented in Section 1.3. These two sections serve to help understand the backgrounds and system models used in this Thesis. In Section 1.4, we provide an outline and summarize the main contributions of this thesis.

1.2 Multipath Fading Environment

The hostile mobile radio propagation environment inhibits the performance of wireless communication systems. There are three commonly seen phenomena in a radio propagation environment [1]. Propagation path loss, caused by the terrestrial losses as well as free space losses, refers to the signal energy decay with distance [2]. The second is the short-term fading, caused by reflecting and scattering by surrounding objects in the channel, refers to the rapid fluctuation of the received signal energy, frequency and phase. The third is the

long-term fading, typically caused by the small-scale topographical variations along the transmission path, and is commonly modeled as slow log-normal shadowing. In this thesis, we consider only short-term multipath fading.

In built-up areas, the mobile antenna is usually well below the surrounding buildings, so there is no direct transmission path, or line-of-sight (LOS) path between the transmitter and the receiver. Propagation is by way of reflecting and scattering of the rays by objects in the transmission path. So the signal waves arrive via several paths simultaneously, from different directions and with different time delays. When multiple waves of the same signal are received at the receiving antenna, the destructive and constructive multipath components result in substantial variations of the received signal envelope, frequency and phase. Secondly, whenever relative motion exists between the transmitter and receiver, there is frequency shift of the received signal due to the Doppler effect. Thus, both the motions of the mobile terminal and of objects around the receiving terminal introduce random frequency modulation. On the other hand, the transmitted signal bandwidth and the fading channel bandwidth decide what type of fading the signal experiences. When the signal bandwidth is smaller than the channel coherence bandwidth, different frequency components of the signal have the same gain in amplitude and the phase of the signal is preserved. This is called flat fading. For wide-band signals, as the frequency separation increases, the behavior of the frequency components becomes uncorrelated. Thus, the received signal strength varies as a function of frequency. This phenomenon is known as frequency selective fading.

1.2.1 Short-term Fading Model

A number of multipath models have been suggested to explain the observed statistical characteristics of the electromagnetic fields. The earliest was due to Ossanna [3]. His model

was based on interference of waves incident and reflected from the flat sides of randomly located buildings. The limitation of Ossanna's model is that it assumes the existence of a direct path between the transmitter and receiver, and is further limited to a restricted range of reflection angles. The more widely used model is the Clarke model.

Clarke's model [4] assumes that the field incident on the mobile antenna is composed of N horizontally traveling plane waves of random phase. These plane waves are vertically polarized with spatial angles of arrival and phase angles which are random and statistically independent. Furthermore, it is assumed the phases are uniformly distributed in the interval $(0, 2\pi)$, or equivalently, the scattering is isotropic.

The resultant electric field component at the mobile, with these assumptions, is

$$E_z(t) = E_0 \sum_{n=1}^N A_n \cos((\omega_c + \omega_n)t + \phi_n) \quad (1.1)$$

where $E_0 A_n$ is the real amplitude of the n th wave in the electric field, ω_c is the carrier frequency, ω_n is the Doppler shift in the n th wave, and ϕ_n is the uniformly distributed random phase. The Doppler shift, or Doppler spread is,

$$\omega_n = \frac{2\pi v}{\lambda} \cos \alpha_n = 2\pi f_m \cos \alpha_n \quad (1.2)$$

where v is the mobile speed, λ is the wavelength of the carrier frequency, and α_n is the azimuthal angle of arrival. The maximum Doppler frequency is defined as $f_m = \frac{v}{\lambda}$. The amplitudes A_n are normalized so that the ensemble average

$$E \left\{ \sum_{n=1}^N A_n^2 \right\} = 1. \quad (1.3)$$

If N is sufficiently large (theoretically infinite, but in practice greater than 6 [5], [2]), then as a consequence of the central limit theorem, E_z is approximately a Gaussian random process.

Rice proved in [6], [7] that we can express E_z as

$$E_z = T_c(t) \cos \omega_c t - T_s(t) \sin \omega_c t, \quad (1.4)$$

where

$$T_c(t) = E_0 \sum_{n=1}^N A_n \cos(\omega_n t + \phi_n) \quad (1.5)$$

$$T_s(t) = E_0 \sum_{n=1}^N A_n \sin(\omega_n t + \phi_n) \quad (1.6)$$

are Gaussian random processes, corresponding to the in-phase and quadrature components of E_z , respectively. Denote T_c and T_s as the Gaussian random variable (RV) corresponding to $T_c(t)$ and $T_s(t)$, at any time t . Rice has shown that they are zero-mean Gaussian with equal variance

$$E(T_c^2) = E(T_s^2) = \frac{E_0^2}{2} = E(|E_z|^2). \quad (1.7)$$

Furthermore, T_c and T_s are uncorrelated and therefore independent at any time t .

Assuming the distribution of power with arrival angle is a uniform distribution, the power spectrum of the electric field can be found as [8]

$$S_{E_z}(f) = \frac{3b}{2\pi f_m} \left[1 - \left(\frac{f - f_c}{f_m} \right)^2 \right]^{-1/2} \quad (1.8)$$

where b is the average power that would be received by an isotropic antenna. From this power spectrum density function (PSD), Rice has obtained the correlation functions of the in-phase and quadrature components $T_c(t)$ and $T_s(t)$,

$$E(T_c(t)T_c(t+\tau)) = E(T_s(t)T_s(t+\tau)) = g(\tau), \quad (1.9a)$$

$$E(T_c(t)T_s(t+\tau)) = -E(T_s(t)T_c(t+\tau)) = h(\tau), \quad (1.9b)$$

$$E(T_c(t)T_c'(t+\tau)) = E(T_s(t)T_s'(t+\tau)) = -E(T_c'(t)T_c(t+\tau)) = -E(T_s'(t)T_s(t+\tau)) = g'(\tau), \quad (1.9c)$$

$$E(T_c(t)T_s'(t+\tau)) = -E(T_s'(t)T_c(t+\tau)) = -E(T_c'(t)T_s(t+\tau)) = -E(T_s(t)T_c'(t+\tau)) = h'(\tau), \quad (1.9d)$$

$$E(T_c'(t)T_c'(t+\tau)) = E(T_s'(t)T_s'(t+\tau)) = -g''(\tau), \quad (1.9e)$$

$$E(T_c'(t)T_s'(t+\tau)) = -E(T_s'(t)T_c'(t+\tau)) = -h''(\tau), \quad (1.9f)$$

where

$$g(\tau) = \int_{f_c-f_m}^{f_c+f_m} S_z(f) \cos(2\pi(f-f_c)\tau) df, \quad (1.10)$$

$$h(\tau) = \int_{f_c-f_m}^{f_c+f_m} S_z(f) \sin(2\pi(f-f_c)\tau) df \quad (1.11)$$

with $S_z(f)$ defined as the PSD of the electric field and it is defined within the range $(f_c - f_m, f_c + f_m)$. Thus, the moments of the in-phase and quadrature components can be found by setting $\tau = 0$ and are given as

$$b_n = (2\pi)^n \int_{f_c-f_m}^{f_c+f_m} S_z(f) (f-f_c)^n \tau df. \quad (1.12)$$

If we apply the PSD (1.8) in (1.12), and as a consequence of the symmetry of the spectrum about f_c , it is straightforward to show that

$$h(\tau) = 0 \quad (1.13)$$

and all b_n equal zero for n odd. When n is even,

$$b_n = b_0 (2\pi f_m)^n \frac{1 \cdot 3 \cdot 5 \cdots (n-1)}{2 \cdot 4 \cdot 6 \cdots n}, \quad (1.14)$$

$$b_0 = E(T_c^2) = E(T_s^2) = g(0), \quad (1.15)$$

$$g(\tau) = b_0 J_0(2\pi f_m \tau) \quad (1.16)$$

where $J_0(\cdot)$ is the zero-order Bessel function of the first kind [9]. The auto-correlation function $g(\tau)$ of the in-phase and quadrature components and the quantities b_n will be used in Section 2.

1.2.2 Rayleigh Fading

A number of models have been proposed to describe the signals transmitted through wireless channels. In (1.4) it is shown the received signal after fading can be expressed as in-phase and quadrature components, both of which are Gaussian processes. The equivalent lowpass signal [10] is thus a complex Gaussian random process,

$$z(t) = r(t)e^{-j\phi(t)} = x(t) + jy(t) \quad (1.17)$$

where $x(t)$ and $y(t)$ are Gaussian distributed at any time t . In urban built-up areas, there is no direct transmission path between the transmitter and the receiver. The signal propagation is through the scattering of the objects in the transmission path. In such an environment, $x(t)$ and $y(t)$ have zero means. At any time t , x and y are zero-mean Gaussian RV's with

$$E(x) = E(y) = 0, \quad \text{Var}(x) = \text{Var}(y) = b_0, \quad E(xy) = 0 \quad (1.18)$$

where $\text{Var}(\cdot)$ is the variance. The received signal envelope, r , is therefore Rayleigh distributed with PDF given by

$$f(r) = \frac{r}{b_0} \exp\left\{-\frac{r^2}{2b_0}\right\} \quad r \geq 0. \quad (1.19)$$

The cumulative distribution function (CDF) of a Rayleigh faded envelope is

$$F(R) = P(r \leq R) = 1 - \exp\left(-\frac{R^2}{2b_0}\right) \quad (1.20)$$

where $P(\mathcal{A})$ is the probability of event \mathcal{A} .

1.2.3 Ricean Fading

When there is a LOS or specular component between the transmitter and the receiver, x and y have non-zero mean m and the envelope of the received fading signal has a Ricean PDF

given by

$$f(r) = \frac{r}{b_0} \exp \left\{ -\frac{(r^2 + s^2)}{2b_0} \right\} I_0 \left(\frac{rs}{b_0} \right) \quad r \geq 0 \quad (1.21)$$

where $s = 2m^2$ is the non-centrality parameter and $I_0(\cdot)$ is the zero-order modified Bessel function of the first kind [9]. Ricean fading is often observed in microcellular and satellite applications where a LOS path exists [11], [12]. The Rice factor K is defined as the power ratio of the specular components to the scattering components as

$$K = \frac{s^2}{2b_0}. \quad (1.22)$$

Setting $K = 0$ corresponds to the Rayleigh fading and $K = \infty$ describes the case without fading. Typical practical values of K are 7dB and 12dB [11]. The CDF of Ricean distributed RV r is given as [10]

$$F(r) = 1 - Q_1 \left(\frac{s}{\sqrt{b_0}}, \frac{r}{\sqrt{b_0}} \right), \quad r \geq 0 \quad (1.23)$$

where $Q_1(a, b)$ is the first-order Marcum Q function given by [13]

$$Q_1(a, b) = e^{-(a^2 + b^2)/2} \sum_{k=0}^{\infty} \left(\frac{a}{b} \right)^k I_k(ab), \quad b > a > 0 \quad (1.24)$$

with $I_k(\cdot)$ defined as the k -order modified Bessel function of the first kind, given by

$$I_k(z) = \sum_{l=0}^{\infty} \frac{1}{l! \Gamma(l + k + 1)} \left(\frac{z}{2} \right)^{k+2l} \quad (|z| < \infty, |arg(z)| < \pi). \quad (1.25)$$

1.2.4 Nakagami- m Fading

The PDF of Nakagami- m fading was introduced by Nakagami in 1960 [14]. Empirical data show that the Nakagami fading model fits observed data better than the Rayleigh, Ricean or log-normal distributions. The Nakagami- m faded signal envelope has PDF

$$f(r) = \frac{2m^m r^{2m-1}}{\Omega^m \Gamma(m)} \exp \left(-\frac{mr^2}{\Omega} \right) \quad r \geq 0, m \geq \frac{1}{2} \quad (1.26)$$

where $\Omega = E(r^2)$, $\Gamma(m)$ is the Gamma function and m is the Nakagami parameter, defined as the ratio of moments,

$$m = \frac{\Omega^2}{E[(r^2 - \Omega)^2]}. \quad (1.27)$$

The Nakagami- m distribution can be used to model fading more or less severe than Rayleigh fading. When $m = \frac{1}{2}$, the Nakagami distribution becomes a one-sided Gaussian distribution. When $m = 1$, the Nakagami distribution becomes the Rayleigh distribution. As m gets larger, it models less severe fading than the Rayleigh. In the limiting case, $m = \infty$ models the channel without fading.

The CDF of Nakagami- m is given in [14] as

$$F(r) = \frac{\Gamma(m, mr^2/\Omega)}{\Gamma(m)} \quad (1.28)$$

where $\Gamma(a, b)$ is the incomplete Gamma function defined as

$$\Gamma(a, b) = \int_0^b z^{a-1} \exp(-z) dz \quad . \quad (1.29)$$

Fig. 1.1 shows a computer simulated Rayleigh fading envelope at signal energy $2b_0 = 1$ and maximum Doppler frequency $f_m = 90$ Hz, corresponding to a mobile moving at 60 mi./hr., and transmitting at 1 GHz. The signal envelope has been normalized to its root-mean-square value, $R_{rms} = \sqrt{E[r^2]}$. It is clearly shown in the 0.5 seconds time window that the signal envelope fluctuates rapidly in a random manner.

1.3 Diversity Methods

In order to reduce the signal fading range or excessive deep fades for both digital and analog systems, diversity combining is widely used, as an alternative to increasing transmission power [15], [16]. The principle of diversity is that, if a number of copies of the same

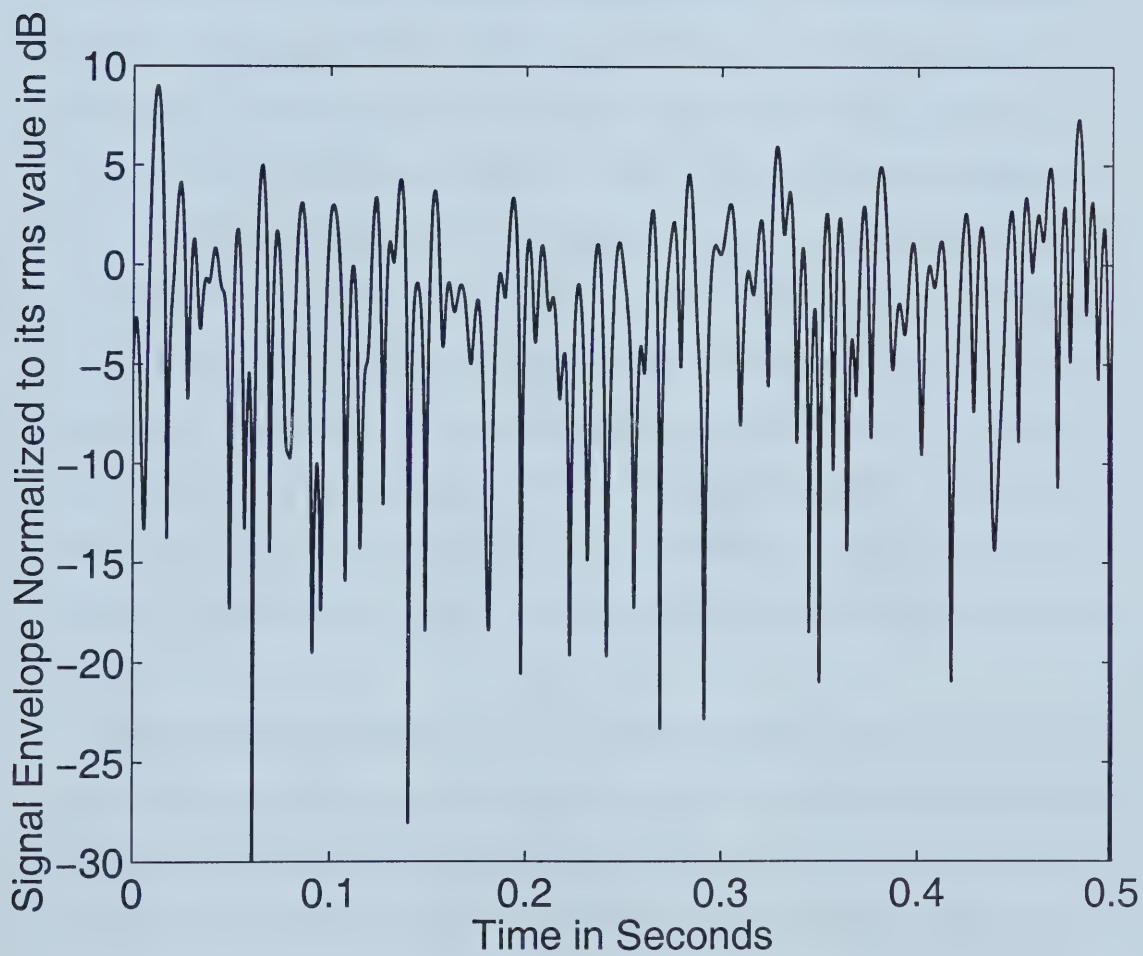


Figure 1.1. Normalized Rayleigh fading signal envelope at $f_m = 90$ Hz.

information bearing signal is available, and they all experience independent fading, then the probability that all copies are in deep fades simultaneously is small.

Generally speaking, there are two types of diversity. Macroscopic diversity, which is used to mitigate the long-term log-normal shadowing, places multiple receiving antennae at different base station sites [17]. Microscopic diversity is used to counteracting the short-term fading, or multipath fading. In our work, we consider only microscopic diversity.

There are a number of ways to obtain the multiple copies of the transmitted signals [18]. Space diversity, most commonly used and preferred for mobile communication engineering, places receiving antennae far enough apart to achieve independent fading. Frequency diversity transmits the same signal at sufficiently spaced carrier frequencies. Polarization diversity is possible when two orthogonal polarizations can be deployed. Multipath diversity, or the RAKE technique, can be achieved in multipath situations when wideband signals are transmitted. The multiple ray reception is obtained by resolving multipath components at different delays by using direct sequence spread spectrum signaling along with a RAKE receiver [19].

There are also many different linear combining methods. The most common combining methods in the literature are maximal ratio combining, equal gain combining and selection combining. According to where the combining is performed, the aforementioned combining methods can be further classified as predetection and postdetection combining. If the signal-to-noise power ratio does not change from the detection, theoretically predetection and postdetection combining are the same. However in real systems, there are practical differences. In this thesis, only predetection combining is considered.

The received baseband equivalent signal at the i_{th} antenna is

$$z_i(t) = r_i(t)e^{j\theta_i(t)} + n_i(t) \quad (1.30)$$

where $n_i(t)$ is the additive white Gaussian noise, $\theta_i(t)$ is the random phase and $r_i(t)$ is the received fading signal envelope at any time t . The general combining weights input channels by complex factors α_i , so the resultant combined signal can be expressed as

$$z(t) = \sum_{i=1}^M \alpha_i z_i(t). \quad (1.31)$$

1.3.1 Maximal Ratio Combining

In maximal ratio combining, input branches are co-phased, and weighted by their signal envelope amplitude to noise power ratios,

$$\alpha_i = \frac{r_i e^{-j\theta_i(t)}}{N} \quad (1.32)$$

where we have assumed that the noise power at each branch is the same and is denoted by N . Fig. 1.2 shows a typical predetection maximal ratio combiner structure. Assuming the noise components of the input branches are mutually independent, the instantaneous output noise power is [8, eqn. 5.2-10]

$$N_{out} = \frac{\sum_{i=1}^M r_i^2}{N}. \quad (1.33)$$

Consequently, the output signal-to-noise ratio (SNR) is given by

$$\gamma_{out} = \frac{r^2}{2N_{out}} = \sum_{i=1}^M \frac{r_i^2}{2N} = \sum_{i=1}^M \gamma_i. \quad (1.34)$$

In particular, the output noiseless signal envelope can be expressed as [8, eqn. 5.2-9]

$$r = \frac{1}{N} \sum_{i=1}^M r_i^2. \quad (1.35)$$

Maximal ratio combining is the optimum combining in terms of the output SNR at each time instant. It is also considered as the most complicated to implement, due to the fact that phase-lock and amplitude weighting must be performed.

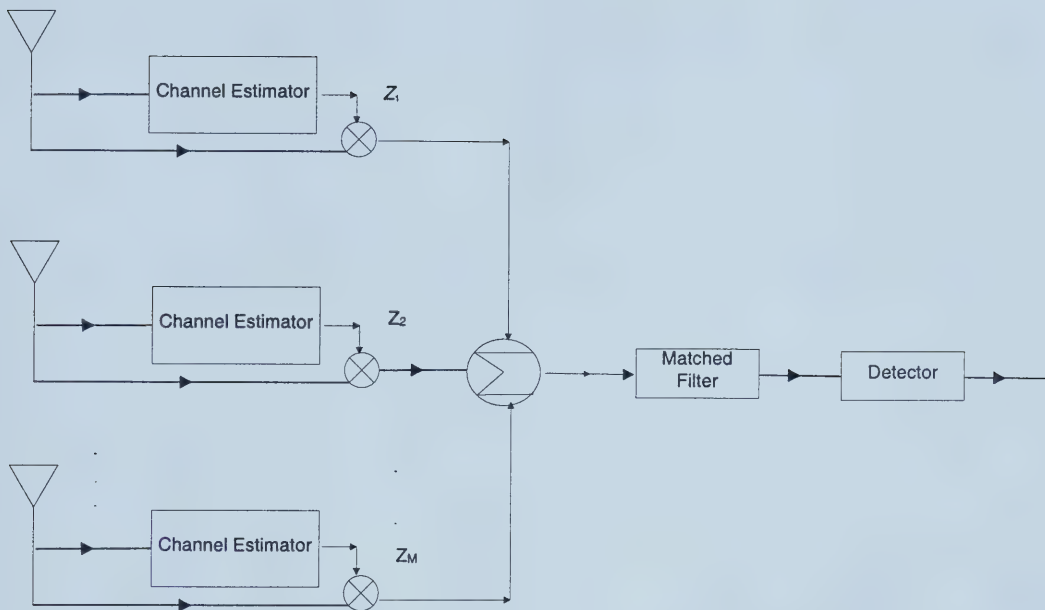


Figure 1.2. Receiver structure of a coherent maximal ratio combiner.

Fig. 1.3 shows the signal envelope after four-branch MRC combining. A unit signal energy and maximum Doppler frequency of 90 Hz is used, the same as previously used in Fig. 1.1. Diversity has significantly improved fading, as deep fades below -10 dB are not seen within the time window of Fig. 1.3, while they are common in Fig. 1.1.

1.3.2 Equal Gain Combining

Equal gain combining is an attractive alternative to MRC, since it provides performance similar to that of MRC but has a reduced complexity. In equal gain combining, branch signals are co-phased, and weighted equally. Thus, the weighting factors α_i are

$$\alpha_i = \frac{e^{-j\theta_i(t)}}{N}. \quad (1.36)$$

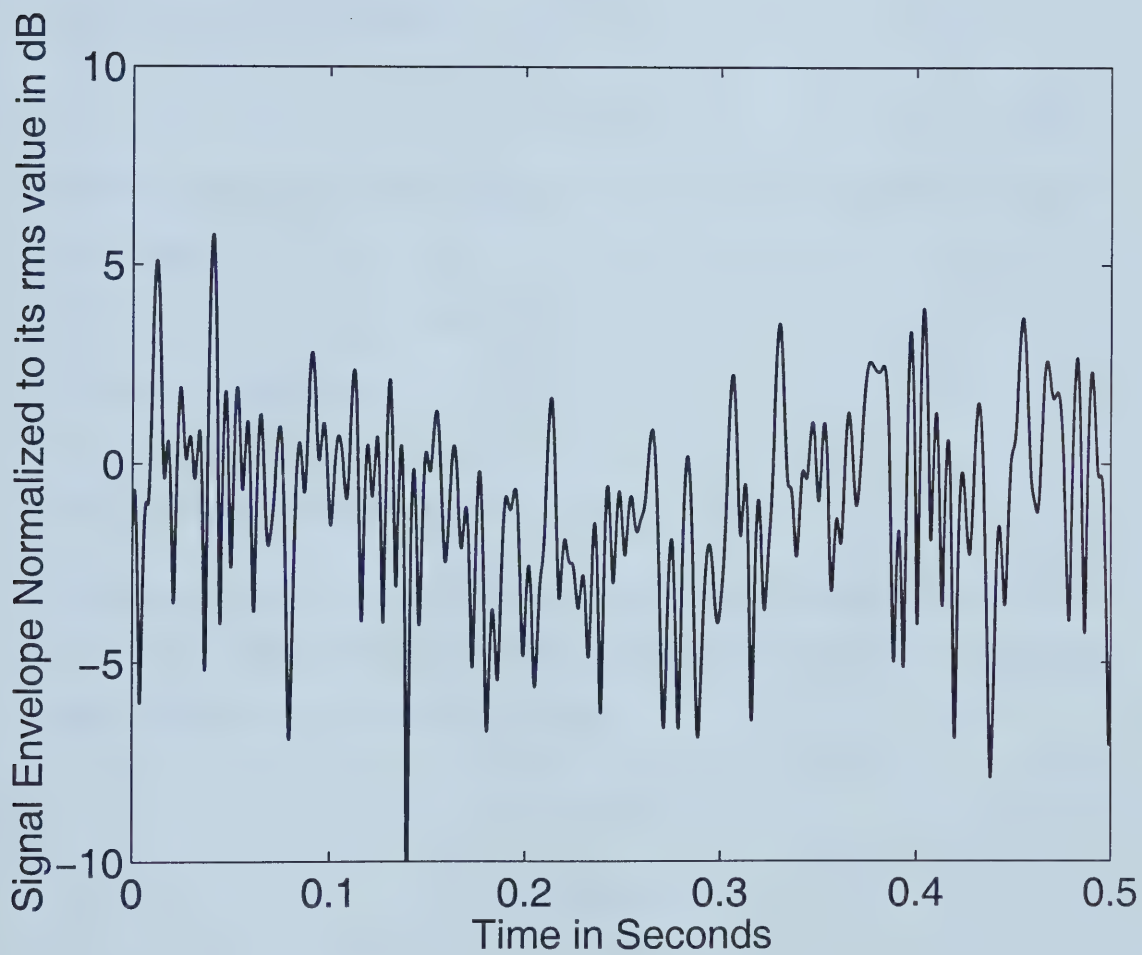


Figure 1.3. Normalized signal envelope of a four-branch maximal ratio combining diversity system operating with iid Rayleigh branches at $f_m = 90$ Hz.

The combined noiseless signal envelope is thus given by [8, eqn. 5.2-17]

$$r = \frac{1}{N} \sum_{i=1}^M r_i. \quad (1.37)$$

The EGC output SNR is obtained as

$$\gamma_{out} = \frac{r^2}{2NM}. \quad (1.38)$$

For EGC operating on iid Rayleigh fading branches, the average output SNR is obtained from (1.38) as

$$E[\gamma] = \frac{b_0}{N} \left[1 + (M-1) \frac{\pi}{4} \right] \quad (1.39)$$

where b_0 is defined in (1.15).

1.3.3 Selection Combining

Selection combining is described, where at any time t , the weighting factors α_i are zero except for the branch with the largest SNR, where it is a constant. Thus, the combiner output signal envelope and SNR are, respectively,

$$r = \max \{r_i\}_{i=1}^M, \quad (1.40)$$

$$\gamma_{out} = \max \{\gamma_i\}_{i=1}^M. \quad (1.41)$$

1.4 Thesis Outline and Contributions

In Chapter 2 we introduce the terminology and concepts of level crossing rate and fade duration. Analytical results on the average level crossing rate and the fade duration of Gaussian and Nakagami processes are given. In Chapter 3 we investigate the average level crossing rate and average fade duration of maximal ratio combining diversity. New exact

closed-form expressions for the two quantities are presented for the case of independent and identically distributed Ricean input branches. The results can be specialized to the Rayleigh case. We also introduce a new method of normalization, which we believe is more physically intuitive. We further extend our research to the case when the input branches of a maximal ratio combiner have unbalanced mean signal energies. New, exact analytical results are obtained for the case of Rayleigh fading branches.

In Chapter 4 we present a new method of computing the average LCR and AFD of an equal gain combined signal envelope using Beaulieu's infinite series [20]. Rayleigh, Ricean and Nakagami fading branches are considered. Precise results are obtained for independent fading branches with both equal and non-identical powers. Numerical computations and simulations are also presented for Ricean fading branches.

In Chapter 5 we investigate the average LCR and AFD in selection combining in generalized fading models. Independent fading of input branches is assumed. Simple, exact closed-form expression are obtained for the commonly used Rayleigh, Ricean and Nakagami fading models. To the best of the authors knowledge, these results are new.

So far we have only considered the case where the input branches are independent. Sometimes the diversity branches are correlated in practical systems. In Chapter 6 we investigate the performance measures of a diversity system in correlated fading. We show that by using a unitary transformation, the performance analysis of a correlated maximal ratio diversity combiner can be solved from an equivalent, independent branch model, which, in general, has unbalanced powers. We also point out that MRC is optimal even without decorrelating the inputs. These results are applied to the level crossing problems. New, exact analytical results for average LCR and AFD of a MRC system in correlated Rayleigh fading are presented.

In the end, we present a summary of the thesis.

Chapter 2

Level Crossing Rate and Fade Duration

It is apparent from Fig. 1.1 that the fading signal envelope fluctuates rapidly. The Rayleigh CDF, as well as the Ricean and the Nakagami CDF are first order statistics of the envelope, which give information of such as the overall percentage of time, or overall percentage of locations, for which the envelope lies below a specific level. First order statistics give no information of how the time is made up. However, system design engineers are interested in the rate of the occurrence of deep fades and the duration of such deep fades [2]. They provide valuable aids in selecting bit rate and frame length, especially in packet-switched systems. Also, they are important parameters in selecting buffer depth for adaptive modulators and code designs for both digital and analog systems. The level crossing rate and the fade duration are quantitative descriptions of the required information.

2.1 Definitions

The level crossing rate at level R is defined as the rate at which the fading signal envelope crosses level R in a positive-going (or negative-going) direction. There has been a consid-

erable amount of work about the level crossing rate of a random process [21]- [26], since it is not only of profound physical and theoretical interest, but is also of practical importance. Rice [6] gave a rather simple expression of the average level crossing rate, N_R , per second in terms of the joint probability density function (JPDF) of the signal envelope, r , and its time derivative, \dot{r} ,

$$N_R = \int_0^\infty \dot{r} f(R, \dot{r}) d\dot{r}. \quad (2.1)$$

The fade duration is defined as the time a fading envelope remains below a specific level after crossing that level in a downward going direction. It is obvious to see that the overall fraction of time that the signal is below a level R is the cumulative distribution function of the envelope. So the average fade duration, which is defined as the first moment of the fade duration, can be computed from

$$T_R = \frac{P_r(r \leq R)}{N_R}. \quad (2.2)$$

2.2 The Average Level Crossing Rate and Average Fade Duration of a Gaussian Process

The derivation of the level crossing rate of a Gaussian process is often quoted from Rice's work in 1945 [6]. He proved that for the Gaussian processes, like those defined in Chapter 1 (1.5) and (1.6), the average level crossing rate N_R of the signal envelope is given by

$$N_R = \frac{R(2\pi)^{-3/2}}{\sqrt{Bb_0}} \int_{-\pi}^{\pi} d\theta \int_0^\infty \dot{r} d\dot{r} \exp \left\{ -\frac{1}{2Bb_0} [B(R^2 - 2Rs \cos \theta + s^2) + (b_0\dot{r} + b_1s \sin \theta)^2] \right\} \quad (2.3)$$

where s is the non-zero mean of T_c and T_s , which are defined in (1.5) and (1.6), respectively, $\tan \theta = -T_s/T_c$, $B = b_0b_2 - b_1^2$ and the b_n 's are given in (1.14) and (1.15). When the power

spectrum $S(f)$ of the Gaussian process is symmetrical about the carrier frequency f_c , as in the Clarke's model (1.8), b_1 is zero and $B = b_0 b_2$. Thus, the integrations in (2.3) can be performed and we have [7, eqn. 4.8]

$$\begin{aligned} N_R &= \left(\frac{b_2}{2\pi}\right)^{1/2} \frac{R}{b_0} I_0\left(\frac{Rs}{b_0}\right) \exp\left(-\frac{R^2 + s^2}{2b_0}\right) \\ &= \left(\frac{b_2}{2\pi}\right)^{1/2} \times [\text{PDF of envelope at the value } R]. \end{aligned} \quad (2.4)$$

Rice has shown in (2.4) that r and \dot{r} are independent, and that \dot{r} is Gaussian distributed with PDF

$$f(\dot{r}) = \frac{1}{\sqrt{2\pi b_2}} \exp\left(-\frac{\dot{r}^2}{2b_2}\right) \quad (2.5)$$

where b_2 can be obtained from (1.14) as

$$b_2 = 2\pi^2 f_m^2 b_0. \quad (2.6)$$

It is easy to see that the same property holds when the mean s of the Gaussian processes T_c and T_s are zero. In other words, the average level crossing rate of a Rayleigh and Ricean fading envelope can be obtained as the PDF of the signal envelope times a scalar, as manifested in (2.4).

From (2.4), the average level crossing rate is a function of the mobile speed, and this is apparent from the appearance of f_m in (2.6). Normalization of N_R by f_m produces the number of level crossings per wavelength and the value is thus independent of the mobile speed. The normalized average level crossing rate of the Rayleigh envelope is [8, eqn. 1.3-37], [2, eqn. 5.44]

$$\frac{N_R}{f_m} = \sqrt{2\pi} \rho \exp\{-\rho^2\} \quad (2.7)$$

where

$$\rho = \frac{R}{R_{rms}} = \frac{R}{\sqrt{2}\sqrt{b_0}}. \quad (2.8)$$

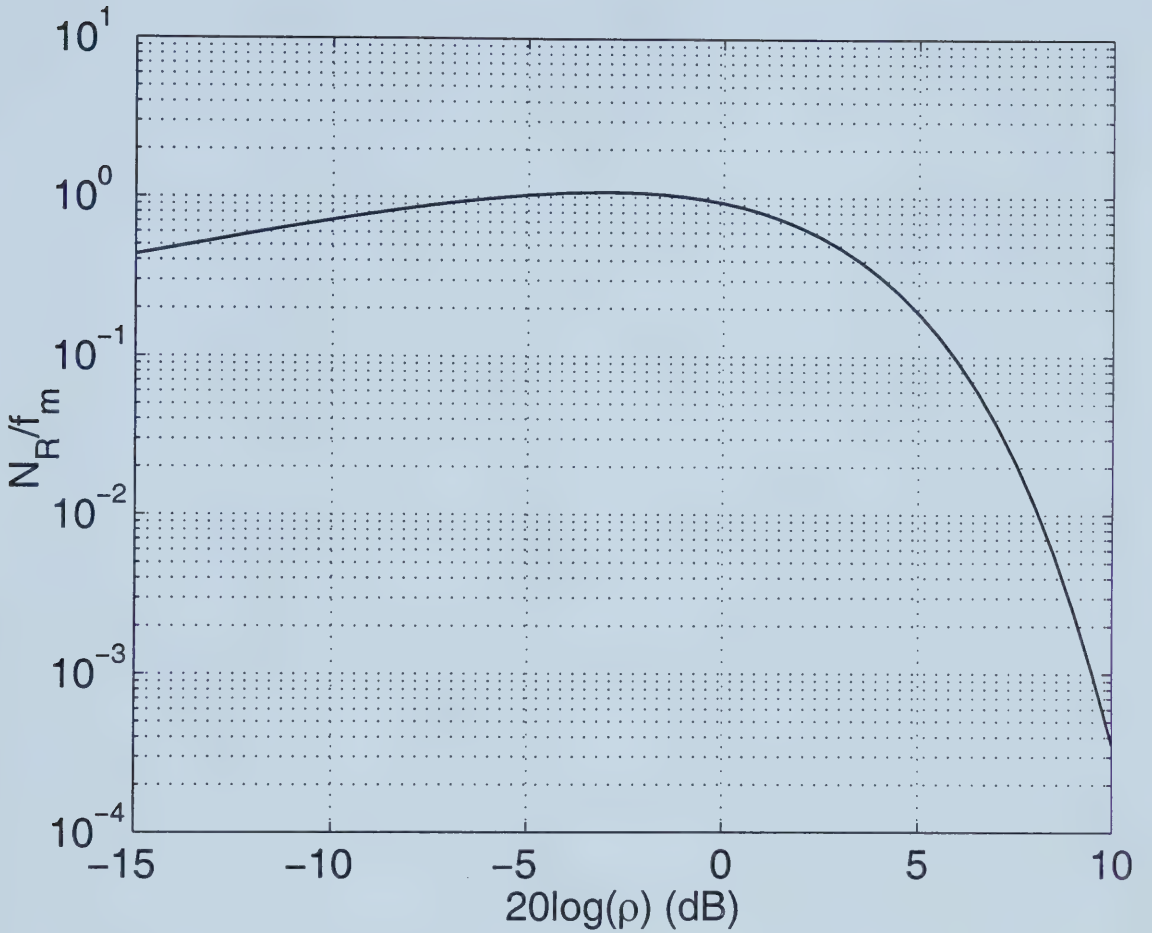


Figure 2.1. Normalized average level crossing rate of a Rayleigh fading envelope.

Fig. 2.1 plots the normalized average LCR vs signal level normalized to the envelope root-mean-square value. It is straightforward to see that the maximum rate occurs at the mode of the Rayleigh distribution $R_{\text{mode}} = \sqrt{b_0}$, i.e. at a level 3 dB below the rms value.

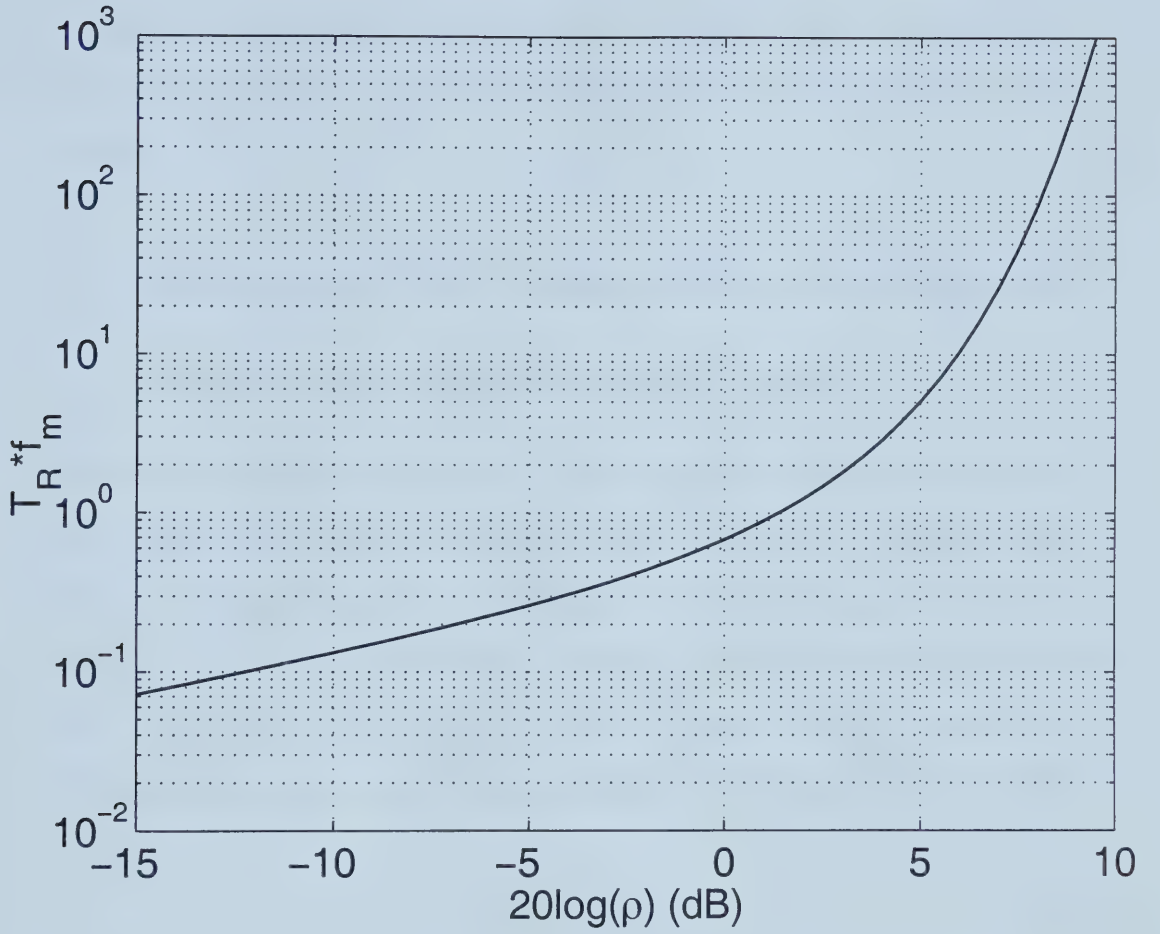


Figure 2.2. Normalized average fade duration of a Rayleigh fading envelope.

For the case of Rayleigh fading, the CDF of r is

$$F(r) = 1 - \exp\left(-\frac{r^2}{2b_0}\right). \quad (2.9)$$

Therefore, the normalized average fade duration is

$$T_R = \frac{\exp(\rho^2) - 1}{\rho f_m \sqrt{2\pi}} \quad (2.10)$$

where $\rho = \frac{R}{R_{rms}}$. Multiplying T_R by f_m gives the average fade duration in wavelengths, which is independent of the mobile speed.

Fig.2.2 illustrates the average fade duration of a Rayleigh fading envelope, where the AFD has been normalized to f_m while the signal level is normalized to the rms value of the envelope.

2.3 The Average Level Crossing Rate and Average Fade Duration of a Nakagami Fading Signal

A method for deriving the average level crossing rate and fade duration of the Rayleigh and Ricean fading models is given in the previous section. The analysis of average level crossing rate and average fade duration of the Nakagami- m fading model is given by Yacoub in [27] for $m = n/2$, with n a nonzero integer number. One important conclusion he derived is that in the Nakagami- m case as in the Rayleigh and Ricean cases, the time derivative of the fading signal envelope, \dot{r} , and the signal envelope, r , are independent random variables, [27, eqn. 14]

$$f(\dot{r}, r) = f(\dot{r}) \times f(r). \quad (2.11)$$

Moreover, the probability density function of the time derivative of the Nakagami- m envelope is also zero-mean Gaussian distributed as are the time derivatives of both Rayleigh and Ricean envelopes, [27, eqn. 13]

$$f(\dot{r}) = \frac{1}{\sqrt{2\pi\dot{\sigma}}} \exp\left(-\frac{\dot{r}^2}{2\dot{\sigma}^2}\right) \quad (2.12)$$

where

$$\dot{\sigma}^2 = \frac{\pi^2 f_m^2 \Omega}{m} \quad (2.13)$$

is the variance of \dot{r} .

Consequently, the average level crossing rate of a Nakagami- m fading signal envelope can be obtained in simple closed-form for $m = n/2$ as ¹

$$N_R = \sqrt{2\pi}f_m \frac{m^{m-1/2}}{\Gamma(m)} \rho^{2m-1} \exp(-m\rho^2) \quad (2.14)$$

where $\rho = R/R_{rms}$ with $R_{rms} = \sqrt{\Omega}$ the root-mean-square value of the signal envelope.

The average fade duration is thus given by [27, eqn. 21]

$$T_R = \frac{\Gamma(m, m\rho^2) \exp(m\rho^2)}{\sqrt{2\pi}f_m m^{m-1/2} \rho^{2m-1}} \quad (2.15)$$

where $\Gamma(a, b)$ is the incomplete gamma function, as previously defined in (1.29).

¹Note that [27, eqn. 17] is incorrect.

Chapter 3

Average Level Crossing Rate and Average Fade Duration of MRC Diversity

It is obvious from (2.1) that to obtain the average level crossing rate and average fade duration of any fading envelope, it is critical to find the JPDF of the signal envelope and its time derivative. As shown in (2.4) and (2.11), it has been proved that the JPDF for single branch reception is the product of two marginal distributions, as the signal envelope and its time derivative are independent random processes. This property, however, may not hold after diversity combining due to the weighting.

Maximal ratio combining is the optimal diversity combining method [15] [8]. It provides the largest output SNR and is an effective way of reducing fading. The level crossing rate and fade duration are thus expected to be changed by MRC diversity. In this chapter, we present the simple closed-form results for the average LCR and AFD of MRC in iid Ricean and Rayleigh fading. The analytical expressions of average LCR and AFD for

MRC in non-identical Rayleigh fading are also obtained.

3.1 System Model

We recall and rewrite here the results needed to derive the expressions of average level crossing rate and average fade duration of a diversity system.

The received baseband equivalent signal at the i_{th} antenna of an M -antenna system is

$$s_i(t) = r_i(t)e^{j\theta_i(t)} + n_i(t) = z_i(t) + n_i(t) \quad (3.1)$$

where $r_i(t)$ is the received fading signal envelope, $\theta_i(t)$ is the random phase, $z_i(t)$ is the equivalent complex signal, and $n_i(t)$ is additive white Gaussian noise. Some most commonly used fading models of $r_i(t)$ are Rayleigh, Ricean and Nakagami fading models, as explained in the Introduction. When the Rayleigh and Ricean models are used, $z_i(t)$ is Gaussian distributed and $r_i(t)$ is the envelope of $z_i(t)$.

The probability densities of the aforementioned models are given in (1.19), (1.21) and (1.26) and are summarized here as

$$f_{\text{Rayleigh}}(r_i) = \frac{r_i}{\sigma_i^2} \exp \left\{ -\frac{r_i^2}{2\sigma_i^2} \right\}, \quad (3.2a)$$

$$f_{\text{Ricean}}(r_i) = \frac{r_i}{\sigma_i^2} \exp \left\{ -\frac{(r_i^2 + s_i^2)}{2\sigma_i^2} \right\} I_0 \left(\frac{r_i s_i}{\sigma_i^2} \right), \quad (3.2b)$$

$$f_{\text{Nakagami}}(r_i) = \frac{2m^m r_i^{2m-1}}{\Omega_i^m \Gamma(m)} \exp \left(-\frac{mr_i^2}{\Omega_i} \right) \quad r_i \geq 0, m \geq \frac{1}{2}. \quad (3.2c)$$

The cumulative distribution functions of these models are given in (1.20), (1.23) and (1.28)

$$F_{\text{Rayleigh}}(r_i) = 1 - \exp \left(-r_i^2 / 2\sigma_i^2 \right), \quad (3.3a)$$

$$F_{\text{Ricean}}(r_i) = 1 - Q_1(s_i/\sigma_i, r_i/\sigma_i), \quad (3.3b)$$

$$F_{\text{Nakagami}}(r_i) = \frac{\Gamma(m, mr_i^2/\Omega_i)}{\Gamma(m)}. \quad (3.3c)$$

The discussion of the level crossing problem of a diversity system in the following chapters is based on the system model (3.1). To investigate the level crossing rate and fade duration, the distribution of the time derivative of the fading signal envelope is needed. Summarizing the results of Chapter 2, the PDFs of \dot{r}_i are

$$f(\dot{r}_i) = \frac{1}{\sqrt{2\pi\dot{\sigma}_i^2}} \exp\left(-\frac{\dot{r}_i^2}{2\dot{\sigma}_i^2}\right) \quad (3.4)$$

with

$$\dot{\sigma}_i^2 = 2\pi^2 f_m^2 \sigma_i^2 \quad (3.5)$$

for the Rayleigh and Ricean distributed envelopes and

$$\dot{\sigma}_i^2 = \frac{\pi^2 f_m^2 \Omega_i}{m} \quad (3.6)$$

for the Nakagami- m envelope; when $2m = n$, n is a non-zero integer.

3.2 Independent and Identically Distributed Ricean Fading Model

3.2.1 The Average Level Crossing Rate

For M -branch MRC diversity, the noiseless output signal envelope is the square summation of input branch signal envelopes, as previously defined in (1.35). When the input signals, $\{r_i\}_{i=1}^M$, are independent and identically distributed Ricean RVs as defined in (3.2b), the combiner output signal envelope r has a non-central chi-square distribution of order $2M$

[10], as it is a squared summation of $2M$ non zero-mean Gaussian RVs. The PDF of r is given by

$$f(r) = \frac{1}{2\sigma^2} \left(\frac{r}{S^2} \right)^{\frac{M-1}{2}} \exp \left\{ -\frac{(r+S^2)}{2\sigma^2} \right\} I_{M-1} \left(\sqrt{r} \frac{S}{\sigma^2} \right) \quad (3.7)$$

where $\sigma_i^2 = \sigma^2$, $S^2 = Ms^2$ and $I_{M-1}(\cdot)$ is the $(M-1)$ th-order modified Bessel function of the first kind [9].

Differentiating (1.35), we have the time derivative of the MRC diversity output signal envelope, \dot{r} , given by

$$\dot{r} = 2 \sum_{i=1}^M r_i \dot{r}_i. \quad (3.8)$$

Given $\{r_i\}_{i=1}^M$, \dot{r} is Gaussian distributed since it is a linear transformation of M Gaussian random variables [28], where \dot{r}_i is defined in (2.5). The conditional distribution of \dot{r} has zero mean since $\{\dot{r}_i\}_{i=1}^M$ have zero means. The conditional variance of \dot{r} is given by

$$\dot{\sigma}^2 = \text{Var}[\dot{r} | \{r_i\}_{i=1}^M] = \text{E}[\dot{r}^2 | \{r_i\}_{i=1}^M] = 4 \sum_{i=1}^M r_i^2 \text{E}[\dot{r}_i^2] \quad (3.9)$$

where we have assumed the input branches are independent. When the input signals are identically distributed, the above equation can be simplified to

$$\dot{\sigma}^2 = 4 \sum_{i=1}^M r_i^2 \dot{\sigma}_i^2 = 8\pi^2 f_m^2 \sigma^2 r \quad (3.10)$$

where (1.35) and (3.5) are used. We note that this conditional distribution of \dot{r} does not depend on individual branches. Instead, it is just a function of the combiner output signal envelope r . Therefore,

$$f(\dot{r} | r) = f(\dot{r} | \{r_i\}_{i=1}^M) = \frac{1}{\sqrt{2\pi\dot{\sigma}^2}} \exp \left(-\frac{\dot{r}^2}{2\dot{\sigma}^2} \right) \quad (3.11)$$

with $\dot{\sigma}^2$ given in (3.10).

Since

$$f(r, \dot{r}) = f(\dot{r} | r) f(r), \quad (3.12)$$

combining (3.7), (3.11) and (3.12) gives the JPDF of the MRC output signal envelope and its time derivative as

$$f(r, \dot{r}) = \frac{1}{\sqrt{2\pi(8\pi^2 f_m^2 \sigma^2 r)}} \exp \left\{ -\frac{\dot{r}^2}{16\pi^2 f_m^2 \sigma^2 r} \right\} \frac{1}{2\sigma^2} \left(\frac{r}{s^2} \right)^{\frac{M-1}{2}} \exp \left\{ -\frac{(r+s^2)}{2\sigma^2} \right\} I_{M-1} \left(\sqrt{r} \frac{s}{\sigma^2} \right). \quad (3.13)$$

An immediate observation is that though r_i and \dot{r}_i are independent, r and \dot{r} are not independent. This is due to the weighting of MRC, which results in the squaring of the channel signal envelopes before summing. Combining (2.1) and (3.13), the average level crossing rate of MRC diversity, operating on iid Ricean fading branch signals, normalized to the maximum Doppler frequency is given by,

$$\frac{N_R}{f_m} = \sqrt{2\pi} \left(\frac{R}{2\sigma^2} \right)^{\frac{1}{2}} \left(\frac{R}{s^2} \right)^{\frac{M-1}{2}} \exp \left\{ -\frac{R+s^2}{2\sigma^2} \right\} \cdot I_{M-1} \left(\sqrt{R} \frac{s}{\sigma^2} \right). \quad (3.14)$$

If we normalize the average level crossing rate to the rms value of the signal envelope at the combiner output, we have

$$\begin{aligned} \frac{N_R}{f_m} &= \sqrt{2\pi} \rho^{\frac{M}{2}} \frac{(\sqrt{M^2(1+K)^2 + M(2K+1)})^{\frac{M}{2}}}{(MK)^{\frac{M-1}{2}}} \\ &\cdot \exp \left\{ -\rho \sqrt{M^2(1+K)^2 + M(2K+1)} - MK \right\} \cdot I_{M-1} \left(2\sqrt{\rho MK \sqrt{M^2(1+K)^2 + M(2K+1)}} \right) \end{aligned} \quad (3.15)$$

where $\rho = R/R_{rms}$ with the root-mean-square envelope level given by

$$R_{rms} = \sqrt{E[r^2]} = \frac{\Omega_i}{1+K} \sqrt{M^2(1+K)^2 + M(2K+1)}. \quad (3.16)$$

Result (3.15) is a closed-form expression for the average level crossing rate of the output signal of MRC diversity operating on Ricean fading input signals. To the best of the author's knowledge, this result is new.

The normalization that we use is also new. Previous work [29], [30] and [31] normalizes the signal level to the rms value of one input branch signal. Our normalization, to the rms value of the diversity combiner output signal, is more physically intuitive and results in a clearer understanding of the diversity behaviors as will be clearly seen in our results for the average level crossing rate and average fade duration.

When the diversity order M becomes large, the maximum level crossing rate occurs at $R = R_{rms}$ and its value can be found using a central limit theorem (CLT) analysis. Define

$$r = \sum_{i=1}^M r_i^2 = \sum_{i=1}^M z_i \quad (3.17)$$

where $\{z_i\}_{i=1}^M$ are iid RVs with mean $\mu = \Omega_i$ and variance [10]

$$\sigma_z^2 = \frac{\Omega_i^2}{(1+K)^2} (1+2K) < \infty. \quad (3.18)$$

According to the Lindeberg-Lévy CLT [32, p. 196], $(r - M\mu)/(\sigma_z\sqrt{M})$ is Gaussian distributed with zero-mean and unit variance. Thus, r is Gaussian distributed with mean $M\mu$ and variance $M\sigma_z^2$ and the PDF of r when M is large is given by

$$f(r) = \sqrt{\frac{1}{2\pi \frac{M\Omega_i^2(1+2K)}{(1+K)^2}}} \exp \left\{ -\frac{(r - M\Omega_i)^2}{\frac{2M\Omega_i^2(1+2K)}{(1+K)^2}} \right\}. \quad (3.19)$$

Combining (2.1), (2.6), (3.10) and (3.13), the normalized average level crossing rate of the output signal envelope r of MRC when the diversity order is large is given by

$$\frac{N_R}{f_m} = \sqrt{\frac{\rho(1+K)}{1+2K}} \sqrt[4]{1 + \frac{1+2K}{M(1+K)^2}} \exp \left\{ -\frac{M(\rho\sqrt{1 + \frac{1+2K}{M(1+K)^2}} - 1)^2(1+K)^2}{2(1+2K)} \right\} \quad (3.20)$$

where

$$R_{rms} = \sqrt{E[r^2]} = \frac{\Omega_i}{1+K} \sqrt{M^2(1+K)^2 + M(1+2K)}.$$

Therefore, almost no level crossings happen at output signal envelope levels different from the rms value but right at $R = R_{rms}$, the normalized average level crossing rate is

$\sqrt{(1+K)/(1+2K)}$. This is because increasing the number of diversity branches makes the fading of scattering components of the signal shallower. In the limiting case as the diversity order approaches infinity, all the signal power becomes concentrated at the rms signal level value.

3.2.2 The Average Fade Duration

The normalized average fade duration is obtained by integrating (3.7) and combining it with (3.15), which gives

$$T_R * f_m = \frac{[1 - Q_M(\sqrt{2KM}, \sqrt{2\rho\sqrt{M^2(1+K)^2 + M(2K+1)}})]}{\sqrt{2\pi}\rho^{\frac{M}{2}}(\sqrt{M^2(1+K)^2 + M(2K+1)})^{\frac{M}{2}}} \exp\{\rho\sqrt{M^2(1+K)^2 + M(2K+1)} + MK\} \cdot \frac{(MK)^{\frac{M-1}{2}}}{I_{M-1}(2\sqrt{\rho MK\sqrt{M^2(1+K)^2 + M(2K+1)}})} \quad (3.21)$$

where $Q_M(\cdot)$ is the generalized Marcum Q function of order M, given by [13]

$$Q_M(a, b) = Q_1(a, b) + e^{-(a^2+b^2)/2} \sum_{k=1}^{M-1} \left(\frac{b}{a}\right)^k I_k(ab) \quad (3.22)$$

with $Q_1(a, b)$ defined in (1.24).

3.2.3 Simulation

Computer simulations were run to justify (3.15) and (3.21). All simulation results were obtained using the inverse fast Fourier transform method of [33] for generating time-correlated Ricean random variates. A sample size of 2^{20} is used, with the digitized maximum Doppler frequency of 0.01.

Fig. 3.1 shows plots of N_R/f_m versus the normalized signal level ρ for five different values of diversity order M . A Rice factor of $K = 7$ dB is used for these curves. Simulation

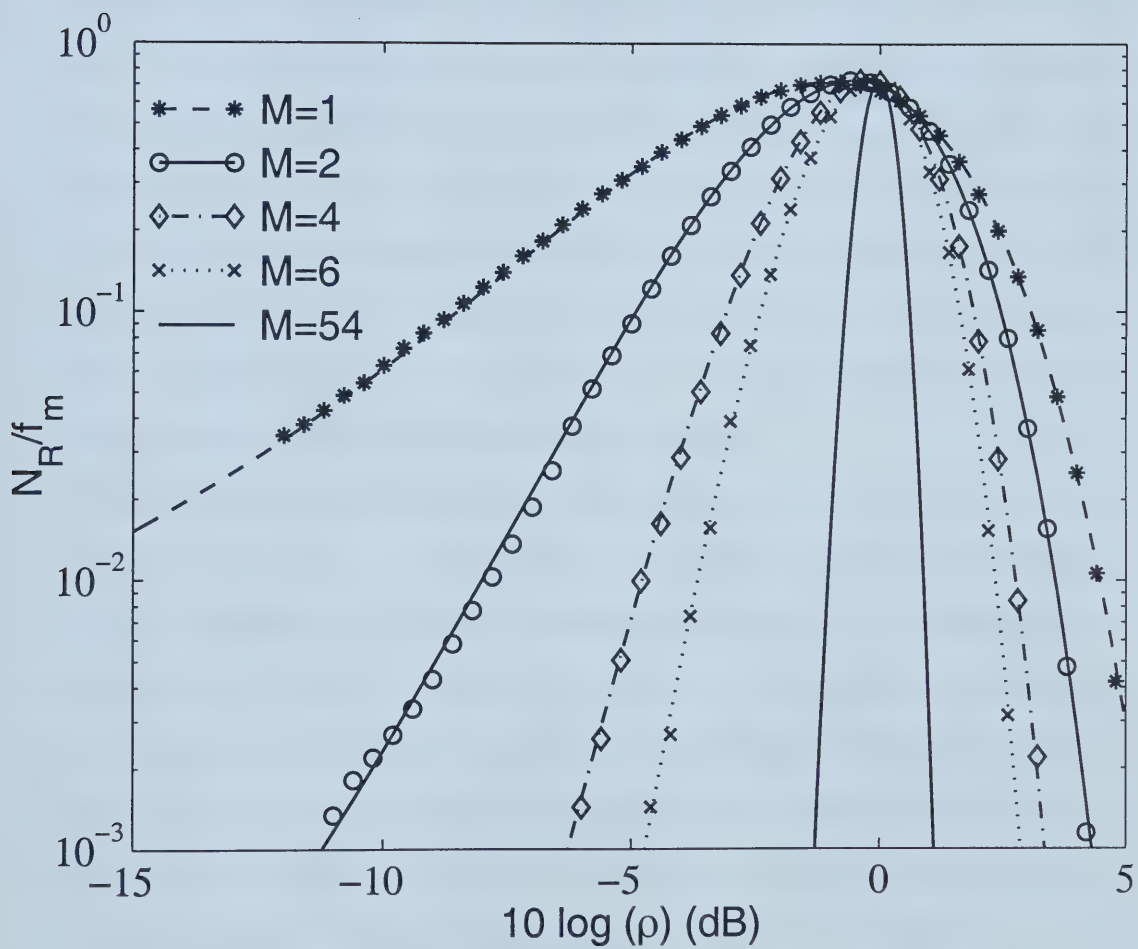


Figure 3.1. Average normalized level crossing rate of MRC for different diversity orders with $K = 7$ dB.

results (the points) are also shown and they are in excellent agreement with the theoretical curves (the lines). As expected, diversity mitigates the effect of fading, which is manifested in Fig. 3.1 in that the level crossing rate becomes smaller and smaller as the diversity order increases whenever the combiner output signal envelope level is below or above its rms value. It is clearly shown in the figure that as the diversity order increases, the average level crossing rate normalized to the rms value and the maximum Doppler frequency bends around $R = R_{rms}$. This important property can only be seen from the normalization we use. For comparison, previous normalization schemes on work of the average LCR of a diversity system, normalize the signal level to the rms value of one input branch signal power, as shown in Fig. 3.2. Instead of bending around the rms value of the combiner output, the average LCR shifts with diversity order increase.

Fig. 3.3 shows the normalized average fade duration as a function of the normalized envelope level ρ . Again, simulation results are in excellent agreement with theoretical results. Corresponding to the behavior previously seen in Fig. 3.1, the fade duration at signal levels below the rms level decreases as the diversity order increases and the duration at levels above the rms level increases, as the signal spends more time around its rms value. In the limiting case when M approaches infinity, the average fade duration of the output signal envelope jumps from zero to infinity as the envelope level passes its rms value from below R_{rms} to above it. This trend is illustrated by the curve $M = 54$ in Fig. 3.3.

This trend can only be observed from the normalization scheme we use, which normalizes the signal levels to the rms value of the MRC combiner output signal envelope. Previous work on the average fade duration [29], [30], [31], normalized to the rms value of one input branch, and it causes the average fade duration to shift with diversity order increase, as shown in Fig. 3.4.

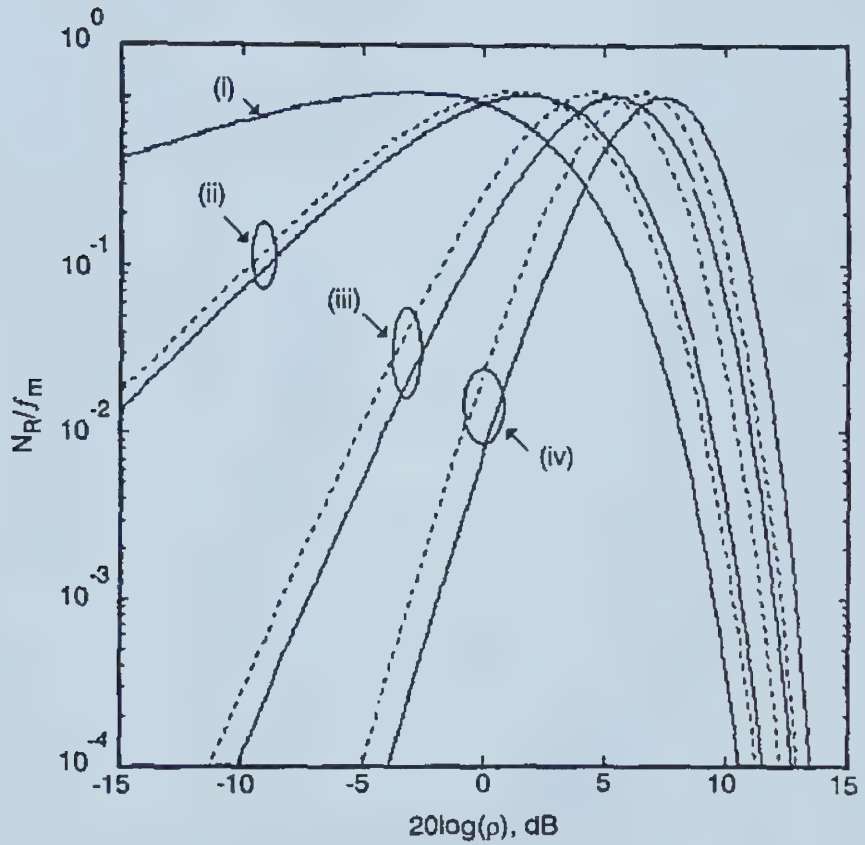


Fig. 1 *Level crossing rate*

..... EGC
 — MRC

(i) no diversity, (ii) $M = 2$, (iii) $M = 4$, (iv) $M = 6$

Figure 3.2. A branch input normalization where the average LCR is normalized to one branch power [Yacoub, *Elect. Letters*, Jan. 2000].

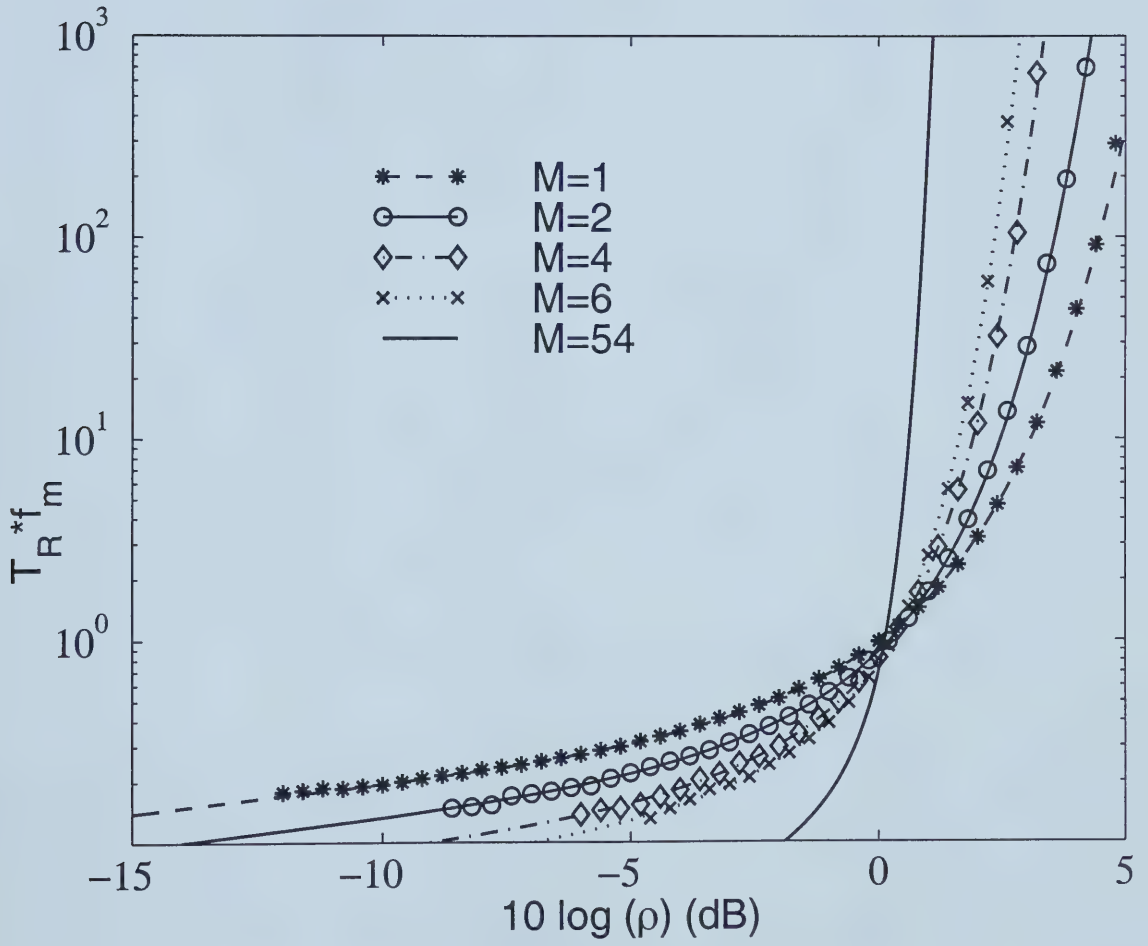
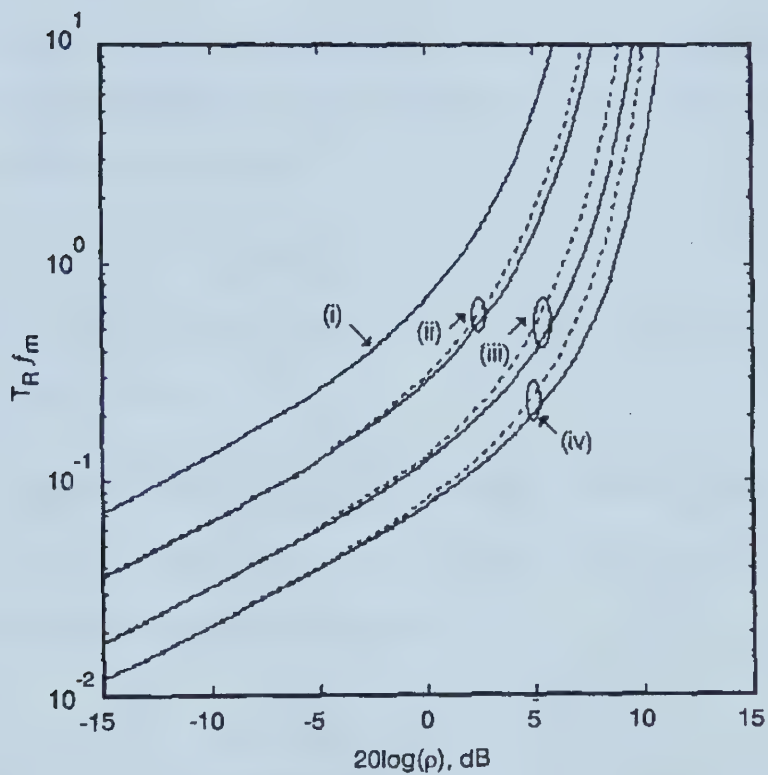


Figure 3.3. Average normalized fade duration of MRC for different diversity orders with $K = 7$ dB.



805/2

Fig. 2 *Average fade duration*

..... EGC

—— MRC

(i) no diversity, (ii) $M = 2$, (iii) $M = 4$, (iv) $M = 6$

Figure 3.4. Branch Input Normalization: AFD normalized to one branch power [Yacoub, *Elect. Letters*, Jan. 2000].

3.3 Independent and Identically Distributed Rayleigh Fading Model

When the input signals, $\{r_i\}_{i=1}^M$, are independent and identically distributed Rayleigh RVs as defined in (3.2a), the combiner output signal envelope r has a chi-square distribution of order $2M$ [10]. The PDF of r is given by

$$f(r) = \frac{r^{M-1}}{(2\sigma^2)^M (M-1)!} \exp\left(-\frac{r}{2\sigma^2}\right). \quad (3.23)$$

Using a similar method to that used in Section 3.2, the JPDF of the MRC output signal envelope and its time derivative is

$$f(r, \dot{r}) = \frac{1}{\sqrt{16\pi^3 f_m^2 \sigma^2 r}} \exp\left(-\frac{\dot{r}^2}{16\pi^2 f_m^2 \sigma^2 r}\right) \frac{r^{M-1}}{(2\sigma^2)^M (M-1)!} \exp\left(-\frac{r}{2\sigma^2}\right). \quad (3.24)$$

With (3.24), the integration of (2.1) can be performed. We have the average LCR at level R normalized to the maximum Doppler frequency as

$$\frac{N_R}{f_m} = \frac{\sqrt{2\pi} R^{M-\frac{1}{2}}}{(2\sigma^2)^{M-\frac{1}{2}} (M-1)!} \exp\left(-\frac{R}{2\sigma^2}\right). \quad (3.25)$$

Result (3.25) was also incorrectly given in [29].

If we normalize the signal levels to the rms value of the MRC combiner output signal envelope, then the normalized average LCR is given by

$$\frac{N_R}{f_m} = \sqrt{2\pi} \frac{(\rho \sqrt{M^2 + M})^{M-\frac{1}{2}}}{(M-1)!} \exp\{-\rho \sqrt{M^2 + M}\} \quad (3.26)$$

where again $\rho = R/R_{rms}$ with $R_{rms} = 2\sigma^2 \sqrt{M^2 + M}$.

The average fade duration of a MRC combiner with iid Rayleigh fading inputs can be found by combining (3.23) and (3.26), which gives

$$T_R * f_m = \frac{\exp(\rho \sqrt{M^2 + M}) - (M-1)! \sum_{k=0}^{M-1} (\rho \sqrt{M^2 + M})^k / k!}{\sqrt{2\pi} (\rho \sqrt{M^2 + M})^{M-1/2}}. \quad (3.27)$$

3.4 Independent Rayleigh Fading Models with Unbalanced Branch Powers

So far we have discussed the average LCR and AFD of maximal ratio combining operating on independent and identically distributed input branches. However, the assumption of identical signal powers of all diversity branches is seldom true in practical systems. First, the propagation paths of the branches of diversity systems are rarely identical. Second, the antennae and/or receiver electronics may also be unbalanced. Third, in the utilization of a RAKE receiver operating in frequency selective fading, the signals at the combiner branches usually have a non-uniform power delay profile [1]. In this section, the average LCR and AFD of MRC diversity combined non-identical Rayleigh fading signals are derived for diversity orders of two, three and four. To the best of the author's knowledge, these results are new.

3.4.1 The Average Level Crossing Rate

Suppose the input branches of a MRC combiner are independent Rayleigh fading signals having different powers. Given $\{r_i\}_{i=1}^M$, the time derivative of the MRC combiner output signal envelope, \dot{r} , is Gaussian distributed given by

$$f(\dot{r}|\{r_i\}_{i=1}^M) = \frac{1}{\sqrt{2\pi\dot{\sigma}^2}} \exp\left\{-\frac{\dot{r}^2}{2\dot{\sigma}^2}\right\} \quad (3.28)$$

with

$$\begin{aligned} \dot{\sigma}^2 &= 4 \sum_{i=1}^M r_i^2 \dot{\sigma}_i^2 \\ &= 8\pi^2 f_m^2 \sum_{i=1}^M r_i^2 \sigma_i^2. \end{aligned} \quad (3.29)$$

We can see from (3.29) that property (3.11) no longer holds, since the conditional PDF of \dot{r} involves information of individual branches. Thus, we cannot express the JPDF of r and \dot{r} in a simple relationship.

For dual-branch MRC, the joint PDF of \dot{r}, r_1 and r_2 can be obtained from (3.2a) and (3.28) as

$$f(\dot{r}, r_1, r_2) = f(\dot{r}|r_1, r_2)f(r_1, r_2) = \frac{1}{\sqrt{2\pi\dot{\sigma}^2}} \exp\left\{-\frac{\dot{r}^2}{2\dot{\sigma}^2}\right\} \frac{r_1}{\sigma_1^2} \exp\left\{-\frac{r_1^2}{2\sigma_1^2}\right\} \frac{r_2}{\sigma_2^2} \exp\left\{-\frac{r_2^2}{2\sigma_2^2}\right\},$$

$$r_1 > 0 \quad \text{and} \quad r_2 > 0. \quad (3.30)$$

Using $u = r_1$ as an auxiliary random variable in the mapping

$$\begin{cases} r = r_1^2 + r_2^2 \\ u = r_1 \\ \dot{r} = \dot{r} \end{cases} \quad (3.31)$$

gives the JPDF of $\{r, u, \dot{r}\}$ as

$$f(r, u, \dot{r}) = \frac{f(\dot{r}, r_1, r_2)}{|J|} \quad (3.32)$$

where J is the Jacobian of the transformation (3.31) given by [28]

$$J = \begin{vmatrix} \frac{\partial r}{\partial r_1} & \frac{\partial r}{\partial r_2} & \frac{\partial r}{\partial \dot{r}} \\ \frac{\partial u}{\partial r_1} & \frac{\partial u}{\partial r_2} & \frac{\partial u}{\partial \dot{r}} \\ \frac{\partial \dot{r}}{\partial r_1} & \frac{\partial \dot{r}}{\partial r_2} & \frac{\partial \dot{r}}{\partial \dot{r}} \end{vmatrix} = -2r_2. \quad (3.33)$$

Thus, the JPDF of (3.32) can be rewritten as

$$f(r, \dot{r}, u) = \frac{1}{\sqrt{8\pi[(\dot{\sigma}_1^2 - \dot{\sigma}_2^2)u^2 + \dot{\sigma}_2^2 r]}} \frac{u}{2\sigma_1^2 \sigma_2^2} \cdot \exp\left\{-\frac{\dot{r}^2}{8[(\dot{\sigma}_1^2 - \dot{\sigma}_2^2)u^2 + \dot{\sigma}_2^2 r]} - \frac{u^2}{2\sigma_1^2} - \frac{r - u^2}{2\sigma_2^2}\right\} U(u)U(r - u^2). \quad (3.34)$$

Combining (3.30) and (3.34) with (2.1), and integrating with respect to u over $(0, \infty)$, the average level crossing rate is given by [9]

$$N_R = \int_0^\infty \dot{r} d\dot{r} \int_{-\infty}^\infty f(R, \dot{r}, u) du. \quad (3.35)$$

Because the integration region is rectangular and the integrand is continuous on this region, we can exchange the order of the integration, which gives

$$\begin{aligned} N_R &= \int_0^{\sqrt{R}} \left(\int_0^\infty \frac{\dot{r}}{\sqrt{2\pi\dot{\sigma}^2}} \exp\left\{-\frac{\dot{r}^2}{2\dot{\sigma}^2}\right\} d\dot{r} \right) \frac{u}{2\sigma_1^2\sigma_2^2} \exp\left\{-\frac{\sigma_2^2 - \sigma_1^2}{2\sigma_1^2\sigma_2^2} u^2 - \frac{R}{2\sigma_2^2}\right\} du \\ &= \frac{1}{\sqrt{2\pi\sigma_1^2\sigma_2^2}} \exp\left\{-\frac{R}{2\sigma_2^2}\right\} \int_0^{\sqrt{R}} u \sqrt{(\dot{\sigma}_1^2 - \dot{\sigma}_2^2)u^2 + \dot{\sigma}_2^2 R} \exp\left\{-\frac{\sigma_2^2 - \sigma_1^2}{2\sigma_1^2\sigma_2^2} u^2\right\} du \\ &\quad \text{change variable } u \text{ by } t = u^2 \\ &= \frac{\sqrt{\pi} f_m}{2\sigma_1^2\sigma_2^2} \exp\left\{-\frac{R}{2\sigma_2^2}\right\} \int_0^R \sqrt{(\sigma_1^2 - \sigma_2^2)t + \sigma_2^2 R} \exp\left\{-\frac{\sigma_2^2 - \sigma_1^2}{2\sigma_1^2\sigma_2^2} t\right\} dt \\ &\quad \text{change variable } t \text{ by } (\sigma_1^2 - \sigma_2^2)t + \sigma_2^2 R = s \\ &= \frac{\sqrt{\pi} f_m}{2\sigma_1^2\sigma_2^2(\sigma_1^2 - \sigma_2^2)} \exp\left\{-\frac{R}{2\sigma_2^2} - \frac{R}{2\sigma_1^2}\right\} \int_{\sigma_2^2 R}^{\sigma_1^2 R} \sqrt{s} \exp\left\{\frac{s}{2\sigma_1^2\sigma_2^2}\right\} ds. \quad (3.36) \end{aligned}$$

Without loss of generality, we assume $\sigma_1^2 > \sigma_2^2$. According to [9, 3.383, pp. 365], the above integral can be expressed by the confluent hypergeometric function. Thus, N_R at level R normalized to the maximum Doppler frequency can be rewritten as

$$\frac{N_R}{f_m} = \frac{\sqrt{\pi} R^{\frac{3}{2}}}{3(\sigma_1^2 - \sigma_2^2)} \left[\frac{\sigma_1}{\sigma_2^2} e^{-\frac{R}{2\sigma_1^2}} {}_1F_1\left(1, \frac{5}{2}; -\frac{R}{2\sigma_2^2}\right) - \frac{\sigma_2}{\sigma_1^2} e^{-\frac{R}{2\sigma_2^2}} {}_1F_1\left(1, \frac{5}{2}; -\frac{R}{2\sigma_1^2}\right) \right] \quad (3.37)$$

where ${}_1F_1(\alpha, \beta; \gamma)$ is the confluent hypergeometric function defined as [9]

$${}_1F_1(\alpha, \beta; \gamma) = 1 + \frac{\alpha \gamma}{\beta \cdot 1} + \frac{\alpha(\alpha+1) \gamma^2}{\beta(\beta+1) 2!} + \frac{\alpha(\alpha+1)(\alpha+2) \gamma^3}{\beta(\beta+1)(\beta+2) 3!} + \dots \quad (3.38)$$

The normalized average LCR given in (3.37) is an important new closed-form result for dual-diversity systems with unequal branch powers.

Following the same approach using r_1, r_2 as the auxiliary variables, the normalized average level crossing rate of the output signal envelope of three-branch MRC can be found as a single definite integral given as

$$\frac{N_R}{f_m} = \frac{\sqrt{\pi}}{6\sigma_1^2\sigma_2^2\sigma_3^2(\sigma_2^2 - \sigma_3^2)} \int_0^R g(x, R) dx \quad (3.39a)$$

with integrand

$$\begin{aligned} g(x, R) = & [(\sigma_1^2 - \sigma_2^2)x + \sigma_2^2 R]^{\frac{3}{2}} \exp \left\{ -\frac{R}{2\sigma_2^2} - \frac{x}{2\sigma_1^2} + \frac{x}{2\sigma_2^2} \right\} {}_1F_1 \left(1, \frac{5}{2}; -\frac{\sigma_1^2 - \sigma_2^2}{2\sigma_2^2\sigma_3^2}x - \frac{R}{2\sigma_3^2} \right) \\ & - [(\sigma_1^2 - \sigma_3^2)x + \sigma_3^2 R]^{\frac{3}{2}} \exp \left\{ -\frac{R}{2\sigma_3^2} - \frac{x}{2\sigma_1^2} + \frac{x}{2\sigma_3^2} \right\} {}_1F_1 \left(1, \frac{5}{2}; -\frac{\sigma_1^2 - \sigma_3^2}{2\sigma_2^2\sigma_3^2}x - \frac{R}{2\sigma_2^2} \right). \end{aligned} \quad (3.39b)$$

Similarly, the average LCR of four-branch MRC can be expressed as

$$\frac{N_R}{f_m} = \frac{\sqrt{\pi}}{12(\sigma_3^2 - \sigma_4^2)\sigma_1^2\sigma_2^2\sigma_3^2\sigma_4^2} \cdot \int_0^R \int_0^{R-x} h(x, y) dy dx \quad (3.40a)$$

where

$$\begin{aligned} h(x, y) = & \exp \left\{ -\frac{R}{2\sigma_3^2} - \frac{x}{2\sigma_1^2} + \frac{x}{2\sigma_3^2} - \frac{y}{2\sigma_2^2} + \frac{y}{2\sigma_3^2} \right\} [\sigma_3^2 R + (\sigma_1^2 - \sigma_3^2)x + (\sigma_2^2 - \sigma_3^2)y]^{\frac{3}{2}} \\ & \cdot {}_1F_1 \left(1, \frac{5}{2}; -\frac{R}{2\sigma_4^2} - \frac{\sigma_1^2 - \sigma_3^2}{2\sigma_3^2\sigma_4^2}x - \frac{\sigma_2^2 - \sigma_3^2}{2\sigma_3^2\sigma_4^2}y \right) - \exp \left\{ -\frac{R}{2\sigma_4^2} - \frac{x}{2\sigma_1^2} + \frac{x}{2\sigma_4^2} - \frac{y}{2\sigma_2^2} + \frac{y}{2\sigma_4^2} \right\} \\ & \cdot [\sigma_4^2 R + (\sigma_1^2 - \sigma_4^2)x + (\sigma_2^2 - \sigma_4^2)y]^{\frac{3}{2}} {}_1F_1 \left(1, \frac{5}{2}; -\frac{R}{2\sigma_3^2} - \frac{\sigma_1^2 - \sigma_4^2}{2\sigma_3^2\sigma_4^2}x - \frac{\sigma_2^2 - \sigma_4^2}{2\sigma_3^2\sigma_4^2}y \right). \end{aligned} \quad (3.40b)$$

Fig. 3.5 shows plots of the average LCR normalized to f_m versus the signal level $\rho = R/R_{rms}$, which has been normalized to its root-mean-square (rms) value after combining, R_{rms} ,

$$R_{rms} = \sqrt{8 \left(\sum_{i=1}^M \sigma_i^4 + \sum_{i=1}^M \sum_{j=i+1}^M \sigma_i^2 \sigma_j^2 \right)}. \quad (3.41)$$

The theoretical results (the lines) are in excellent agreement with the simulation (the points).

An exponentially decaying power delay profile model [1] is used in Fig. 3.5 where

$$\sigma_i^2 = \sigma_1^2 \exp(-\delta(i-1)), \quad i = 1, 2, \dots, M \quad (3.42)$$

with $\delta = 1$. The simulator of Young and Beaulieu [33] is used to generate the Rayleigh random variates. The double integral of (3.40) was easily computed in Matlab within 320 seconds for 26 values (points in the graph) using a 1.1 GHz AMD Athlon processor running Linux. It is clearly shown that diversity mitigates fading, as the average LCR becomes smaller when the diversity order increases. On the other hand, the MRC diversity system performance degrades in terms of reducing the LCR when the mean branch signal powers are unbalanced. Nonetheless, as pointed out by Barrow [34] and Halpern [35], the system performance is acceptable with reasonable imbalance of mean signal strengths of input branches. It is proved in [35] that significant diversity improvement can be observed for selection, equal gain and maximal ratio diversity combining for imbalance less than 6 dB. For MRC, our case show that imbalance as high as 10 dB (three-branch MRC in our case) can be tolerated.

3.4.2 The Average Fade Duration

The cumulative distribution function (CDF) of the combined signal of MRC can be obtained in closed-form by integrating the product of M -PDFs in (3.2a) as

$$F(R) = 1 - \sum_{i=1}^M \frac{\sigma_i^{2(M-1)} \exp\left\{-\frac{R}{2\sigma_i^2}\right\}}{\prod_{j=1, j \neq i}^M (\sigma_i^2 - \sigma_j^2)}. \quad (3.43)$$

Therefore, using (2.2), (3.43) and (3.37), one has the AFD of dual-branch MRC

$$T_R * f_m = \frac{3 \left(\sigma_1^2 - \sigma_2^2 - \sigma_1^2 e^{-\frac{R}{2\sigma_1^2}} - \sigma_2^2 e^{-\frac{R}{2\sigma_2^2}} \right)}{\sqrt{\pi} R^{\frac{3}{2}} \left[\frac{\sigma_1}{\sigma_2^2} e^{-\frac{R}{2\sigma_1^2}} {}_1F_1\left(1, \frac{5}{2}; -\frac{R}{2\sigma_2^2}\right) - \frac{\sigma_2}{\sigma_1^2} e^{-\frac{R}{2\sigma_2^2}} {}_1F_1\left(1, \frac{5}{2}; -\frac{R}{2\sigma_1^2}\right) \right]}. \quad (3.44)$$

Eqn. (3.44) is a new closed-form result for the AFD of dual-branch MRC diversity with unequal branch powers.

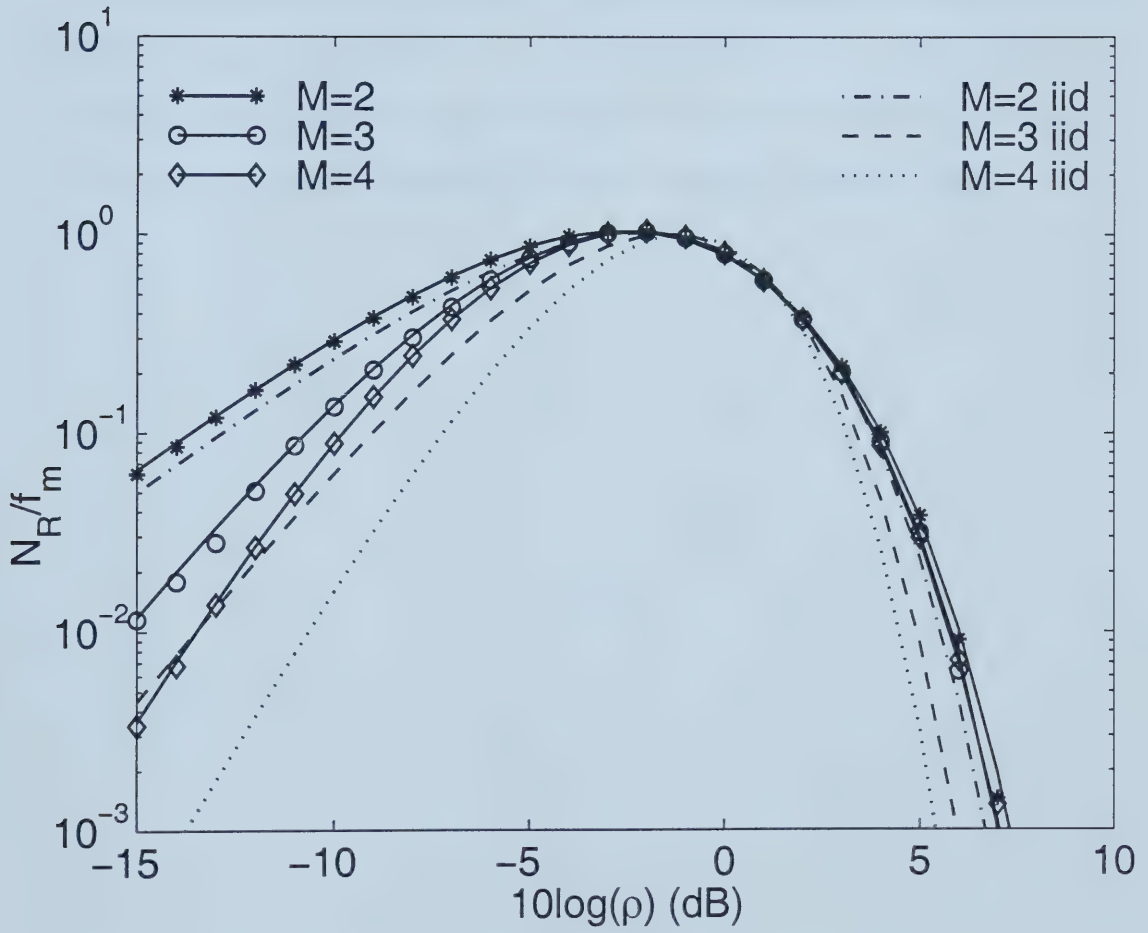


Figure 3.5. The average normalized LCR of MRC for branch signals with an exponentially decaying input signal power profile with decay factor 1.

Similarly, the AFD of three- and four-branch MRC can be found by combining (2.2) with (3.43) and (3.39) with (3.40), respectively. To the best of the author's knowledge, results (3.37) to (3.40) and (3.44) are new. Fig. 3.6 shows the normalized AFD of MRC as a function of the normalized envelope level $\rho = R/R_{rms}$. The lines are theoretical results and the points are simulation results. As expected, diversity improves the AFD as the signal spends more time around its rms value. However, curves for $M = 4$ show that an imbalance of branch powers degrades the benefit of diversity, especially at high signal levels.

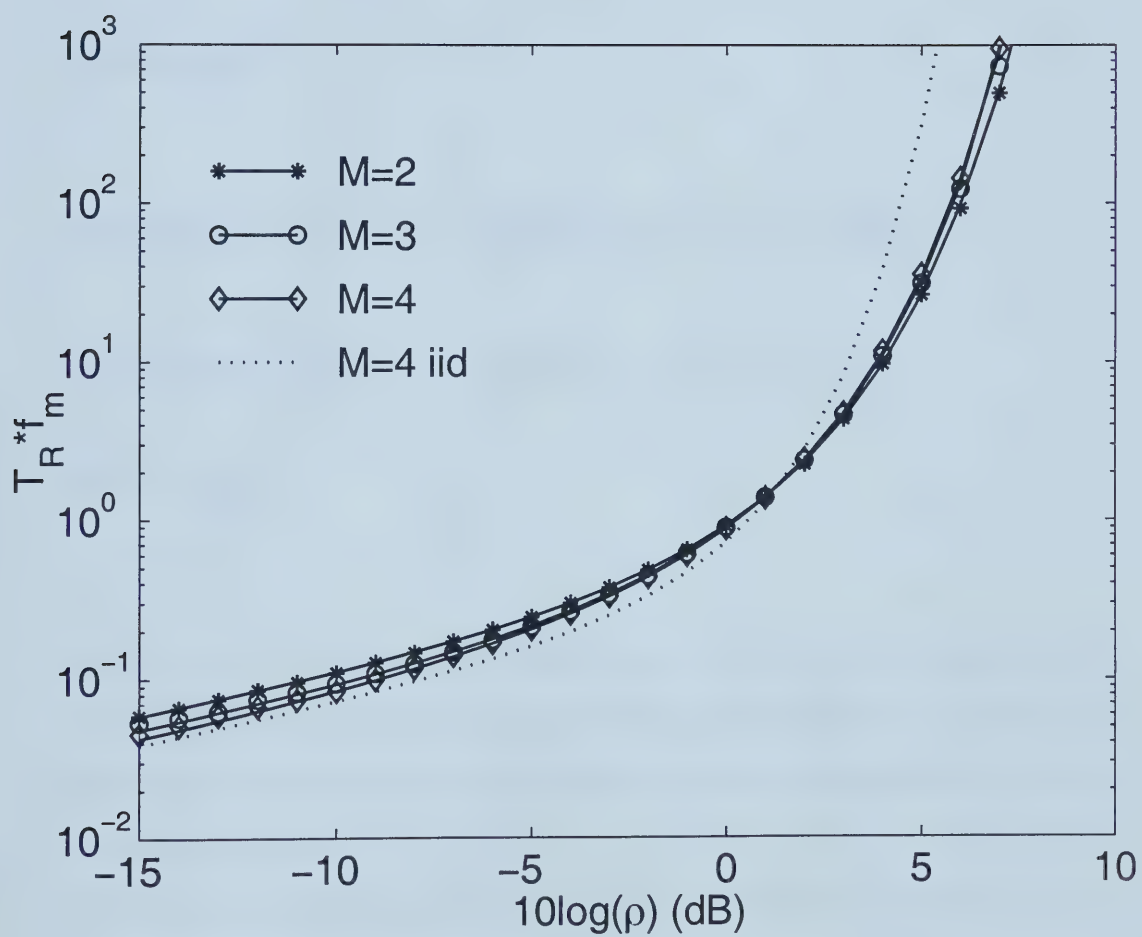


Figure 3.6. The normalized AFD of MRC for branch signals with an exponentially decaying input signal power profile with decay factor 1.

Chapter 4

Average Level Crossing Rate and Average Fade Duration of EGC Diversity

Equal gain combining is an appealing combining method. It provides performance similar to a maximal ratio combiner, but with considerably reduced complexity. In equal gain combining, all branches are cophased and summed, so the receiver does not need to track the branches constantly.

Previous work on the average level crossing rate and fade duration of EGC diversity systems can be found in [30], where the two parameters were obtained in closed-form for dual-branch EGC with correlated Rayleigh inputs. Lee proposed an approximation of the average level crossing rate and fade duration of an equal gain predetection system in [31], where he expressed the average LCR as the probability density function times a function of the direction of the motion. The branch signals are assumed to be partially correlated. More recently, Yacoub [29] studied the level crossing rate of EGC diversity with independent

and identically distributed Rayleigh fading branches, and he expressed the final result as an $(M - 1)$ -fold integral. In this chapter, we investigate the average level crossing rate and fade duration of an EGC diversity system for generalized fading models. An approximate Fourier series method is used to give a precise approximation for the LCR and AFD of the combined signal.

4.1 General Expressions for Level Crossing Rate and Fade Duration

In EGC, received signals are cophased before they are summed. The noiseless signal envelope r at the combiner output is as previously defined in (1.37)

$$r = \sum_{i=1}^M r_i. \quad (4.1)$$

The time derivative \dot{r} of the combiner output is

$$\dot{r} = \sum_{i=1}^M \dot{r}_i \quad (4.2)$$

where r_i and \dot{r}_i have the density defined in (3.2b) and (3.4), respectively. Since $\{r_i\}_{i=1}^M$ are independent, \dot{r} is Gaussian distributed with zero mean and variance

$$\dot{\sigma}^2 = \sum_{i=1}^M \dot{\sigma}_i^2 \quad (4.3)$$

where $\dot{\sigma}_i^2$ is given in (3.5). From (4.3), it is easy to see that $f(\dot{r}|\{r_i\}_{i=1}^M) = f(\dot{r})$. So \dot{r} and r are independent, which is different from the maximal ratio combining case. Therefore, in EGC diversity,

$$f(r, \dot{r}) = f(r) \cdot f(\dot{r}) \quad (4.4)$$

and the average level crossing rate of EGC diversity is given as

$$\begin{aligned} N_R &= \int_0^\infty \dot{r} f(R) f(\dot{r}) d\dot{r} \\ &= f(R) \cdot \sqrt{\frac{\sigma^2}{2\pi}}. \end{aligned} \quad (4.5)$$

Similarly, according to (2.2), the average fade duration can be expressed as

$$T_R = \frac{1 - F(R)}{N_R} \quad (4.6)$$

where $F(R) = P(r \geq R)$ is the complement of the CDF of the signal envelope at the output of the combiner. As long as we know the density and distribution of the signal envelope at the combiner output, we can use the PDF and CDF of r directly in (4.5) and (4.6) to get the average level crossing rate and average fade duration, respectively.

4.2 Obtaining the PDF of the Equal Gain Output Signal Envelope

It is proved in the previous section that the computation of the average level crossing rate and fade duration of a equal gain diversity system depends on finding the PDF and CDF of the combined signal envelope. Unfortunately, the distribution of the summation of M independent Rayleigh, Ricean or Nakagami random variables is not known in closed-form for M greater than two. In this chapter, we propose a precise approximation using the infinite series method introduced by Beaulieu in [20].

4.2.1 Ricean Fading

Let r be the sum of M independent Ricean RVs $\{r_i\}_{i=1}^M$ with the PDF given in (3.2b). It is shown in [20] that the PDF and CDF of r can be computed within a determined accuracy

as

$$f(r) = \lim_{T \rightarrow \infty} \frac{4}{T} \sum_{\substack{n=1 \\ n \text{ odd}}}^{\infty} A_n \cos \theta_n \quad (4.7a)$$

$$F(r) = P_r(R \geq r) \cong \frac{1}{2} + \frac{2}{\pi} \sum_{\substack{n=1 \\ n \text{ odd}}}^{\infty} \frac{A_n \sin(\theta_n)}{n} \quad (4.7b)$$

with

$$A_n = \prod_{i=1}^M A_{in} \quad (4.7c)$$

$$\theta_n = \sum_{i=1}^M \theta_{in} \quad (4.7d)$$

$$A_{in} = \sqrt{E^2[\cos(n\omega r_i)] + E^2[\sin(n\omega r_i)]} \quad (4.7e)$$

$$\begin{aligned} \theta_{in} &= \arctan \left(\frac{E[\sin(n\omega(r_i - \varepsilon))]}{E[\cos(n\omega(r_i - \varepsilon))]} \right) \\ &= \arctan \left(\frac{E[\sin(n\omega r_i)] \cos \varepsilon - E[\cos(n\omega r_i)] \sin \varepsilon}{E[\cos(n\omega r_i)] \cos \varepsilon + E[\sin(n\omega r_i)] \sin \varepsilon} \right) \end{aligned} \quad (4.7f)$$

where

$$\varepsilon = \frac{r}{M} \quad (4.7g)$$

and

$$\omega = \frac{2\pi}{T}. \quad (4.7h)$$

The parameter T controls the accuracy of the result [20].

4.2.1.1 Independent Ricean Fading Branches with Non-identical Powers

The aforementioned Beaulieu Series can be applied to the sum of any M independent random variable, even if they have non-identical means and variances. Define

$$\Phi_{R_i} = E[\cos(n\omega r_i)] \quad (4.8)$$

¹In this equation, θ_{in} must be chosen to be in the correct one of four quadrants.

and

$$\Phi_{I_i} = E[\sin(n\omega r_i)]. \quad (4.9)$$

It is obvious that Φ_{R_i} and Φ_{I_i} are important quantities in obtaining the PDF and CDF of r . Combining (4.8) and (4.9) with (4.7e) and (4.7f), one has that

$$A_{in} = \sqrt{\Phi_{R_i}^2 + \Phi_{I_i}^2} \quad (4.10)$$

and

$$\theta_{in} = \tan^{-1} \left\{ \frac{\Phi_{I_i} \cos\left(\frac{n\omega r}{M}\right) - \Phi_{R_i} \sin\left(\frac{n\omega r}{M}\right)}{\Phi_{R_i} \cos\left(\frac{n\omega r}{M}\right) + \Phi_{I_i} \sin\left(\frac{n\omega r}{M}\right)} \right\}. \quad (4.11)$$

For independent Ricean RVs $\{r_i\}_{i=1}^M$,

$$\begin{aligned} \Phi_{R_i} &= E[\cos(n\omega r_i)] \\ &= \int_0^\infty \frac{x}{\sigma_i^2} \exp\left(-\frac{s_i^2 + x^2}{2\sigma_i^2}\right) \cos(n\omega x) I_0\left(\frac{x s_i}{\sigma_i^2}\right) dx \\ &= \exp\left(-\frac{s_i^2}{2\sigma_i^2}\right) \int_0^\infty u \exp\left(-\frac{u^2}{2}\right) \cos(n\omega \sigma_i u) I_0\left(\frac{s_i u}{\sigma_i}\right) du. \end{aligned} \quad (4.12)$$

The above integral does not have a direct closed-form solution. If we express the modified Bessel function as a infinite series

$$I_0(z) = \sum_{k=0}^{\infty} \frac{1}{(k!)^2} \left(\frac{z}{2}\right)^{2k} \quad (|z| < \infty), \quad (4.13)$$

we have

$$\begin{aligned} \Phi_{R_i} &= \exp\left(-\frac{s_i}{2\sigma_i^2}\right) \sum_{k=0}^{\infty} \int_0^\infty \frac{(s_i u)^{2k} u}{(2\sigma_i)^{2k} (k!)^2} \exp\left(-\frac{u^2}{2}\right) \cos(n\omega \sigma_i u) du \\ &= \exp\left(-\frac{s_i}{2\sigma_i^2}\right) \sum_{k=0}^{\infty} \frac{s_i^{2k}}{(2\sigma_i^2)^k k!} {}_1F_1\left(k+1, \frac{1}{2}, -\frac{n^2 \omega^2 \sigma_i^2}{2}\right) \\ &= \exp\{-K_i\} \sum_{k=0}^{\infty} \frac{K_i^k}{k!} {}_1F_1\left(k+1, \frac{1}{2}, -\frac{n^2 \omega^2 \sigma_i^2}{2}\right) \end{aligned} \quad (4.14)$$

where $K_i = s_i^2/2\sigma_i^2$ is the Rice factor of each input branch, as previously.

Similarly, $E[\sin(n\omega r_i)]$ can be expressed as an infinite series as

$$\begin{aligned}
\Phi_{I_i} &= E[\sin(n\omega r_i)] \\
&= \exp\left(-\frac{s_i}{2\sigma_i^2}\right) \sum_{k=0}^{\infty} \int_0^{\infty} \frac{s_i^{2k} u^{2k+1}}{(2\sigma_i)^{2k} (k!)^2} \exp\left(-\frac{u^2}{2}\right) \sin(n\omega \sigma_i u) du \\
&= \frac{n\omega}{\sqrt{2\sigma_i^2}} \exp(-K_i) \sum_{k=0}^{\infty} \frac{\Gamma(k + \frac{3}{2})}{(k!)^2} K_i^k {}_1F_1\left(k + \frac{3}{2}, \frac{3}{2}, -\frac{n^2 \omega^2 \sigma_i^2}{2}\right).
\end{aligned} \tag{4.15}$$

Thus, to obtain the PDF and CDF of the sum of Ricean RVs, both ${}_1F_1(k, 1/2, -a)$ and ${}_1F_1(k + 3/2, 3/2, -a)$ where k is an integer are needed. It is shown in [36] that ${}_1F_1(k + 3/2, 3/2, -a)$ can be rewritten as a finite series given by

$${}_1F_1\left(k + \frac{3}{2}, \frac{3}{2}, -a\right) = e^{-a} \sum_{i=0}^k \frac{(-1)^i \binom{k}{i} 2^i a^i}{(2i+1)!!} \tag{4.16}$$

where $\binom{k}{i}$ is the binomial coefficient and

$$(2i+1)!! = (2i+1)(2i-1)\cdots 3 \cdot 1. \tag{4.17}$$

A more efficient way to compute this confluent hypergeometric function is to use a recursive method. For non negative integer k , define A_k as [37]

$$A_k = {}_1F_1\left(k + \frac{3}{2}, \frac{3}{2}, -a\right). \tag{4.18}$$

Then it is easy to prove that

$$A_0 = e^{-a} \tag{4.19}$$

and

$$A_1 = \frac{2}{3} \left(-a + \frac{3}{2}\right) e^{-a}. \tag{4.20}$$

For $k \geq 2$, A_k can be written as

$$A_k = \frac{1}{2k+1} [(-2a+4k-1)A_{k-1} + 2(1-k)A_{k-2}]. \tag{4.21}$$

The recursive expressions to compute ${}_1F_1(k, 1/2, -a)$ is shown in [36, Appendix B] for positive integer k . For $k \geq 2$,

$${}_1F_1\left(k, \frac{1}{2}, -a\right) = \frac{1}{k-1} \left[\left(-a + \frac{4k-5}{2}\right) {}_1F_1\left(k-1, \frac{1}{2}, -a\right) + \frac{3-2k}{2} {}_1F_1\left(k-2, \frac{1}{2}, -a\right) \right]. \quad (4.22)$$

It has been shown in [20] that for a small argument a ,

$${}_1F_1\left(1, \frac{1}{2}, -a\right) = e^{-a} - e^{-a} \sum_{i=0}^{\infty} \frac{a^i}{(2i-1)i!} \quad (4.23a)$$

is convenient for computation and for large and medium argument a ,

$${}_1F_1\left(1, \frac{1}{2}, -a\right) = \frac{-1}{2a} \left[1 + \frac{1 \cdot 3}{2a} + \frac{1 \cdot 3 \cdot 5}{(2a)^2} + \frac{1 \cdot 3 \cdot 5 \cdot 7}{(2a)^3} + \dots \right]. \quad (4.23b)$$

Furthermore,

$${}_1F_1\left(0, \frac{1}{2}, -a\right) = 1. \quad (4.24)$$

With (4.22), (4.23) and (4.24), the computation of the hypergeometric function ${}_1F_1(k, 1/2, -a)$ can be performed.

4.2.1.2 Independent Ricean Branches With Identical Signal Powers

When the input branches are independent and identically distributed, (4.7a) becomes

$$f(r) = \lim_{T \rightarrow \infty} \frac{4}{T} \sum_{\substack{n=1 \\ n \text{ odd}}}^{\infty} (A_{in})^M \cos(M\theta_{in}) \quad (4.25)$$

and (4.7b) becomes

$$F(r) = \frac{1}{2} + \frac{2}{\pi} \sum_{\substack{n=1 \\ n \text{ odd}}}^{\infty} \frac{A_{in}^M \sin(M\theta_{in})}{n} \quad (4.26)$$

where A_{in} and θ_{in} are independent of i and are given by (4.7e) and (4.7f), respectively.

4.2.1.3 Simulation and Numerical Computation

Combining (4.8) and (4.9) with (4.7a) to (4.7h) gives the PDF and CDF of the combiner output signal envelope r when operating on iid Ricean input branches. The average level crossing rate and fade duration can thus be computed within a determined accuracy. It is worthwhile to note that the selection of T in (4.25) is not critical [20], although more terms are needed for a given accuracy if it is chosen larger than the minimum value needed to obtain the given accuracy. The infinite series (4.25) and (4.26) converge faster for larger values of diversity order M . In general, increasing the number of terms improves the accuracy. At $M = 1$, signal level 5 dB, with $T = 3.56$, only 11 terms are needed for accuracy of 10^{-9} .

Fig. 4.1 shows both the theoretical results and simulated results for the average level crossing rate, normalized to the maximum Doppler frequency, of EGC in Ricean fading, as a function of the rms value of the output signal, which is given as

$$\begin{aligned} R_{rms} &= \sqrt{E[r^2]} \\ &= \sqrt{\frac{M\Omega}{1+K}} \sqrt{1+K + \frac{(M-1)\pi}{4} {}_1F_1^2\left(-\frac{1}{2}, 1, -K\right)}. \end{aligned} \quad (4.27)$$

A Rice factor $K = 7$ dB is used for these examples and five different branch orders are examined.

Fig. 4.2 shows theoretical values and simulated results for the average fade duration of EGC. The parameter T is chosen between 80 and 90 to generate these two plots, and typically 300 terms are required to reach the accuracy of 10^{-9} with the choice of $T = 98$. The agreement between simulation results and theoretical results is excellent in all cases. Previously, approximations to the average level crossing rate and average fade duration of EGC normalized to the rms value of one branch of the input signal for Rayleigh fading were given in [31]. Exact analytical expressions normalized to the rms value of one branch

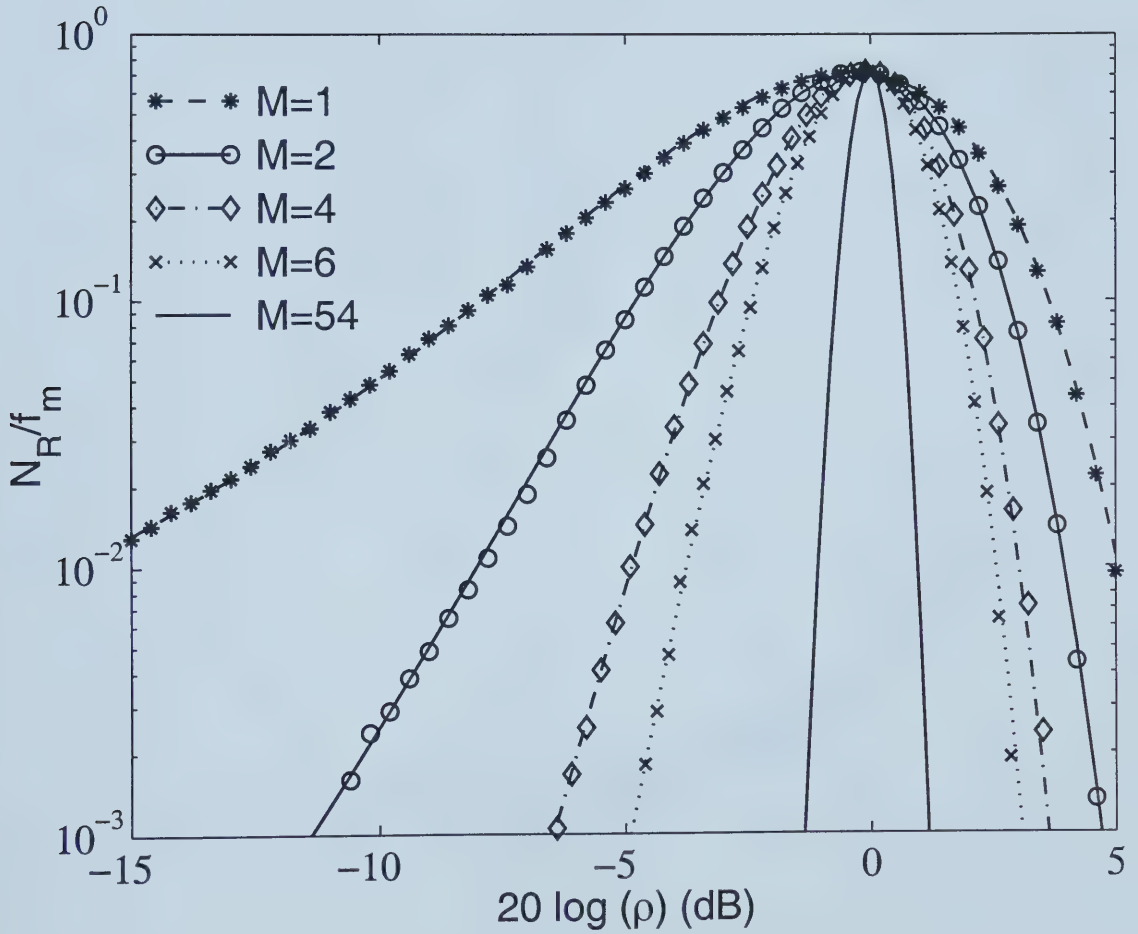


Figure 4.1. Average normalized level crossing rate of EGC operating on iid Ricean fading branches for different diversity orders with $K = 7$ dB.

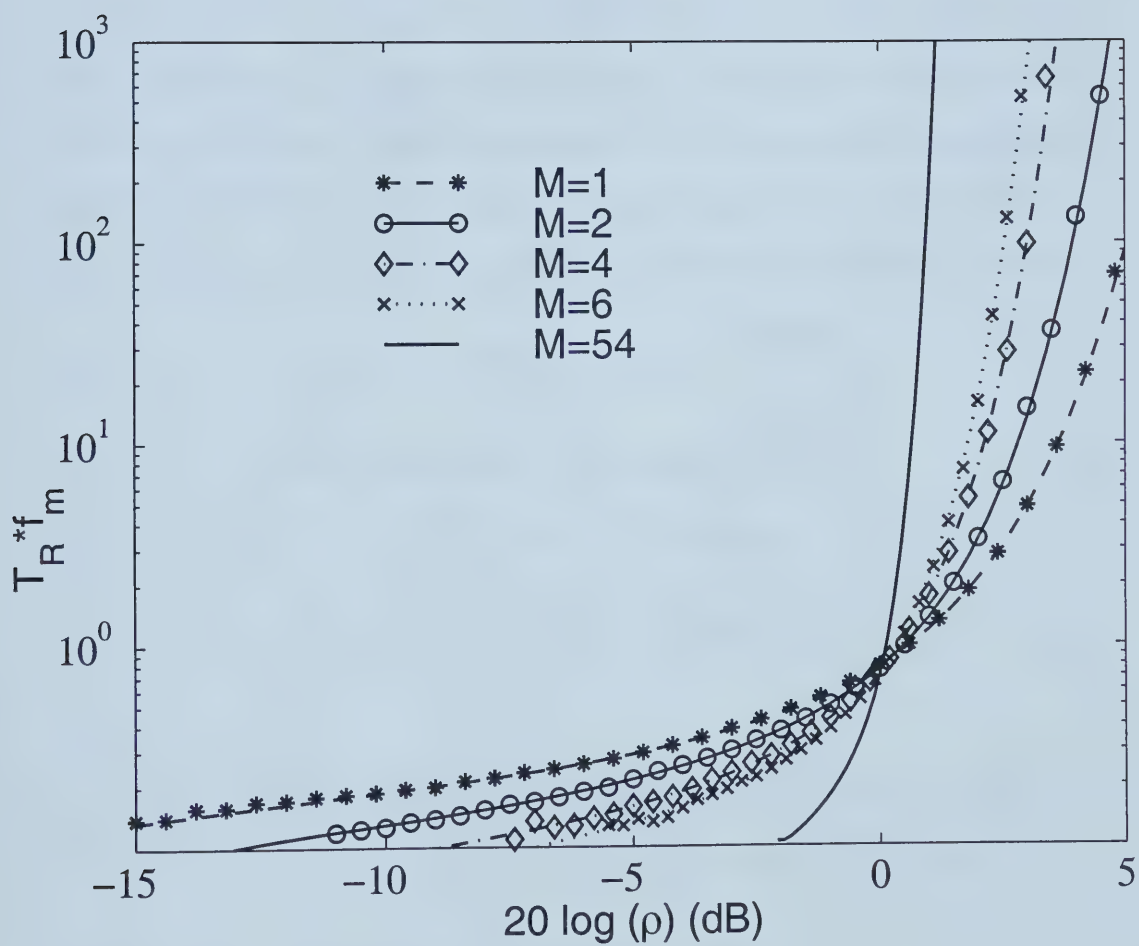


Figure 4.2. Average normalized fade duration of EGC operating on iid Ricean fading branches for different diversity orders with $K = 7$ dB.

of the input signal, given as M -fold iterated integrals were given in [29].

4.2.2 Rayleigh Fading

Similar procedures can be carried out to find the PDF and CDF of the equal gain combiner output signal envelope r , when the input branches are independent Rayleigh random variables at any time instant. Using the infinite series method, Beaulieu gave the expressions of the PDF and CDF of the sum of M Rayleigh random variables in [20]. With PDFs of input branches given in (3.2a), Φ_{R_i} and Φ_{I_i} , defined in (4.8) and (4.9) respectively, are given by

$$\Phi_{R_i} = E[\cos(n\omega r_i)] = {}_1F_1\left(1, \frac{1}{2}, -\frac{n^2\omega^2\sigma_i^2}{2}\right) \quad (4.28)$$

$$\Phi_{I_i} = E[\cos(n\omega r_i)] = \sqrt{\frac{\pi}{2}}n\omega\sigma_i \exp\left(-\frac{n^2\omega^2\sigma_i^2}{2}\right). \quad (4.29)$$

Combining (4.28) and (4.29) with (4.7e) and (4.7f), we have [20, eqn. 31]

$$A_{in} = \sqrt{\left[{}_1F_1\left(1, \frac{1}{2}, -\frac{n^2\omega^2\sigma_i^2}{2}\right)\right]^2 + \frac{\pi}{2}n^2\omega^2\sigma_i^2 \exp\left(-n^2\omega^2\sigma_i^2\right)} \quad (4.30)$$

and

$$\theta_{in} = \tan^{-1} \left\{ \frac{\sqrt{\frac{\pi}{2}}n\omega\sigma_i \exp\left(-\frac{n^2\omega^2\sigma_i^2}{2}\right) \cos\left(\frac{n\omega r}{M}\right) - {}_1F_1\left(1, \frac{1}{2}, -\frac{n^2\omega^2\sigma_i^2}{2}\right) \sin\left(\frac{n\omega r}{M}\right)}{{}_1F_1\left(1, \frac{1}{2}, -\frac{n^2\omega^2\sigma_i^2}{2}\right) \cos\left(\frac{n\omega r}{M}\right) + \sqrt{\frac{\pi}{2}}n\omega\sigma_i \exp\left(-\frac{n^2\omega^2\sigma_i^2}{2}\right) \sin\left(\frac{n\omega r}{M}\right)} \right\}. \quad (4.31)$$

Efficient ways to compute ${}_1F_1(1, \frac{1}{2}, -a)$ are given in (4.23).

4.2.3 Nakagami Fading

Closed-form solutions can also be found for Φ_{R_i} and Φ_{I_i} for Nakagami fading branches defined in (3.2c). Suppose the input Nakagami branches are independent and have distinct

Nakagami parameters m_i , as well as mean signal energies Ω_i . One has that [38, eqn. (77), p. 24, p. 80]

$$\Phi_{R_i} = {}_1F_1 \left(m_i, \frac{1}{2}; -\frac{n^2\omega^2\Omega_i}{4m_i} \right) \quad (4.32)$$

$$\Phi_{I_i} = {}_1F_1 \left(m_i + \frac{1}{2}, \frac{3}{2}; -\frac{n^2\omega^2\Omega_i}{4m_i} \right). \quad (4.33)$$

Therefore, combining (4.7e) and (4.7f) with (4.32) and (4.33) gives

$$\begin{aligned} A_{in} &= \sqrt{\Phi_{R_i}^2 + \Phi_{I_i}^2} \\ &= \sqrt{\left[{}_1F_1 \left(m_i, \frac{1}{2}; -\frac{n^2\omega^2\Omega_i}{4m_i} \right) \right]^2 + \left[{}_1F_1 \left(m_i + \frac{1}{2}, \frac{3}{2}; -\frac{n^2\omega^2\Omega_i}{4m_i} \right) \right]^2} \end{aligned} \quad (4.34)$$

and

$$\begin{aligned} \theta_{in} &= \tan^{-1} \left\{ \frac{\Phi_{I_i} \cos \left(\frac{n\omega r}{M} \right) - \Phi_{R_i} \sin \left(\frac{n\omega r}{M} \right)}{\Phi_{R_i} \cos \left(\frac{n\omega r}{M} \right) + \Phi_{I_i} \sin \left(\frac{n\omega r}{M} \right)} \right\} \\ &= \tan^{-1} \left\{ \frac{{}_1F_1 \left(m_i + \frac{1}{2}, \frac{3}{2}; -\frac{n^2\omega^2\Omega_i}{4m_i} \right) \cos \left(\frac{n\omega r}{M} \right) - {}_1F_1 \left(m_i, \frac{1}{2}; -\frac{n^2\omega^2\Omega_i}{4m_i} \right) \sin \left(\frac{n\omega r}{M} \right)}{{}_1F_1 \left(m_i, \frac{1}{2}; -\frac{n^2\omega^2\Omega_i}{4m_i} \right) \cos \left(\frac{n\omega r}{M} \right) + {}_1F_1 \left(m_i + \frac{1}{2}, \frac{3}{2}; -\frac{n^2\omega^2\Omega_i}{4m_i} \right) \sin \left(\frac{n\omega r}{M} \right)} \right\}. \end{aligned} \quad (4.35)$$

To the best of the author's knowledge, the application of the precise infinite series to computing the average level crossing rate and the average fade duration is new.

Chapter 5

Average Level Crossing Rate and Average Fade Duration of SC Diversity

A selection combiner picks the branch with the largest SNR and is perhaps one of the simplest micro-diversity combining methods [15]. Despite the importance of level crossing rate and fade duration in fading channel communication system design, only the LCR and AFD of two-branch SC diversity are known and only for the case of equal branch powers [30]. As pointed out in Section 3.4, it is very difficult to have uniform signal energy on all diversity branches in practical systems. It is shown in [34] that having unbalanced mean branch signal powers degrades diversity system performance for diversity combiners. However, the system performance is acceptable when the imbalance is reasonable. In this chapter, we derive simple closed-form solutions for the average level crossing rate and average fade duration of a SC output signal envelope, assuming that the input signals are independent with unequal average powers. The results are valid for arbitrary diversity orders, and are obtained for Rayleigh, Ricean and Nakagami fading distributions. To the best of the author's knowledge, these results are new.

5.1 Average Level Crossing Rate

It has been shown in Chapter 2 that for single branch reception, the time derivative of the branch signal, \dot{r}_i , is a zero-mean Gaussian process independent of r_i for the Rayleigh, Ricean and Nakagami fading models.

Given M receiving branches and assuming the noise powers of the input branches are the same, we can write the selection combiner output signal envelope r simply as the largest input signal envelope, *i.e.*,

$$r = \max(r_1, r_2, \dots, r_M) \quad (5.1)$$

and

$$\dot{r} = \dot{r}_i, \quad \text{if } r_i = \max(\{r_k\}_{k=1}^M). \quad (5.2)$$

To obtain the JPDP for calculating the average level crossing rate, we consider the joint CDF of r and \dot{r} of the SC output.

Note that the events

$$\mathcal{A}_i = \{r_i \text{ is the max of } \{r_k\}_{k=1}^M\}, \quad i = 1, 2, \dots, M \quad (5.3)$$

form a partition. Thus, the JCDF of r and \dot{r} can be expressed as a summation

$$F(r, \dot{r}) = F(r, \dot{r} | \mathcal{A}_1)P(\mathcal{A}_1) + \dots + F(r, \dot{r} | \mathcal{A}_M)P(\mathcal{A}_M) \quad (5.4)$$

where $P(\mathcal{A}_i)$ is the probability of event \mathcal{A}_i and

$$\begin{aligned} F(r, \dot{r} | \mathcal{A}_i) &= F(r, \dot{r} | r_i \text{ is max of } \{r_k\}_{k=1}^M) \\ &= P(r_i < r, \dot{r}_i < \dot{r} | r_i \text{ max}). \end{aligned} \quad (5.5)$$

Since \dot{r}_i is independent of r_i for all i , the above conditional JCDF can be expressed as

$$F(r, \dot{r} | \mathcal{A}_i) = P(r_i < r | r_i \text{ max})P(\dot{r}_i < \dot{r} | r_i \text{ max}) = \frac{P(r_i < r, r_i \text{ max})}{P(\mathcal{A}_i)}P(\dot{r}_i < \dot{r}). \quad (5.6)$$

Denote the probability of the event $\{r_i \text{ max and } r_i < r\}$ as $P_i(r)$, which can be written as

$$P_i(r) = \int_0^r f_{r_i}(x) \prod_{k=1, k \neq i}^M F_{r_k}(x) dx. \quad (5.7)$$

Now combining (5.6) with (5.4), the joint CDF of r and \dot{r} is given by

$$F(r, \dot{r}) = \sum_{i=1}^M P_i(r) \cdot F_{\dot{r}_i}(\dot{r}). \quad (5.8)$$

Differentiating (5.8) with respect to r and \dot{r} , the JPDP of r and \dot{r} for selection diversity is

$$f(r, \dot{r}) = \sum_{i=1}^M f_{\dot{r}_i}(\dot{r}) \cdot f_{r_i}(r) \prod_{k=1, k \neq i}^M F_{r_k}(r). \quad (5.9)$$

From (5.9), the PDF of r can be obtained as

$$f(r) = \sum_{i=1}^M f_{r_i}(r) \prod_{k=1, k \neq i}^M F_{r_k}(r). \quad (5.10)$$

The PDF of \dot{r} is obtained by setting $r = \infty$ in (5.7) and (5.8) and then differentiating to give

$$\begin{aligned} f(\dot{r}) &= \sum_{i=1}^M P_i(\infty) \cdot f_{\dot{r}_i}(\dot{r}) \\ &= \sum_{i=1}^M P(\mathcal{A}_i) \cdot f_{\dot{r}_i}(\dot{r}). \end{aligned} \quad (5.11)$$

We observe that (5.10) specializes to the result given in [17, eqn. 10-17] for the Rayleigh case. Interestingly, one can prove using (5.10) and (5.11) with (5.9) that the SC output signal envelope r and its time derivative \dot{r} are not independent, though r_i and \dot{r}_i are independent for the individual branches. Physically, a large branch power implies a larger derivative (scaling). Thus, after combining, the magnitudes of r and \dot{r} are correlated. This effect is absent when the branch powers are equal. Finally, the average level crossing rate of the selection combiner output signal envelope can be found by combining (2.1), (2.6), (2.13) and (5.9) to give

$$N_R = \sum_{i=1}^M \sqrt{\frac{\dot{\sigma}_{\dot{r}_i}^2}{2\pi}} f_{r_i}(r) \prod_{k=1, k \neq i}^M F_{r_k}(r). \quad (5.12)$$

Result (5.12) applies to any fading model of SC so long as the envelope and its derivative for all the of individual branches are independent. Normalizing the level crossing rate by the maximum Doppler frequency, the results for Rayleigh, Ricean and Nakagami fading models are, respectively,

$$\frac{N_R}{f_m \text{ Rayleigh}} = \sqrt{\pi} \sum_{k=1}^M \frac{R}{\sigma_k} \exp\left(-\frac{R^2}{2\sigma_k^2}\right) \prod_{j=1, j \neq k}^M \left(1 - \exp\left(-\frac{R^2}{2\sigma_j^2}\right)\right) \quad (5.13a)$$

$$\frac{N_R}{f_m \text{ Ricean}} = \sqrt{\pi} \sum_{k=1}^M \frac{R}{\sigma_k} \exp\left(-\frac{R^2}{2\sigma_k^2}\right) I_0\left(\frac{R s_k}{\sigma_k^2}\right) \prod_{j=1, j \neq k}^M \left(1 - Q_1\left(\frac{s_j}{\sigma_j}, \frac{R}{\sigma_j}\right)\right) \quad (5.13b)$$

$$\frac{N_R}{f_m \text{ Nakagami}} = \sqrt{2\pi} \frac{m^{m-1/2} R^{2m-1}}{\Gamma^M(m)} \sum_{k=1}^M \frac{1}{\Omega_k^{m-1/2}} \exp\left(-\frac{mR^2}{\Omega_k}\right) \prod_{j=1, j \neq k}^M \Gamma\left(m, \frac{mR^2}{\Omega_j}\right). \quad (5.13c)$$

Result (5.13) can be specialized to the independent and identically distributed (iid) input cases as

$$\frac{N_R}{f_m \text{ Rayleigh}} = \sqrt{\pi} M \frac{R}{\sigma} \exp\left(-\frac{R^2}{2\sigma^2}\right) \left(1 - \exp\left(-\frac{R^2}{2\sigma^2}\right)\right)^{M-1} \quad (5.14a)$$

$$\frac{N_R}{f_m \text{ Ricean}} = \sqrt{\pi} M \frac{R}{\sigma} \exp\left(-\frac{R^2}{2\sigma^2}\right) I_0\left(\frac{R s}{\sigma^2}\right) \left(1 - Q_1\left(\frac{s}{\sigma}, \frac{R}{\sigma}\right)\right)^{M-1} \quad (5.14b)$$

$$\frac{N_R}{f_m \text{ Nakagami}} = \sqrt{2\pi} M \frac{m^{m-1/2} R^{2m-1} \Gamma\left(m, \frac{mR^2}{\Omega}\right)}{\Omega^{m-1/2} \Gamma^M(m)} \exp\left(-\frac{mR^2}{\Omega}\right). \quad (5.14c)$$

To the best of the authors' knowledge, results (5.12), (5.13) and (5.14) are new. Fig. 5.1 shows plots of N_R/f_m versus the normalized signal level $\rho = R/R_{rms}$ for different diversity orders in Rayleigh fading. The root-mean-square value of the combiner signal envelope can be obtained from (5.10) as

$$R_{rms} = \sqrt{E(r^2)} = \sqrt{2 \sum_{i=1}^M h_i} \quad (5.15)$$

where

$$h_1 = \sum_{k=1}^M \sigma_k^2 \quad (5.16)$$

$$h_2 = - \sum_{k_1=1}^{M-1} \sum_{k_2=k_1+1}^M \frac{\sigma_{k_1}^2 \sigma_{k_2}^2}{\sigma_{k_1}^2 + \sigma_{k_2}^2} \quad (5.17)$$

and

$$h_i = (-1)^{i+1} \cdot \sum_{k_1=1}^{M-i+1} \sum_{k_2=k_1+1}^{M-i+2} \cdots \sum_{k_i=k_{i-1}+1}^M \frac{\sigma_{k_1}^2 \sigma_{k_2}^2 \cdots \sigma_{k_i}^2}{\sigma_{k_1}^2 \sigma_{k_2}^2 \cdots \sigma_{k_{i-1}}^2 + \sigma_{k_1}^2 \sigma_{k_3}^2 \cdots \sigma_{k_i}^2 + \cdots + \sigma_{k_2}^2 \sigma_{k_3}^2 \cdots \sigma_{k_{i-1}}^2 \sigma_{k_i}^2}. \quad (5.18)$$

An exponentially decaying branch power delay profile model [1] is used in Fig. 5.1 where $\sigma_i^2 = \sigma_1^2 \exp(-\delta(i-1))$, $i = 1, 2, \dots, M$ with $\delta = 0.25$. Simulation results (the points) are also shown and they are in excellent agreement with the theoretical curves (the lines). All simulation results were obtained using the inverse fast Fourier transform method [33] for generating time-correlated Rayleigh random variates. The results are compared with the average LCR in iid Rayleigh fading models. As expected, diversity mitigates the effect of fading, which is manifested in Fig. 5.1 in that the average LCR becomes smaller and smaller as the diversity order increases whenever the combiner output signal envelope level is below or above its rms value. It is clearly seen in the figure that as the diversity order increases, the average level crossing rate normalized to the rms value and the maximum Doppler frequency bends around $R = R_{rms}$. On the other hand, curves for $M = 6$ show that non-uniform distribution of diversity branch powers degrades the performance of diversity when compared with iid inputs. The larger the imbalance between the input branches, the larger the level crossing rate and the smaller the improvement gained from using diversity in the sense of reducing fading. Using more diversity branches will not bring much improvement in terms of LCR when the unbalance of signal powers is large, as manifested in Fig. 5.1 where the branch signal power decays exponentially and $M = 15$.

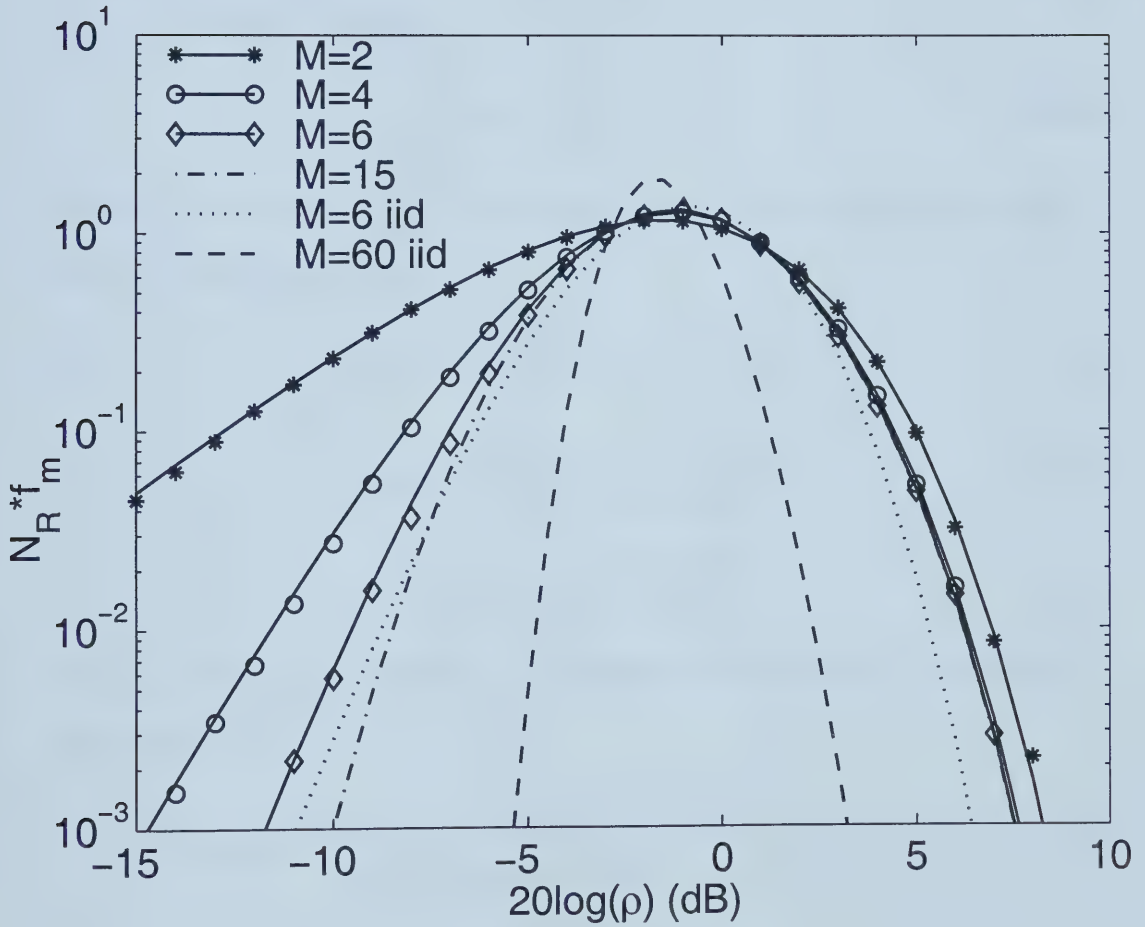


Figure 5.1. Average normalized level crossing rate of SC for different diversity orders with exponentially decaying mean branch signal power profile with decay factor 0.25.

5.2 Average Fade Duration

The average fade duration of the output of a selection combiner is obtained by combining (2.2) and (5.13). The cumulative distribution functions of the SC output signal envelope of various fading models are found as

$$F(r) = \prod_{i=1}^M F_{r_i}(r). \quad (5.19)$$

Therefore, the CDFs of the selection combiner output signal envelope of the Rayleigh, Ricean and Nakagami models are

$$F_{\text{Rayleigh}}(r) = \prod_{i=1}^M \left(1 - \exp\left(-\frac{r^2}{2\sigma_i^2}\right) \right) \quad (5.20a)$$

$$F_{\text{Ricean}}(r) = \prod_{i=1}^M \left(1 - Q_1\left(\frac{s_i}{\sigma_i}, \frac{r}{\sigma_i}\right) \right) \quad (5.20b)$$

$$F_{\text{Nakagami}}(r) = \prod_{i=1}^M \frac{\Gamma\left(m, \frac{mr^2}{\Omega_i}\right)}{\Gamma(m)} \quad (5.20c)$$

Thus the AFD of SC, normalized to the maximum Doppler frequency in non-identical fading is given by

$$T_R * f_{m\text{Rayleigh}} = \frac{\prod_{k=1}^M \left(1 - \exp\left(-\frac{R^2}{2\sigma_k^2}\right) \right)}{\sqrt{\pi} \sum_{k=1}^M \frac{R}{\sigma_k} \exp\left(-\frac{R^2}{2\sigma_k^2}\right) \prod_{j=1, j \neq k}^M \left(1 - \exp\left(-\frac{R^2}{2\sigma_j^2}\right) \right)} \quad (5.21a)$$

$$T_R * f_{m\text{Ricean}} = \frac{\prod_{k=1}^M \left(1 - Q_1\left(\frac{s_k}{\sigma_k}, \frac{R}{\sigma_k}\right) \right)}{\sqrt{\pi} \sum_{k=1}^M \frac{R}{\sigma_k} \exp\left(-\frac{R^2}{2\sigma_k^2}\right) I_0\left(\frac{Rs_k}{\sigma_k^2}\right) \prod_{j=1, j \neq k}^M \left(1 - Q_1\left(\frac{s_j}{\sigma_j}, \frac{R}{\sigma_j}\right) \right)} \quad (5.21b)$$

$$T_R * f_{m\text{Nakagami}} = \frac{\prod_{k=1}^M \Gamma\left(m, \frac{mR^2}{\Omega_k}\right)}{\sqrt{2\pi} m^{m-1/2} R^{2m-1} \sum_{k=1}^M \frac{1}{\Omega_k^{m-1/2}} \exp\left(-\frac{mR^2}{\Omega_k}\right) \prod_{j=1, j \neq k}^M \Gamma\left(m, \frac{mR^2}{\Omega_j}\right)}. \quad (5.21c)$$

Result (5.21) can be specialized to the iid model by setting the signal powers equal, giving

$$T_R * f_{m\text{Rayleigh}} = \frac{\sigma \left(\exp \left(\frac{R^2}{2\sigma^2} \right) - 1 \right)}{\sqrt{\pi}MR} \quad (5.22a)$$

$$T_R * f_{m\text{Ricean}} = \frac{\sigma \exp \left(\frac{R^2}{2\sigma^2} \right) \left(1 - Q_1 \left(\frac{s}{\sigma}, \frac{R}{\sigma} \right) \right)}{\sqrt{\pi}MR I_0 \left(\frac{R_s}{\sigma^2} \right)} \quad (5.22b)$$

$$T_R * f_{m\text{Nakagami}} = \frac{\Omega^{m-1/2} \exp \left(\frac{mR^2}{\Omega} \right) \Gamma \left(m, \frac{mR^2}{\Omega} \right)}{\sqrt{2\pi}Mm^{m-1/2}R^{2m-1}}. \quad (5.22c)$$

To the best of the author's knowledge, results (5.21) and (5.22) are new. Fig. 5.2 shows the normalized AFD as a function of the normalized envelope level ρ , where $\rho = R/R_{rms}$. Again, simulation results are in excellent agreement with theoretical results. Corresponding to the behaviour previously seen in Fig. 5.1, the fade duration at signal levels below the rms level decreases as the diversity order increases and the duration at levels above the rms level increases, as the signal spends more time around its rms value. Comparing the results of non-identical fading with the iid model for $M = 6$, it is clearly seen that having unequal diversity branch signal powers degrades the performance of diversity, and the degradation is more severe when the normalized signal level is large.

5.3 Discussion of Correlated Inputs

Since (5.8) is also valid when the input signals to the SC are correlated, it is straightforward to see that the average LCR of SC operating on correlated branches can be obtained if the quantities $\{P_i(r)\}_{i=1}^M$ are known. The result is written directly from (5.8) and (2.1) as

$$N_{R\text{correlated}} = \sum_{i=1}^M P'_i(r) \sqrt{\frac{\dot{\sigma}_{r_i}^2}{2\pi}} \quad (5.23)$$

where $P'_i(r)$ is the derivative of $P_i(r)$ with respect to r . Then (5.23) with (2.2) gives the average fade duration.

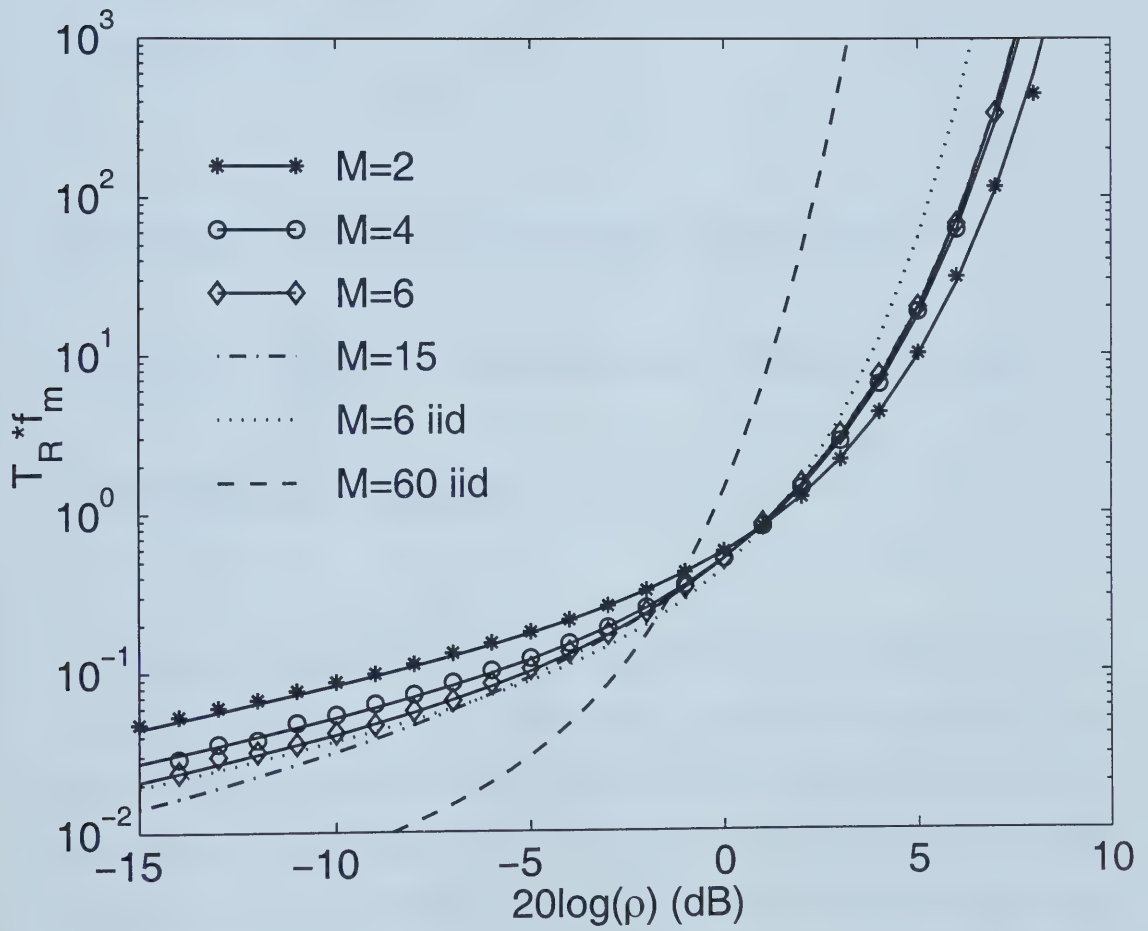


Figure 5.2. Average normalized fade duration of SC for different diversity orders with exponentially decaying mean branch signal power profile with decay factor 0.25.

Chapter 6

Average Level Crossing Rate and Average Fade Duration of Diversity in Correlated Fading

So far we have discussed the level crossing rate problem in diversity systems where the input branches of a diversity combiner are assumed to experience independent fading. However, in practical communication systems, the branches are often correlated [18], [39], [40], such as is the case for antennae with close spacing in space diversity, insufficient frequency spacing due to frequency allocation restrictions in frequency diversity, inadequate delay due to storage or delay limitations in time diversity, etc. In space diversity, a complete decorrelation of the diversity branches at a base station may require at least 50 wavelengths of the transmitted signal. Measured data show that correlation between adjacent branches at the base station is typically 0.7 or higher due to the space limitation. Compact receiver design may also imply highly correlated antennae in a portable receiver. Therefore, it is of great interest for researchers to investigate diversity systems with correlated receiving

branches.

Since the achievable diversity gain is strictly related to the degree of statistical correlation among the fading of the branches [40], one can expect that branch correlation degrades diversity system performance and reduces the effectiveness of the diversity in mitigating fading. However, it was proved in [18] and [41] that a large portion of the diversity effectiveness can be retained even when significant correlation exists. This is due to the fact that deep fades, usually considered as rare events, do not occur more often at inputs simply because of the high cross-correlation of the branches. Feeney and Adachi [41] investigated the average level crossing rate and fade duration of two-branch diversity systems in correlated fading. They showed with experimental data that even with high branch correlation, the maximal ratio diversity still significantly reduces the average level crossing rate, as the average fade duration changes little with correlation increase. Their experiments further proved the well known fact that the advantage of a two-branch diversity system can still be obtained for a cross-correlation as large as 0.7.

In this chapter, we first present a general statement about performance analysis of a maximal ratio diversity system with correlated input branches. Then we apply the conclusion to obtaining the average level crossing rate and fade duration for MRC operating on correlated Rayleigh fading branches. To the best of the author's knowledge, these results are new.

6.1 Optimal Maximal Ratio Combining with Correlated Diversity Branches

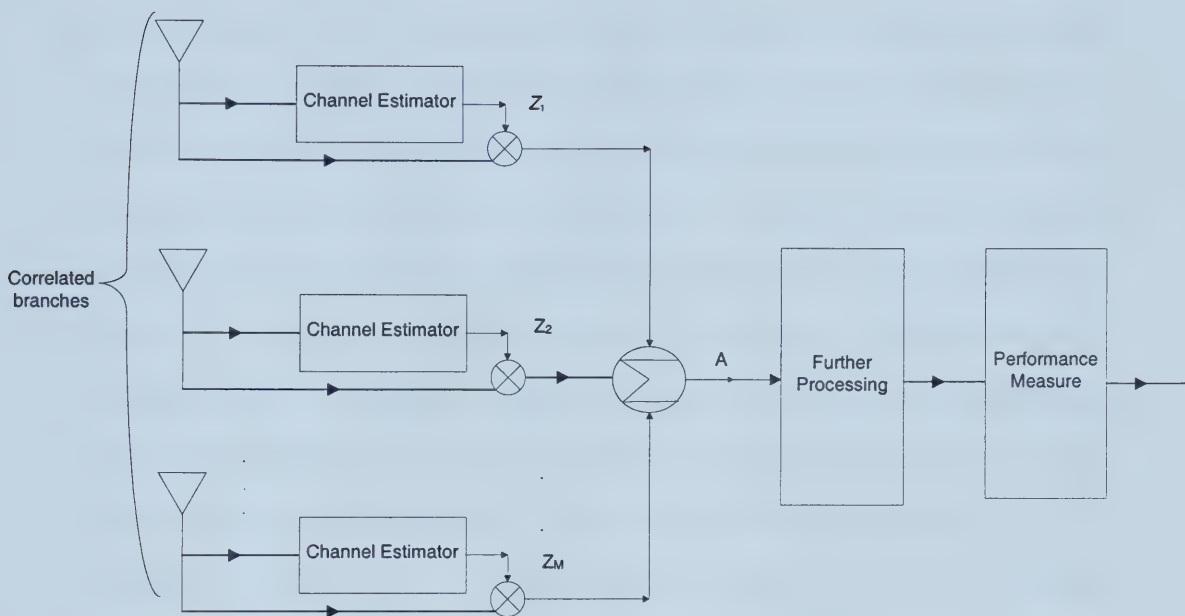
Maximal ratio combining is the optimum theoretical diversity combining method for branch signals having an arbitrary signal amplitude fading distribution [15]. Much recent work has examined various performances of MRC in additive white Gaussian noise (AWGN) for cases where the diversity branches are correlated, for example, outage probabilities [40] and symbol error rates [42], [39].

In this section, we prove the following two facts which provide insight into MRC as well as being useful canonical tools for determining various performance measures of MRC operating with correlated branch signals in Rayleigh fading:

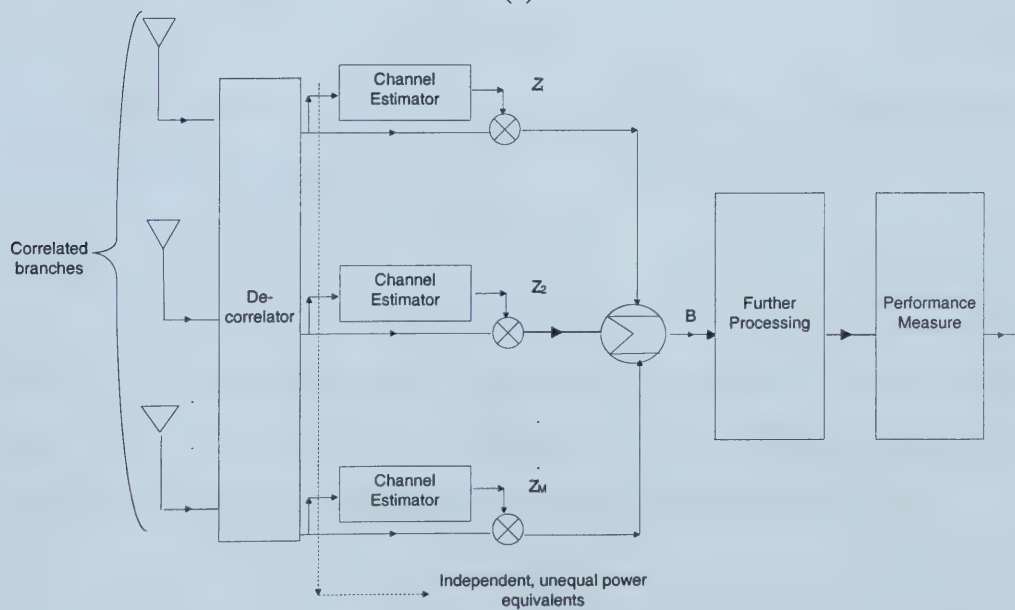
Fact 1: Any performance measure of a MRC diversity system operating with correlated input branch signals in AWGN is identical to the performance of an equivalent MRC diversity system operating with uncorrelated (and, hence, independent) input branch signals.

Fact 2: Any performance measure of a MRC diversity system operating with correlated signals in AWGN and branch weights chosen according to the signal amplitude-to-noise power ratios of the *correlated* branches is identical to the performance measure of a MRC diversity system operating with optimally decorrelated (and, hence, independent) branch signals and weights chosen according to the uncorrelated branch signal amplitude-to-noise power ratios.

Fig. 6.1 clarifies the propositions of Fact 1 and Fact 2. Fact 1 states that the performance of a MRC diversity system operating with correlated input signals can always be expressed as the performance of an equivalent MRC diversity system operating with appropriately determined independent input signals, regardless of the performance measure. Fact 2 states



(a)



(b)

Figure 6.1. Coherent maximal ratio combining operating on correlated inputs, (a) without decorrelation (b) with decorrelation.

that optimal performance is achieved without decorrelating the correlated input signals, weighting the input branch signals as though they were independent. This is a significant insight and powerful result that leads to savings in complexity and cost in receiver designs. Recent literature seems to indicate that this point is not well understood. For example, [43] examines the two-dimensional special case of Fact 1 but has no discussion of the optimality of the system, as established in Fact 2 here; reference [40] points out that MRC operating on independent branch input signals is optimal, but makes no statement about the optimality of MRC when operating on correlated branches. The proofs follow in the next paragraph.

Proof: Using vector notation in (3.1), let \mathbf{s} , \mathbf{z} and \mathbf{n} be the column vectors of M complex Gaussian random variables, corresponding to the received signals, branch inputs and additive noises at any time t , respectively. Then we have $\mathbf{z} = [z_1 \ z_2 \ \dots \ z_M]^T$ and

$$\mathbf{s} = \mathbf{z} + \mathbf{n}. \quad (6.1)$$

We assume the noise powers on all input branches are the same and that they are independent of the signals, which gives

$$E[\mathbf{z}\mathbf{n}^H] = \mathbf{0} \quad (6.2)$$

$$N = E[\mathbf{n}\mathbf{n}^H] = N_0 I \quad (6.3)$$

where $\{\cdot\}^H$ is the conjugate transpose, N is the correlation matrix of the Gaussian noise, $E[n_i n_i^*] = N_0$, $i = 1, 2, \dots, M$ is the noise power of one branch, and I is the identity matrix. The signal-to-noise power ratio (SNR) of each channel is given by [8, eqn. 5.2-1]

$$\gamma_i = \frac{r_i^2}{2N_0}. \quad (6.4)$$

Thus, the noiseless MRC combiner output signal envelope r [8, eqn. 5.2-9], as well as the output SNR γ , can be written in terms of the Euclidean norm of the vector \mathbf{z} ,

$$r = \frac{\sum_{i=1}^M r_i^2}{N_0} = \frac{\mathbf{z}^H \mathbf{z}}{N_0} = \frac{\|\mathbf{z}\|^2}{N_0} \quad (6.5)$$

$$\gamma = \sum_{i=1}^M \gamma_i = \frac{\mathbf{z}^H \mathbf{z}}{2N_0} = \frac{\|\mathbf{z}\|^2}{2N_0}. \quad (6.6)$$

Suppose the input branches $\{z_i(t)\}_{i=1}^M$ are correlated. The correlation matrix

$$R = E[\mathbf{z}\mathbf{z}^H] \quad (6.7)$$

of the complex Gaussian vector \mathbf{z} is Hermitian. Therefore, all the eigenvalues $\{\lambda_i\}_{i=1}^M$ of R are real, and R has a complete set of orthonormal eigenvectors $\{\mathbf{q}_i\}_{i=1}^M$. Furthermore, R is unitarily diagonalizable [44]. Denote matrix Q as the complete set of orthonormal eigenvectors of R ,

$$Q = [\mathbf{q}_1 \quad \mathbf{q}_2 \quad \dots \quad \mathbf{q}_M]. \quad (6.8)$$

It can be proved that Q is unitary and thus, R can be diagonalized by Q , which gives

$$R = Q\Lambda Q^H \quad (6.9)$$

with $\Lambda = \text{diag}(\lambda_1 \quad \lambda_2 \quad \dots \quad \lambda_M)$. If we apply this unitary transformation (6.8) on the received signals \mathbf{s} before combining, we obtain a new vector $\hat{\mathbf{s}} = Q^H \mathbf{s}$, which is the sum of uncorrelated, hence independent signals and additive noise, given by

$$\hat{\mathbf{s}} = \hat{\mathbf{z}} + \hat{\mathbf{n}} \quad (6.10)$$

and

$$\hat{R} = E[\hat{\mathbf{z}}\hat{\mathbf{z}}^H] = \Lambda. \quad (6.11)$$

Furthermore, it is easy to see that the unitary transformation does not change the correlation matrix of the noise, and the noise is still independent of the signals. One has

$$E[\hat{\mathbf{z}}\hat{\mathbf{n}}^H] = Q^H E[\mathbf{z}\mathbf{n}^H]Q = \mathbf{0} \quad (6.12)$$

and

$$\hat{N} = E[\hat{\mathbf{n}}\hat{\mathbf{n}}^H] = Q^H E[\mathbf{n}\mathbf{n}^H]Q = Q^H N_0 I Q = N_0 I = N. \quad (6.13)$$

Then, after the transformation, the combiner output signal envelope \hat{r} and SNR $\hat{\gamma}$ is, respectively,

$$\hat{r} = \frac{\hat{\mathbf{z}}^H \hat{\mathbf{z}}}{\hat{N}_0} = \frac{\mathbf{z}^H \mathbf{Q} \mathbf{Q}^H \mathbf{z}}{N_0} = \frac{\mathbf{z}^H \mathbf{z}}{N_0} = r \quad (6.14a)$$

$$\hat{\gamma} = \frac{\hat{\mathbf{z}}^H \hat{\mathbf{z}}}{2\hat{N}_0} = \frac{\mathbf{z}^H \mathbf{Q} \mathbf{Q}^H \mathbf{z}}{2N_0} = \frac{\mathbf{z}^H \mathbf{z}}{2N_0} = \gamma. \quad (6.14b)$$

Thus, the unitary diagonalization (6.8) does not change the statistics of the combiner output signal envelope, nor the SNR. Furthermore, the equivalent independent signals' powers, given by the diagonal elements of the correlation matrix \hat{R} , are eigenvalues of the correlation matrix R before transformation. With reference to Fig. 6.1, the signal components at points A and B are identical. The noise processes at these two points have identical statistics. Therefore, the receiver structures of Fig. 6.1 (a) and Fig. 6.1 (b) are both optimal and all performance measures of MRC operating on correlated Rayleigh fading input branches can be obtained from the results of those quantities of independent, non-identical branch powers models, by replacing the branch signal powers $2\sigma_i^2$, $i = 1, 2, \dots, M$ with the eigenvalues λ_i .

6.2 Average Level Crossing Rate and Average Fade Duration in Correlated Fading

In the previous section, we pointed out that the performance of a maximal ratio combiner operating with correlated branches can be obtained from an equivalent model with independent and usually unbalanced branches. We now apply this result to our level crossing problems.

We showed that the maximal ratio combiner output signal envelope is essentially the Euclidean norm of the input signals, which is preserved after the unitary transformation.

Thus, the unitary transformation does not change the statistics of the combiner output signal envelope. The same property can be observed for the time derivative of the combiner output signal envelope, which is given by differentiating (6.5)

$$\dot{r} = 2 \sum_{i=1}^M r_i \dot{r}_i = 2 \operatorname{Re}\{\mathbf{z}^H \dot{\mathbf{z}}\}. \quad (6.15)$$

If we apply the unitary transformation (6.8) on \mathbf{z} , the time derivative of the combiner output becomes

$$\hat{r} = 2 \operatorname{Re}\{\hat{\mathbf{z}}^H \hat{\dot{\mathbf{z}}}\} = 2 \operatorname{Re}\{\mathbf{z}^H Q Q^H \dot{\mathbf{z}}\} = 2 \operatorname{Re}\{\mathbf{z}^H \dot{\mathbf{z}}\} = \dot{r}. \quad (6.16)$$

Eqn. (6.16) shows that the statistics of the time derivative of the combiner output do not change after unitary transformation. Consequently, we can expect that performance measures involving the maximal ratio combined output signal envelope and its time derivative, as well as the output signal-to-noise ratio, can be obtained from the equivalent model where the branches are independent.

To compute the average level crossing rate and average fade duration, the first step is to find the eigenvalues λ_i and corresponding orthonormal eigenvectors \mathbf{q}_i of the correlation matrix R . Then, the results of MRC with unequal power, independent branches, given in Chapter 3, Section 3.4, can be applied. The root-mean-square value of the output signal envelope, R_{rms} , is computed from (3.41) by replacing $2\sigma_i^2$ with λ_i . The average LCR and AFD can be obtained from (3.37), (3.39) and (3.40) by replacing $2\sigma_i^2$ with λ_i . The average level crossing rate of two-branch MRC in correlated Rayleigh fading is

$$\frac{N_R}{f_m} = \frac{2\sqrt{2\pi}R^{\frac{3}{2}}}{3(\lambda_1 - \lambda_2)} \left[\frac{\sqrt{\lambda_1}}{\lambda_2} e^{-\frac{R}{\lambda_1}} {}_1F_1\left(1, \frac{5}{2}; -\frac{R}{\lambda_2}\right) - \frac{\sqrt{\lambda_2}}{\lambda_1} e^{-\frac{R}{\lambda_2}} {}_1F_1\left(1, \frac{5}{2}; -\frac{R}{\lambda_1}\right) \right]. \quad (6.17)$$

For three-branch MRC, the result is

$$\frac{N_R}{f_m} = \frac{2\sqrt{2\pi}}{3\lambda_1\lambda_2\lambda_3(\lambda_2 - \lambda_3)} \int_0^R g(x, R) dx \quad (6.18a)$$

with integrand

$$g(x, R) = [(\lambda_1 - \lambda_2)x + \lambda_2 R]^{\frac{3}{2}} \exp \left\{ -\frac{R}{\lambda_2} - \frac{x}{\lambda_1} + \frac{x}{\lambda_2} \right\} {}_1F_1 \left(1, \frac{5}{2}; -\frac{\lambda_1 - \lambda_2}{\lambda_2 \lambda_3} x - \frac{R}{\lambda_3} \right) \\ - [(\lambda_1 - \lambda_3)x + \lambda_3 R]^{\frac{3}{2}} \exp \left\{ -\frac{R}{\lambda_3} - \frac{x}{\lambda_1} + \frac{x}{\lambda_3} \right\} {}_1F_1 \left(1, \frac{5}{2}; -\frac{\lambda_1 - \lambda_3}{\lambda_2 \lambda_3} x - \frac{R}{\lambda_2} \right). \quad (6.18b)$$

Finally, for four-branch MRC in correlated fading,

$$\frac{N_R}{f_m} = \frac{2\sqrt{2\pi}}{3(\lambda_3 - \lambda_4)\lambda_1\lambda_2\lambda_3\lambda_4} \cdot \int_0^R \int_0^{R-x} h(x, y) dy dx \quad (6.19a)$$

where

$$h(x, y) = \exp \left\{ -\frac{R}{\lambda_3} - \frac{x}{\lambda_1} + \frac{x}{\lambda_3} - \frac{y}{\lambda_2} + \frac{y}{\lambda_3} \right\} [\lambda_3 R + (\lambda_1 - \lambda_3)x + (\lambda_2 - \lambda_3)y]^{\frac{3}{2}} \\ \cdot {}_1F_1 \left(1, \frac{5}{2}; -\frac{R}{2\lambda_4} - \frac{\lambda_1 - \lambda_3}{2\lambda_3\lambda_4} x - \frac{\lambda_2 - \lambda_3}{2\lambda_3\lambda_4} y \right) - \exp \left\{ -\frac{R}{2\lambda_4} - \frac{x}{2\lambda_1} + \frac{x}{2\lambda_4} - \frac{y}{2\lambda_2} + \frac{y}{2\lambda_4} \right\} \\ \cdot [\lambda_4 R + (\lambda_1 - \lambda_4)x + (\lambda_2 - \lambda_4)y]^{\frac{3}{2}} {}_1F_1 \left(1, \frac{5}{2}; -\frac{R}{2\lambda_3} - \frac{\lambda_1 - \lambda_4}{2\lambda_3\lambda_4} x - \frac{\lambda_2 - \lambda_4}{2\lambda_3\lambda_4} y \right). \quad (6.19b)$$

To the best of the author's knowledge, results (6.17), (6.18) and (6.19) are new.

Matlab simulations were run to justify our results. As an example, we consider an M -ary linear array with spacings equal to one wavelength between adjacent branch antennae [17, eqn. 10-58]. The $(i, j)_{th}$ element of the normalized correlation matrix R is given by

$$R_{ij} = J_0(\beta d_{ij}) \quad (6.20)$$

where $J_0(\cdot)$ is the zero-order Bessel function of the first kind, $d_{ij} = (i - j)\lambda$, $\beta = \frac{2\pi}{\lambda}$, and λ is the wavelength. Thus,

$$R = \begin{vmatrix} 1 & J_0(\beta d_{12}) & J_0(\beta d_{13}) & \cdots & J_0(\beta d_{1M}) \\ J_0(\beta d_{21}) & 1 & J_0(\beta d_{23}) & \cdots & J_0(\beta d_{2M}) \\ \vdots & \vdots & \vdots & \ddots & \vdots \\ J_0(\beta d_{M1}) & J_0(\beta d_{M2}) & \cdots & \cdots & 1 \end{vmatrix}. \quad (6.21)$$

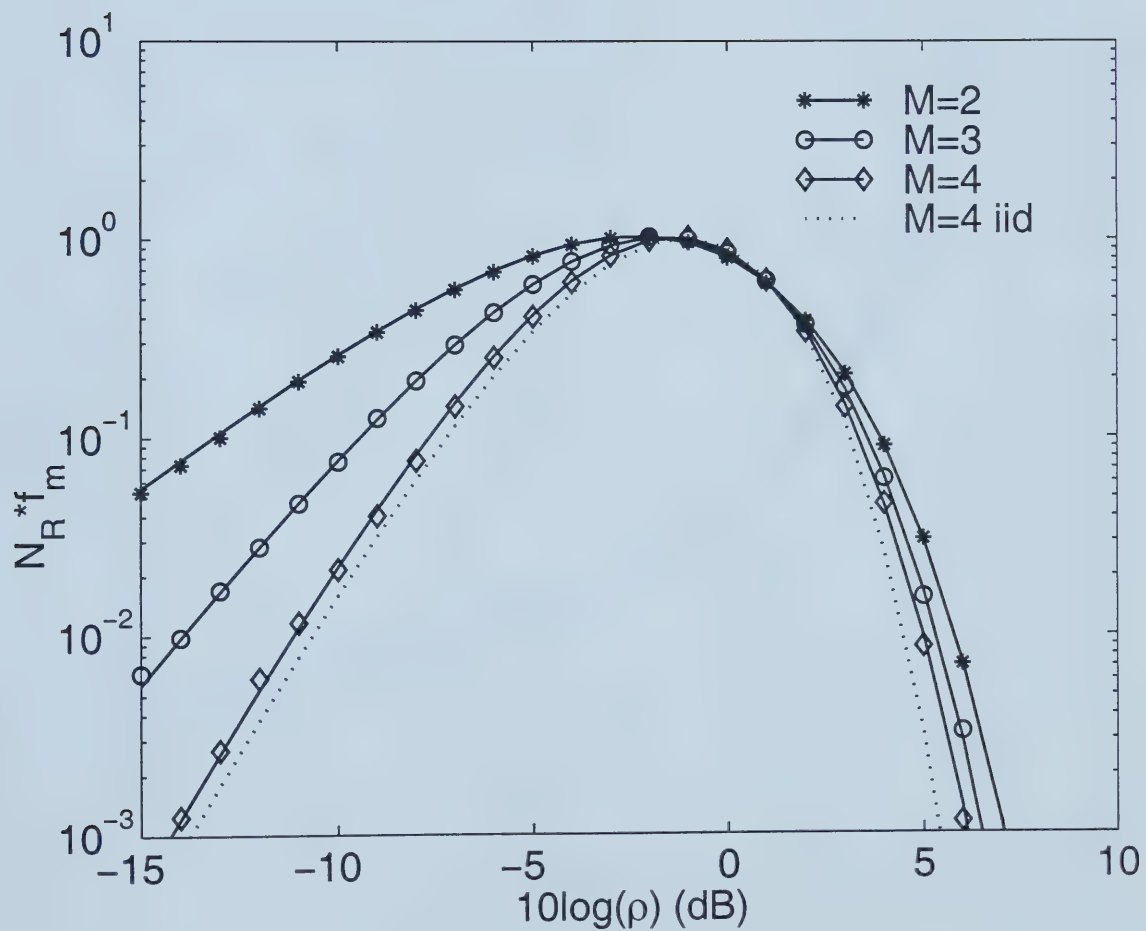


Figure 6.2. The average normalized LCR of MRC with adjacent branch spacings equal to one wavelength.

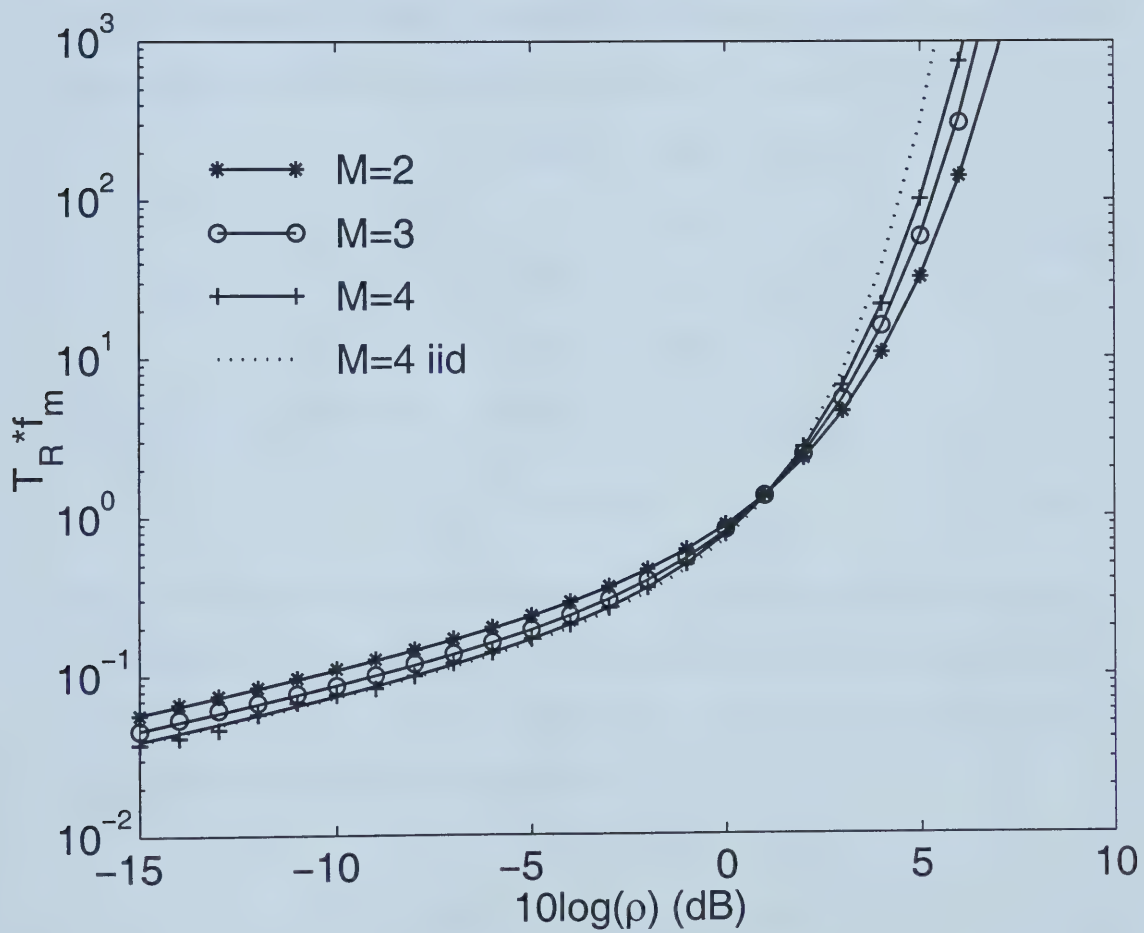


Figure 6.3. The normalized AFD of MRC with adjacent branch spacings equal to one wavelength.

Fig. 6.2 shows the normalized average LCR of MRC with branch correlations defined in (6.20). Fig. 6.3 illustrates the normalized AFD of the same system. The signal levels have been normalized to the rms value of the combiner output signal, R_{rms} . The simulator of Beaulieu and Merani [45] is used to generate the Rayleigh fading sequences with specified cross-correlations. For four-branch MRC, the correlation matrix in (6.21) becomes

$$R = \begin{vmatrix} 1 & 0.2203 & -0.1812 & 0.1575 \\ 0.2203 & 1 & 0.2203 & -0.1812 \\ -0.1812 & 0.2203 & 1 & 0.2203 \\ 0.1575 & -0.1812 & 0.2203 & 1 \end{vmatrix}. \quad (6.22)$$

The Rayleigh envelope correlation, defined as

$$R_r = E[r_i r_j], \quad (6.23)$$

can be obtained from the complex correlation (6.7), since the envelope correlation $R_{r_{ij}}$ is closely related to $|R_{ij}^2|$ [18], the squared magnitude of the complex cross-correlation of the Gaussian processes. The closeness is shown in detail in [18, Table 10-10-1] and [46]. In our example, the envelope correlation is given by

$$R_r = \begin{vmatrix} 1 & 0.0485 & 0.0328 & 0.0248 \\ 0.0485 & 1 & 0.0485 & 0.0328 \\ 0.0328 & 0.0485 & 1 & 0.0485 \\ 0.0248 & 0.0328 & 0.0485 & 1 \end{vmatrix}. \quad (6.24)$$

It is clearly shown in Fig. 6.2 that the analytical results are in excellent agreement with simulation. Diversity mitigates fading as the combiner signal envelope stays around its rms value. The branch correlation degrades the performance of MRC in terms of reducing fading, but is almost negligible when the correlation is small, as shown by curves at $M = 4$.

To see the performance of maximal ratio combining when the branch correlation is high, we show in Fig. 6.4 the average level crossing rate of MRC when the branches have equal envelope correlation

$$(a) \quad R_{rij} = 0.604 \quad i \neq j$$

$$(b) \quad R_{rij} = 0.748 \quad i \neq j$$

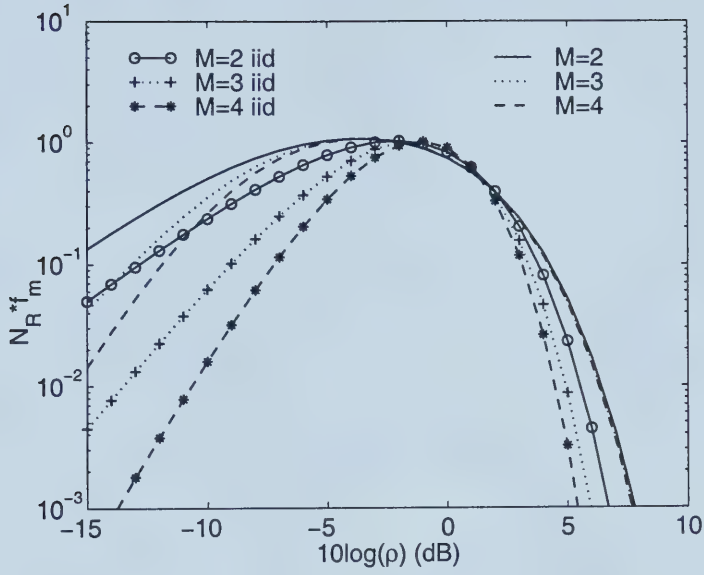
$$(c) \quad R_{rij} = 0.932 \quad i \neq j.$$

The behavior is similar to the behavior described by Feeney and Adachi in [41]. Maximal ratio combining is still an effective way of reducing fading, even when the branch correlation is high. The influence of branch correlation is more obvious at low signal levels.

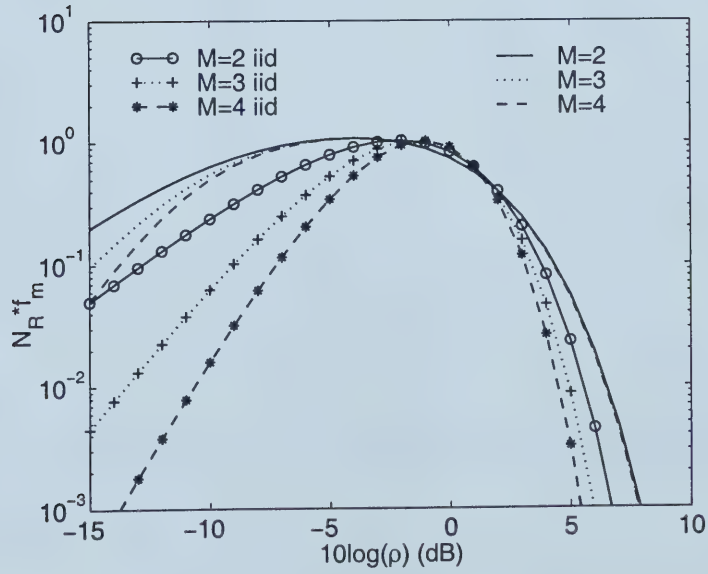
Fig. 6.5 shows the average fade duration of MRC in correlated fading. The input branches have envelope correlation matrix R_r

$$R_r = \begin{vmatrix} 1 & 0.604 & 0.604 \\ 0.604 & 1 & 0.604 \\ 0.604 & 0.604 & 1 \end{vmatrix}. \quad (6.25)$$

The results in Fig. 6.5 further validate Adachi's statement [41] that the high branch correlation does not have a strong impact on the average fade duration.

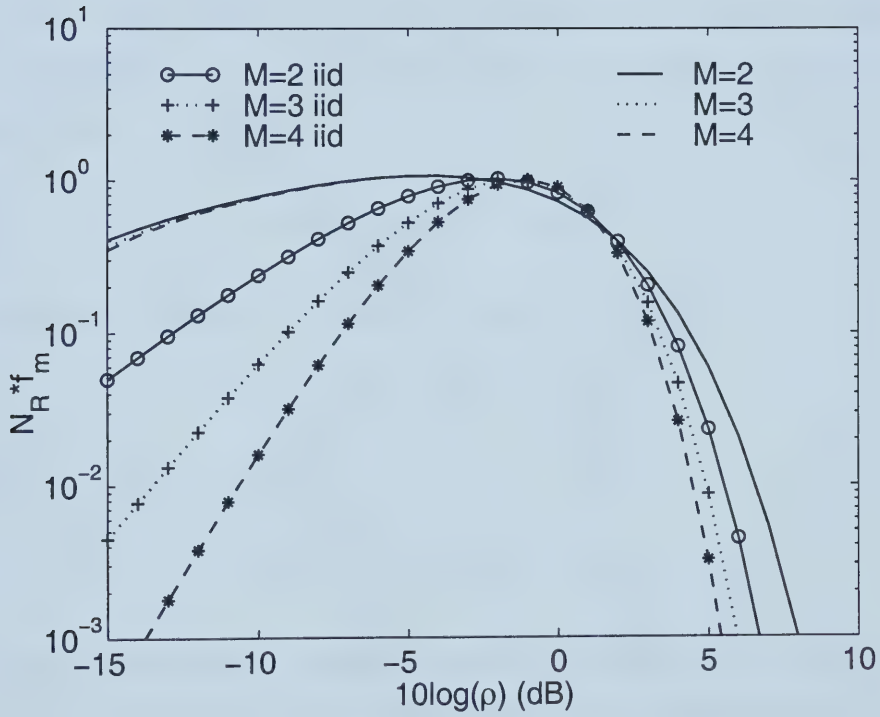


(a) $R_{ij} = 0.604$



(b) $R_{ij} = 0.748$

Figure 6.4. The average normalized LCR of MRC in Rayleigh fading with equal correlations between all branches.



(c) $R_{rij} = 0.932$

Figure 6.4. The average normalized LCR of MRC in Rayleigh fading with equal correlations between all branches.

6.3 Discussion of EGC and SC in Correlated Fading

It is worthwhile to note that the method to convert a correlated MRC case to an equivalent independent MRC case does not apply to equal gain diversity or selection diversity. This is due to the fact that linear transformation is length preserving, but an EGC or a SC output signal is not a length measure of the inputs. According to the vector norm theory [44], there are three frequently encountered vector norms. The Euclidean norm (or l_2 norm) on a complex vector space given by

$$\sqrt{r} = \|\mathbf{z}\|_2 = (|z_1|^2 + \cdots + |z_M|^2)^{1/2}, \quad (6.26)$$

the sum norm (or l_1 norm) on a complex vector space given by

$$r = \|\mathbf{z}\|_1 = |z_1| + \cdots + |z_M| \quad (6.27)$$

and the max norm (or l_∞ norm),

$$r = \|\mathbf{z}\|_\infty = \text{MAX}(|z_1|, \cdots, |z_M|). \quad (6.28)$$

We note that these definitions correspond to our definition of the diversity combiner output signal envelope of MRC, EGC and SC, respectively. We showed in Section 6 that a unitary matrix transformation on the complex vector \mathbf{z} does not change its Euclidean norm, as such a transformation diagonalizes the correlation matrix of vector \mathbf{z} . A matrix that satisfies

$$\|Bx\| = \|x\| \quad \text{for all } x \quad (6.29)$$

is said to be an isometry matrix for the vector norm $\|\cdot\|$. Isometry matrices of the sum norm look like permutation matrices except that the “+1” entries are replaced by arbitrary complex numbers with absolute value 1. Furthermore, if B^H is the isometry group of the sum norm, then B is in the isometry group of the max norm, and vice versa [44, pp. 266,

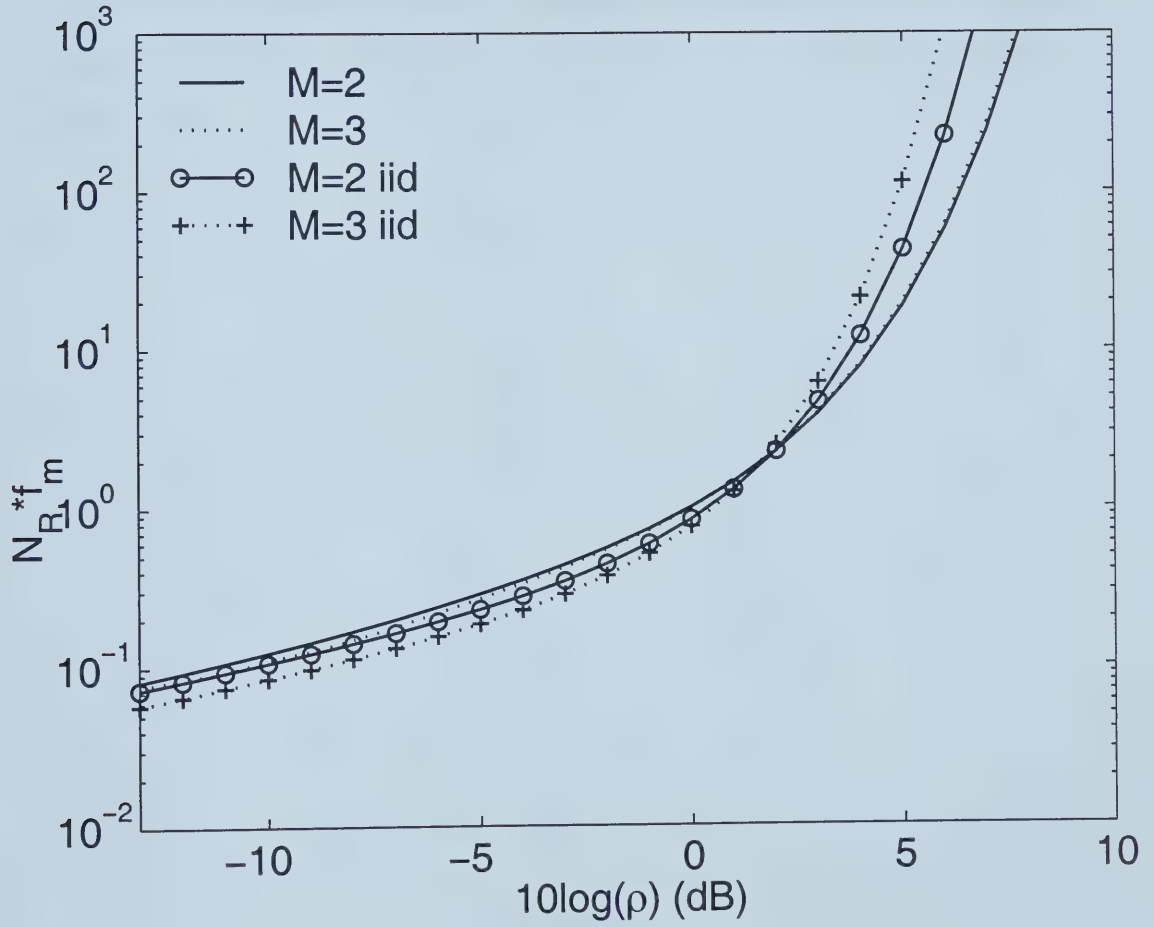


Figure 6.5. The normalized AFD of MRC in Rayleigh fading with equal correlations between all branches of $R_{r_{ij}} = 0.604$.

267]. We can easily prove that, for a general correlation matrix R , the unitary matrix U that diagonalizes R , as in (6.9), cannot be the permutation like matrix. In other words, a unitary transformation that diagonalizes the correlation matrix of the complex vector will change the vector's sum norm and max norm¹. Consequently, applying the unitary transformation directly to the complex vector does not help to solve performance measures problems of EGC and SC.

¹The conclusions about EGC and SC diversity systems in [43] are incorrect.

Chapter 7

Summary and Conclusions

Multipath propagation causes signal fading in wireless systems. The rate of occurrence of signal fades and the durations of the fades are important parameters for the design of wireless communication systems. They provide valuable aid in the selection of codes for digital communication systems and outage probabilities for digital and analog systems. Diversity is often used to mitigate fading and maximal ratio combining diversity is the optimal receiver diversity combining scheme, while equal gain combining offers performance close to that of MRC but with reduced complexity. Selection diversity is perhaps the simplest microdiversity method. The effect of diversity is to reduce fading and thus, the level crossing rate and the fade duration are expected to be altered by diversity. Despite the importance of average level crossing rate and fade duration in system design, only limited literature can be found about level crossing problems of diversity systems.

This thesis gives a relatively complete discussion of the average level crossing rate and fade duration of maximal ratio combining, equal gain combining and selection diversity systems. The Rayleigh, Ricean and Nakagami fading models are considered.

In summary,

1. New, exact, closed-form expressions for the average LCR and AFD of MRC operating with iid Ricean branches were obtained for arbitrary diversity orders and arbitrary Rice factor.
2. New, exact, closed-form expressions for the average LCR and AFD of dual MRC with unbalanced inputs were presented. New, exact analytical results were also obtained for three- and four-branch MRC when the input Rayleigh fading branches have non-identical mean signal energy. The branches are assumed to experience independent fading.
3. New normalization scheme in solving the level crossing problems of a diversity system was introduced. We normalized the signal levels to the rms value of the combiner output signal. It is more physically intuitive compared to the commonly normalization method where the rms value of one input branch signal was used.
4. Precise approximation of the average LCR and AFD of EGC diversity was presented using the infinite series method. Results were obtained for Rayleigh, Ricean and Nakagami fading models.
5. New, simple closed-form expressions for the average LCR and AFD of SC diversity were obtained for the Rayleigh, Ricean and Nakagami models. The results are valid for arbitrary diversity orders and arbitrary branch powers, identical or unbalanced.
6. New insights into the performance measures of MRC in correlated Rayleigh fading were presented. On one hand, any performance measure of a MRC diversity system operating with correlated input branch signals is identical to the performance of an equivalent MRC diversity system operating with uncorrelated (and, hence, independent) input branch signals. The average LCR and AFD of a MRC system in corre-

lated fading were obtained using this method. On the other hand, the performance of a MRC system with correlated signals and branch weights chosen according to the signal amplitude-to-noise power ratios of the correlated branches is identical to the performance of a MRC system with optimally decorrelated (and, hence, independent) branch signals and weights chosen according to the uncorrelated branch signal amplitude-to-noise powers ratios.

We can observe from the results for the average level crossing rate and average fade duration of various diversity models that diversity is an effective way of mitigating fading. With the diversity order increase, the average level crossing rate drops at signals level below and above its rms value, as the signal spends more time around its rms level. The average fade duration at signal levels below the rms value decreases with diversity order increase and increases with diversity order increase at levels above the rms value.

The ideal diversity gain is based on the assumption that all diversity branches are iid. When the branch powers are unbalanced, or branches are correlated, we lose some of the diversity advantage. It is shown in this thesis that reasonable diversity branch imbalance is acceptable. Also diversity system can tolerate a rather high value of branch correlation in terms of reducing the average level crossing rate. The average fade duration changes little with the branch correlation increase.

References

- [1] T. S. Rappaport, *Wireless Communications: Principles and Practice*, Prentice Hall PRT, 1996.
- [2] J. D. Parsons, *The Mobile Radio Propagation Channel*, Halsted Press, New York, 1992.
- [3] J. F. Ossanna, "A model for mobile radio fading due to building reflections: Theoretical and experimental fading waveform power spectra," *Bell Syst. Tech. J.*, , no. 43, pp. 2935–2971, 1964.
- [4] R. H. Clarke, "A statistical theory of mobile radio reception," *Bell Syst. Tech. J.*, , no. 44, pp. 1779–1803, 1965.
- [5] W. R. Bennett, "Distribution of the sum of randomly phased components," *Quart. Appl. Math.*, , no. 5, pp. 385–393, 1948.
- [6] S. O. Rice, "Mathematical analysis of the level crossing and duration of fades of the signal from an energy density mobile radio antenna," *Bell Sys. Tech. J.*, pp. 46–156, January 1945.
- [7] S. O. Rice, "Statistical properties of a sine wave plus noise," *Bell System Tech. J.*, vol. 27, pp. 109–157, January 1948.

- [8] W. C. Jakes, Ed., *Microwave Mobile Communication*, IEEE Press, 1993.
- [9] I. S. Gradshteyn and I. M. Ryzhik, *Table of Integrals, Series, and Products*, Academic Press Inc, 1994.
- [10] J. G. Proakis, *Digital Communications*, Mc-Graw Hill, 3 edition, 1995.
- [11] R. Bultitude and G. Bedal, "Propagation characteristics on microcellular urban mobile radio channels at 910 mhz," *IEEE Journal on Selected Areas in Communications*, vol. 7, pp. 31–39, Jan. 1989.
- [12] R. Steele, "The cellular environment of lightweight handheld portables," *IEEE Communications Magazine*, pp. 20–29, 1989.
- [13] J. I. Marcum, "A statistical theory of target detection by pulsed radar: mathematical appendix," *IEEE Transactions on Information Theory*, vol. 6, pp. 59–267, April 1960.
- [14] M. Nakagami, "The m -distribution- A general formula of intensity distribution of rapid fading," in *Statistical Methods in Radio Wave Propagation*, W. G. Hoffman, Ed., pp. 3–36. Pergamon Press, Oxford, 1960.
- [15] D. G. Brennan, "Linear diversity combining techniques," *Proc. IRE*, vol. 47, pp. 1075–1101, June 1959.
- [16] P. R. J. Parsons, M. Henze and M. Withers, "Diversity techniques for mobile radio reception," *IEEE Trans. Veh. Tech.*, vol. 25, pp. 75–85, 1976.
- [17] W. C. Y. Lee, *Mobile Communications Engineering*, McGraw-Hill, New York, 1992.
- [18] S. S. M. Schwartz, W. R. Bennett, *Communication systems and techniques*, McGraw-Hill, New York, 1966.

- [19] G. L. Stüber, *Principles of Mobile Communications*, Kluwer, Boston, 1996.
- [20] N. C. Beaulieu, "An infinite series for the computation of the complementary probability distribution function of a sum of independent random variables and its application to the sum of Rayleigh random variables," *IEEE Trans. Commun.*, vol. 38, pp. 1463–1474, September 1990.
- [21] M. Kac, "On the average number of real roots of a random algebraic equation," *Bull. Amer. Math. Soc.*, vol. 49, pp. 314–319, 1943.
- [22] M. Kac and D. Slepian, "Large excursions of Gaussian processes," *Ann. Math. Statist.*, vol. 30, pp. 1215–1228, 1959.
- [23] J. D. Bendat, *Principles and Applications of Random Noise Theory*, Wiley, New York, 1958.
- [24] M. R. Leadbetter and J. D. Cryer, "The variance of the number of zeros of a stationary normal process," *Bull. Amer. Math. Soc.*, vol. 71, pp. 561–563, 1965.
- [25] C. W. Helstrom, "The distribution of the number of crossings of a Gaussian stochastic process," *IRE Trans. Inform. Theory*, vol. 3, pp. 232–237, December 1957.
- [26] S. O. Rice, "Distribution of the duration of fades in radio transmission: Gaussian noise model," *Bell. Syst. Tech. J.*, , no. 3, pp. 581–635, May 1958.
- [27] M. Yacoub, J. Bautista, and L. de R. Guedes, "On higher order statistics of the Nakagami- m distribution," *IEEE Trans. Veh. Tech.*, vol. 48, pp. 790–794, May 1999.
- [28] A. Papoulis, *Probability, Random Variables, and Stochastic Processes*, McGraw-Hill, New York, 3 edition, 1991.

- [29] M. D. Yacoub, C. da Silva, and J. V. Bautista, "Second-order statistics for equal gain and maximal ratio diversity-combining reception," *Electron. Lett.*, pp. 382–384, January 2000.
- [30] F. Adachi, M. T. Feeney, and J. D. Parsons, "Effects of correlated fading on level crossing rates and average fade durations with predetection diversity reception," *IEE Proc., Pt. F*, vol. 135, pp. 11–17, February 1988.
- [31] W. C. Y. Lee, "Level crossing rates of an Equal-Gain predetection diversity combiner," *IEEE Trans. Commun.*, vol. 18, pp. 417–426, August 1970.
- [32] M. Fisz, *Probability Theory and Mathematical Statistics*, Robert E. Krieger Publishing Co., Inc., 1980.
- [33] D. J. Young and N. C. Beaulieu, "The generation of correlated Rayleigh random variates by inverse Discrete Fourier Transform," *IEEE Trans. Commun.*, vol. 48, pp. 1114–1127, July 2000.
- [34] B. B. Barrow, "Diversity combination of fading signals with unequal mean strengths," *IEEE Trans. Commun. Sys.*, vol. 11, pp. 73–78, March 1963.
- [35] S. W. Halpern, "The effect of having unequal branch gains in practical predetection diversity systems for mobile radio," *IEEE Trans. Veh. Tech.*, vol. 26, no. 1, pp. 94–105, February 1977.
- [36] N. C. Beaulieu and A. A. Abu-Dayya, "Analysis of equal gain diversity on nakagami fading channels," *IEEE Trans. Commun.*, vol. 39, pp. 225–234, February 1991.
- [37] A. Abu-Dayya and N. C. Beaulieu, "Microdiversity on Rician fading channels," *IEEE Trans. Commun.*, vol. 42, pp. 2258–2267, June 1994.

- [38] F. Oberhettinger, *Fourier Transforms of Distributions and their Inverses*, Academic, New York, 1973.
- [39] Q. T. Zhang, "Maximal-ratio combining over Nakagami fading channels with an arbitrary branch covariance matrix," *IEEE Trans. Veh. Tech.*, vol. 48, no. 4, pp. 1141–1150, July 1999.
- [40] G. F. P. Lombardo and M. M. Rao, "MRC performance for binary signals in Nakagami fading with general branch correlation," *IEEE Trans. Commun.*, vol. 47, no. 1, pp. 44–52, January 1999.
- [41] M. T. Feeney and F. Adachi, "The performance of various diversity combiners on signals received at a base station site," in *IERE Conf. Proc.*, Dec. 1985.
- [42] E. Perahia and G. J. Pottie, "On diversity combining for correlated slowly flat-fading Rayleigh channels," in *Proc. IEEE International Conference on Communication*, May 1994, pp. 342–346.
- [43] G. B. L. Fang and A. Kot, "New method of performance analysis for diversity reception with correlated Rayleigh-fading signals," *IEEE Trans. Veh. Tech.*, vol. 49, no. 5, pp. 1807–1812, September 2000.
- [44] R. A. Horn and C. R. Johnson, *Matrix Analysis*, Cambridge University Press, Cambridge, 1999.
- [45] N. C. Beaulieu and M. L. Merani, "Generation of multiple Rayleigh fading sequences with specified cross-correlations," to appear in *European Transactions on Telecommunications*, 2001.

- [46] J. N. Pierce and S. Stein, “Multiple diversity with non-independent fading,” *Proc. IRE*, vol. 48, pp. 89–104, January 1960.

Vita

Name:

Xiaofei Dong

Education:

University of Alberta, January 2001-present.

M.Sc, (Electrical and Computer Engineering), 2001.

Queen's University, September 1999- December 2000.

M.Sc. (Electrical and Computer Engineering), transferred.

Xian Jiaotong University, P.R. China, 1995-99.

B.Sc/Eng. (Electrical Engineering), 1999.

Experience:

Research Assistant, University of Alberta,

Department of Electrical and Computer Engineering, 2001-present.

Teaching Assistant, University of Alberta,

Department of Electrical and Computer Engineering, 2001.

Research Assistant, Queen's University,

Department of Electrical and Computer Engineering, 1999-2000.

Teaching Assistant, Queen's University,

Department of Electrical and Computer Engineering, 1999-2000.

Awards:

IEEE Student Travel Grant Award, ICC2001.

Queen's Graduate Fellowship, 1999.

Queen's Graduate Award, 2000.

University Scholarship, Xian Jiaotong University, 1995-1999.

Publications:

X. Dong and N.C. Beaulieu, "Average level crossing rate and average fade duration of MRC and EGC diversity," *IEEE International Conference on Communications 2001*, ICC2001, pp. 1078-1083, Helsinki, Finland, June 2001.

X. Dong and N. C. Beaulieu, "Average level crossing rate and average fade duration of selection diversity", to appear in *IEEE Communications Letters*, 2001.

X. Dong and N. C. Beaulieu, "Average level crossing rate and average fade duration of diversity methods," Blakefest Workshop, Victoria, Canada, June 7-8, 2001.

X. Dong and N. C. Beaulieu, "Average level crossing rate and average fade duration of maximal ratio diversity with unbalanced channels," submitted, *IEEE Communications Letters*, May 2001.

X. Dong and N. C. Beaulieu, "Average level crossing rate and fade duration of MRC and EGC diversity in Ricean fading", submitted, *IEEE Transactions on Communication*, Oct. 2000.

X. Dong and N. C. Beaulieu, "Optimal maximal ratio combining with correlated branches," submitted, *IEEE Communications Letters*, June 2001.

X. Dong and N. C. Beaulieu, "Average level crossing rate and average fade duration of maximal ratio diversity in unbalanced and correlated fading channels," submitted, *IEEE Wireless Communications and Networking Conference*, WCNC 2002.

University of Alberta Library



0 1620 1492 0530

B45458